



**UNIVERSIDAD  
DE ANTIOQUIA**

**DESIGN AND CONTROL INTEGRATION OF A  
REACTIVE DISTILLATION COLUMN FOR ETHYL  
LACTATE PRODUCTION**

**Chem. Eng. NATALY JOHANA CASTRILLÓN MADRIGAL**

**Universidad de Antioquia  
Facultad De Ingeniería, Departamento De Ingeniería Química  
Medellín, Colombia  
2020**



Design and Control Integration of a Reactive Distillation Column for Ethyl Lactate  
Production

**Chem. Eng. Nataly Johana Castrillón Madrigal**

Thesis work presented as a partial requirement to qualify for:  
**Master's Degree in Chemical Engineering**

Advisor:

Professor. Dr. Ing. Silvia Ochoa Cáceres

Research line:

Modelling and Simulation Processes

Research group:

SIDCOP

Universidad de Antioquia

Facultad De Ingeniería, Departamento De Ingeniería Química

Medellín, Colombia

2020

## **ACKNOWLEDGMENTS**

*Throughout our lives we take different decisions, about our culture, our food, our likes, our future, and in some moments we decide to make some voyages of learning. On this road we learn a lot, even more than hoped for, in my case, as I received so many unexpected and valuable lessons that it now only remains for me to express my thanks. This master's degree is more than a new professional qualification for my curriculum vitae, it has been a life experience, since it taught me how to get lost and how to go back, to find myself. It taught me to let myself be guided and accompanied, reiterating that in this life all that we learn is useful, that all people who arrive in our lives have a lot to bring to us, and something too that one can contribute. And it was in this during this journey that I found so many beautiful and nice people that I haven't mentioned in these paragraphs. To them I express my deepest esteem and my sincere acknowledgment.*

*Thanks to my quartet of classmates Cesar Garcia, Diana Grajales, Isis Hernández, and Victor López, because with them the postgraduate studies were amazing, filled with learning and laughter. I thank them for their support and friendship, the best possible example of the way such relationships can be built between professionals. A special acknowledgment to Diana Grajales because only somebody so in love with studying and chemical engineering can understand me and help me to rediscover my inspiration, thanks so much. To the teacher Adriana Villegas, thank you for giving me cardiopulmonary resuscitation in a time of agony, because when my PC was broken, she helped me with all her tools and time to allow me to continue.*

*To my advisor Dr. Silvia Ochoa, the most intelligent person, the best teacher and person that I know, thanks for your lessons, advice, and mainly your patience and good talks about the academy and life, maybe I need another thesis to express to her all my gratitude. When I met my advisor, I said that I loved the modeling and simulation of processes and saw that with her I could learn a lot about the programing applied to chemical engineering. I wasn't wrong in my thinking, by contrast, I underestimated this, because not only had I met a great teacher with wide knowledge in mathematics, thermodynamics, control, simulation, amongst other areas of science, and other great quantity of mental capacities, but also I found an excellent person who shares her expertise,*

*and shows more than just interest in her students but interest in the people who are her students, and she helps you to grow as such. Thank you for making sure my postgraduate studies were not just another technical stage, thank you for making me a better person and better professional, and mainly thank you for allowing me to get to know you, and for believing in me, because although I had bad days she always was my cornerstone, motivating and improving my skills and working on my weaknesses, and never allowing me to decline, reminding me of the reasons why I chose to research in modeling and simulation of processes. And finally, a thousand apologies for not always being at her level, and for not being able to take more advantage of her knowledge.*

*To my family, who are always in each one of my goals, thank you for believing in me. To my brothers who are the most amazing men that I know, whose strength is the best example of overcoming. To my sisters who are a big momentum and motivation. And to my mom, because your greatness and temperance have made me who I am. Finally, I appreciate life through each of you as your teaching has allowed me to grow as a person and a professional.*

*To my eternal sigh, because you always give me a new breath.*

## TABLE OF CONTENTS

1. STATE OF THE ART .....	12
1.1. Ethyl Lactate .....	12
1.2. Methodologies for Design and Control integration.....	16
2. THEORETICAL FRAMEWORK.....	22
2.1. Ethyl Lactate production in Reactive Distillation (RD) Columns .....	22
2.2. Traditional Design.....	24
2.3. Integrated Design and Control .....	25
2.3.1. Problem Definition.....	32
2.3.2. Obtaining of a Phenomenological Based Semiphsical Model (PBSM).....	32
2.3.3. Selection of Manipulated Variables and Determination of the Available Interval.	32
2.3.4. Definition of the Objective Function .....	33
2.3.5. Scenarios Selection .....	34
2.3.6. Constrained Optimization .....	34
2.3.7. Control System Design .....	34
3. MODELING AND SIMULATION OF THE ETHYL LACTATE PROCESS BY REACTIVE DISTILLATION .....	35
3.1. Description of the system to be modeled .....	35
3.2. Phenomenological Based Semiphsical Model (PBSM).....	36
3.3. Model Simulation.....	46
3.3.1. Data required for Simulation .....	47
3.3.2. Dynamic simulation of the distillation column.....	49
3.4. Model validation .....	55
3.5. Sensitivity Analysis.....	64
4. DESIGN AND CONTROL INTEGRATION OF A REACTIVE DISTILLATION COLUMN FOR ETHYL LACTATE PRODUCTION.....	69
4.1. Application of the methodology.....	69
4.1.1. Problem Definition.....	69
4.1.2. Obtaining of a Phenomenological Based Semiphsical Model (PBSM).....	69
4.1.3. Selection of Manipulated Variables and Determination of the Available Interval.	70
4.1.4. Definition of the Objective Function .....	77
4.1.5. Scenarios Selection .....	82

4.1.6.	Constrained optimization.....	85
4.1.7.	Control system Design.....	90
4.2.	Results.....	93
4.2.1.	Constrained optimization problem.....	93
4.2.2.	Results of the Control System Implementation.....	101
5.	COMPARISON: INTEGRATED vs. TRADITIONAL SEQUENTIAL DESIGN.....	105
5.1.	Optimization results for traditional design.....	107
5.2.	Integrated vs Traditional design.....	107
6.	CONCLUSIONS AND FUTURE RESEARCH.....	112
6.1.	Future Work:.....	113
	REFERENCES.....	114
	APPENDIX.....	118

## LIST OF FIGURES

<i>Fig. 1 Internal distribution of a Reactive Distillation Column.....</i>	23
<i>Fig. 2 Design and Control Methodology proposed by Ochoa [8].....</i>	31
<i>Fig. 3 Reactive Distillation column for Ethyl Lactate production.....</i>	36
<i>Fig. 4 Internal distribution of a Reactive Distillation Column.....</i>	37
<i>Fig. 5 Scheme of a typical tray .....</i>	38
<i>Fig. 6 Dynamic behavior of the Temperature at some stages in the distillation column .....</i>	50
<i>Fig. 7 Dynamic behavior of the Holdup at some stages in the distillation column.....</i>	50
<i>Fig. 8 Dynamic behavior of the Ethanol mole fraction at some stages in the distillation column.....</i>	51
<i>Fig. 9 Dynamic behavior of the Lactic Acid mole fraction at some stages in the distillation column.....</i>	51
<i>Fig. 10 Dynamic behavior of the Temperature at some stages in reactive distillation column ...</i>	52
<i>Fig. 11 Dynamic behavior of the Holdup at some stages in reactive distillation column .....</i>	53
<i>Fig. 12 Dynamic behavior of the Ethanol mole fraction at some stages in reactive distillation column.....</i>	53
<i>Fig. 13 Dynamic behavior of the Lactic Acid mole fraction at some stages in reactive distillation column.....</i>	54
<i>Fig. 14 Dynamic behavior of the Ethyl Lactate mole fraction at some stages in reactive distillation column .....</i>	54
<i>Fig. 15 Temperature profile in the distillation column.....</i>	57
<i>Fig. 16 Liquid molar fraction profile in the distillation column.....</i>	57
<i>Fig. 17 Vapor molar fraction profile in the distillation column .....</i>	58
<i>Fig. 18 Internal flows profile in the distillation column .....</i>	58
<i>Fig. 19 Temperature profile in the reactive distillation column.....</i>	61
<i>Fig. 20 Mole fraction profile at the liquid in the reactive distillation column .....</i>	61
<i>Fig. 21 Mole fraction profile at the vapor in the reactive distillation column .....</i>	62
<i>Fig. 22 Internal flows (Liquid and vapor) profiles in the reactive distillation column .....</i>	62
<i>Fig. 23 Effect of Diameter in the conversion and Ethyl Lactate molar fraction at Bottoms .....</i>	66
<i>Fig. 24 Effect of Boilup ratio in the conversion and Ethyl Lactate molar fraction at Bottoms....</i>	67
<i>Fig. 25 Effect of Feed molar ratio in the conversion and Ethyl Lactate molar fraction at Bottoms .....</i>	67
<i>Fig. 26 Effect of Reflux ratio in the conversion and Ethyl Lactate molar fraction at Bottoms ....</i>	68
<i>Fig. 27 Effect of Total catalyst loading in the conversion and Ethyl Lactate molar fraction at Bottoms .....</i>	68
<i>Fig. 28 Digraph .....</i>	72
<i>Fig. 29 Definition of the Objective function[31, 42, 48] .....</i>	79
<i>Fig. 30 Catalyst placed on the tray[52].....</i>	81
<i>Fig. 31 Disturbances effects in Rectifying zone.....</i>	82
<i>Fig. 32 Disturbances effects in Reactive zone .....</i>	83
<i>Fig. 33 Disturbances effects in Stripping zone .....</i>	83
<i>Fig. 34 Disturbances effects in Condenser .....</i>	84

<i>Fig. 35 Disturbances effects in Reboiler.....</i>	<i>84</i>
<i>Fig. 36 Control loops for the Reactive Distillation Column.....</i>	<i>92</i>
<i>Fig. 37 Optimization results for integrated design in function of Rzone in \$USD.....</i>	<i>96</i>
<i>Fig. 38 Temperature control in Rectifying zone (<math>x_1</math>). Temperature in tray 2 (top) and Reflux flow rate (bottom) .....</i>	<i>102</i>
<i>Fig. 39 Temperature control in Reactive zone (<math>x_2</math>). Temperature in tray <math>N_1 + N_2 - 1</math> (top) and Lactic Acid feed stream (bottom).....</i>	<i>103</i>
<i>Fig. 40 Temperature control in Stripping zone (<math>x_3</math>). Temperature in tray <math>N+1</math> (top) and Reboiler heat duty (bottom) .....</i>	<i>103</i>
<i>Fig. 41 Level control in the Condenser (<math>x_4</math>). Condenser level (top) and Flow of Distillate (bottom).....</i>	<i>104</i>
<i>Fig. 42 Level control in the Reboiler (<math>x_5</math>). Reboiler level (top) and Flow of Bottoms (bottom) .</i>	<i>104</i>
<i>Fig. 43 General Process Design Algorithm (for Traditional and Integrated Design): Thicker lines indicate steps that are exclusive for Integrated Design Procedure. ....</i>	<i>106</i>
<i>Fig. 44 Profit comparison for integrated and traditional design in \$USD .....</i>	<i>108</i>



## LIST OF TABLES

Table 1 Works about Ethyl Lactate applications and production .....	15
Table 2 Recent Works on the Design- Control integration topic.....	18
Table 3 Classification of variables.....	44
Table 4 Description of subscripts .....	46
Table 5 Kinetic parameters, design parameters and feed conditions.....	48
Table 6 Properties of pure substances and system parameter .....	48
Table 7 Summary streams, Aspen vs MATLAB simulation in distillation column.....	59
Table 8 Summary streams, Aspen vs MATLAB simulation in reactive distillation column .....	63
Table 9 Sensitivity analysis applying 50% of change to the nominal value.....	64
Table 10 Simulated Experimental Design and Results for Sensitivity Analysis.....	65
Table 11 Input variables classification .....	70
Table 12 Chemical compatibility for building materials [49] .....	80
Table 13 Comparison of principal factors for selection tray type .....	80
Table 14 Factors and values for Objective Function calculation [42, 48, 54].....	81
Table 15 Scenarios selected for trajectories.....	85
Table 16 Optimal decision variables.....	94
Table 17 Comparison of results for integrated design in function of Rzone .....	97
Table 18 Optimization results with heuristic $HT/Diam = 5$ for integrated design.....	101
Table 19 Tuning parameters for PI controllers .....	101
Table 20 Optimal values of decision variables for the traditional design.....	107
Table 21 Comparison results for Integrated (Int.) and Traditional (Trad.) design .....	110
Table 22 Optimization results with heuristic $HT/Diam = 5$ for traditional design.....	111
Table 23 Initial condition for model simulation .....	118

## ABSTRACT

Nowadays, the worldwide tendency to obtain environmentally friendly products through the use of safe and stable production processes, minimizing the energy consumption (i.e. using energy integration), and avoiding products out of specification, are an important motivation for applying a process design methodology that incorporates controllability issues since the earliest design stages. Although the topic of design-control integration has been a research topic investigated from different fronts for more than thirty-five years, it was in 2005 where a methodology incorporating local practical controllability issues for nonlinear systems was proposed. Such methodology allows designing processes that fulfill some controllability criteria, which assures that the resulted design will be controllable from the modern control theory.

The mentioned design-control integration methodology was applied in this work for designing a reactive distillation column for producing ethyl lactate, an important green solvent. Production of this green solvent has gained great attention worldwide since it is seen as an excellent alternative for replacing petroleum-based solvents. As with any green product that intends to replace oil-based products, ethyl lactate production needs to be improved (in terms of its economic feasibility) to have an actual chance for replacing the petroleum-based solvents at a worldwide scale. One of the proposals for improving the economic feasibility of this green solvent, is to produce it in a reactive distillation column system, which would reduce the energy consumption, increasing the process profit.

The design-control methodology applied here involved several steps. First, the development of a first principles-based model is required. Unfortunately, experimental data for a reactive distillation system for ethyl lactate production are scarce. Therefore, the model was identified and validated using data generated by running simulations in Aspen Plus. After model validation, simulated data were used in conjunction with knowledge of the process (obtained from technical literature) to select the state variables to be controlled. Then the manipulated and controlled variables were paired by applying digraphs theory, which avoids linearization of the nonlinear model. After this, local practical controllability metrics were formulated for being used as constraints during the optimization step of the design-control methodology. Besides the controllability metrics, physical constraints as well as product specifications constraints were included in the optimization. To compare the integrated design methodology with a traditional design methodology, the optimization was also run but considering only the physical and product specifications as constraints, but not the controllability metrics. Results of the comparison of the integrated design and the traditional design methodologies have shown that the design obtained by using the design control methodology leads to a higher profit while fulfilling all the constraints.

A key factor in the design of the reactive distillation column is the ratio between the number of trays in the rectification zone and the stripping zone. Therefore, the optimization was run for several values of this ratio. Then the best case for this ratio was used for finally designing the column under the design–control methodology. Furthermore, as defining a ratio between the column length and column diameter is a common practice in the traditional design of distillation columns, in this work, such ratio was also included as a constraint in the optimization problem, to investigate how it impacted the optimal design results. It was observed that such type of constraint is not suitable for being included in the design of the reactive distillation column for the analyzed case study.

**Keywords:** *Design and Control Integration, Reactive Distillation Colum, Ethyl Lactate, Local practical controllability*

## 1. STATE OF THE ART

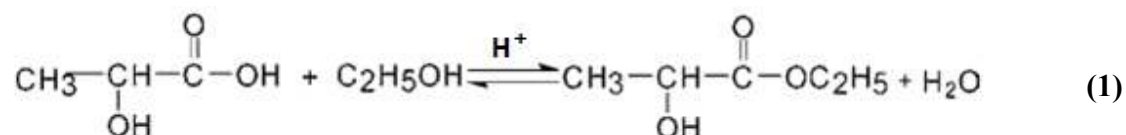
Generally, the main objective of process design is to propose the flowsheet, equipment, and operating conditions for a specific process to obtain the desired product(s). Then, the control system design is carried out for fulfilling the quality requirements whereas safety and environmental constraints are found. Therefore, classic process design is seen to be separated from the control system design. This is often called a sequential process design approach. However, this kind of approach is claimed to be very time consuming and expensive (i.e. re-design is required if no process control can be implemented for the required control objectives at the designed process). Furthermore conflicts and competitions between economic and controllability objectives are usually present (Sharifzadeh, 2013). Since the 1940s, the paradigm of simultaneous process design and control (e.g. Design-Control Integration) have emerged (Pastora Vega, De Rocco, Revollar, & Francisco, 2014) to attend the drawbacks of the sequential approach for facing the characteristics of modern chemical processes, and to enable the application of Process Systems Engineering (PSE) tools for improving the process design (Sharifzadeh, 2013). Simultaneous Process Design and Control is still a very active research area, as it will be shown in this section.

In this chapter, the state of the art is reviewed in two main topics. First, a quick overview of the more important facts on the ethyl lactate production process, which is the case study addressed in this work. Second, the most relevant works published until now on the topic Design-Control Integration will be reviewed.

### 1.1. Ethyl Lactate

Ethyl lactate ( $C_5H_{10}O_3$ ) belongs to the family of lactates that are known as green solvents. It is widely used in paints, gums, dyes, oils, detergents, food additives, cosmetics, and pharmaceutical industries, between others. Ethyl lactate is especially attractive due to its physicochemical properties, such as its high boiling point, low surface tension, and low vapor pressure. Furthermore, this product has started to replace harmful solvents like toluene, acetone, and Xylene. This means, that there is an attractive and increasing market for the use of ethyl lactate as a solvent for a wide range of industrial uses (Lomba, Giner, Zuriaga, Gascón, & Lafuente, 2014).

Currently, the most used method to obtain Ethyl Lactate is the one based on the Lactic acid esterification with ethanol in presence of a strong acid catalyst (heterogeneous or homogenous catalysis as it is explained in 2.1), as it is shown in the following reaction:



According to Gao et al (2007) and Pereira et al (2011), ethyl lactate is one of the most promising green solvents due to its very favorable toxicological properties (it does not show any potential health risks). Furthermore, from an economic viewpoint, the replacement of traditional solvents by Ethyl lactate is favored considering that the raw materials in the process (ethanol and lactic acid) are produced from carbohydrate feedstocks at very low and competitive prices. The use of carbohydrates as a starting point for ethyl lactate production leads to a renewable product, and thus sustainable, not rising from petrochemical sources (Gao, Zhao, Zhou, & Huang; C. S. Pereira, Silva, & Rodrigues, 2011). Ethyl lactate production processes based on the lactic acid esterification can be divided into two main schemes:

- a. **Processes with a reactor followed by separation units:** Two kinds of processes can be distinguished. First, the one in which the reaction mixture is subjected to reduced-pressure flash separation, and the overhead stream (ethyl lactate, water, and ethanol) is fed to a fractional distillation column. In the second, a near-azeotropic water/ethanol mixture is extracted, with a subsequent recovery of ethanol by dehydration using molecular sieves follow of a separation in a distillation column. However, these processes are expensive and less efficient than the technologies that integrate the reaction and separation steps (C. S. Pereira et al.).
- b. **Processes Using Intensification Strategies:** In general, all these processes are more compact and energetically efficient. This kind of process includes those based on membranes technologies, chromatographic reactors, membrane coupled to distillation, and reactive distillation (C. S. Pereira et al.). Precisely, the reactive distillation technology is the one used as a case study in this work. Section 2.1 shows the theoretical framework for the operation of reactive distillation columns.

Table 1 summarizes the most relevant recent works on ethyl lactate production in Reactive Distillation Columns.

**Table 1 Works about Ethyl Lactate applications and production**

<b>Paper</b>	<b>Contribution</b>
(2010) Investigation of ethyl lactate reactive distillation process (Gao et al.)	Design variables, optimal operating conditions, and the kinetics are obtained for the production of ethyl lactate by esterification of lactic acid and ethanol using a solid super-acid catalyst in a reactive distillation column.
(2011) Process Intensification for Ethyl Lactate Production Using Reactive Distillation (Lunelli, de Morais, Maciel, & Maciel Filho)	An NRTL model parameter set has been established to predict the composition and temperatures for the system components. The simulation was carried out with Aspen Plus.
(2011) Ethyl lactate as a solvent: Properties, applications and production processes – a review (C. S. Pereira et al.)	A comprehensive description of the main topics of Ethyl Lactate, with a summary of some production processes, advantages, and disadvantages.
(2014) Conversion of lactides into ethyl lactates and value-added products (Bykowski, Grala, & Sobota)	A method for $Mg(OR)_2$ mediated lactide alcoholysis is presented, where complete consumption of lactide was reported, therefore obtaining very high yields under ambient conditions.

## 1.2. Methodologies for Design and Control integration

The development of the chemical process industry, the advances in technologies, the environmental awareness, the safety requirements, and the high-quality exigencies have generated the necessity of designing controllable processes that operate under stable conditions, satisfying product specifications and environmental regulations while energy consumption is minimized. These demands are not easy to satisfy by the traditional process design methodology, which is dedicated entirely to the process design, and just after the design is finished, the process control system design comes into consideration. Designing in such a sequential manner frequently results in uncontrollable processes or expensive projects for the installation of the control structure. Some methodologies have been suggested, where it is proposed to design the control system along with the process equipment's (i.e. simultaneously and not sequentially as the usual approach). One of these works is developed by Ochoa (Ochoa, 2005) where a methodology for design and control integration is proposed, based on the state controllability concept. The mentioned work introduces the concept of local practical controllability which is used as a base for providing metrics in order to assure process controllability. Such methodology has the advantage of being based on a semi-physical based first principles that doesn't require linearization, allowing to work in the time domain. The work by Ochoa (Ochoa, 2005) will be used as a starting point for developing the design-control integration of a reactive distillation column for the Ethyl Lactate production. Furthermore, other studies already reported in the literature, like the works by Sharifzadeh (2013) and Vega et al. (2014), will serve also for guiding the development of this Master thesis. In the following, some of the main approaches that have been proposed in the literature for addressing the Design- Control integration problem, are described.

- Controllability index-based approaches coupled with optimization: this kind of approaches (generally multi-objective) search the minimum of an objective function that involves capital and operating costs and the fulfillment a specific controllability index. Relative gain array, the condition number, the disturbance condition number, or the integral errors are common criteria used as "controllability indicators". One of the main drawbacks of these approaches is that usually a steady state model of the process is considered which limits the solution of the problem to a region near to the nominal value, however some economic costs referred to



variability of product aren't into considerations (Luis A Ricardez-Sandoval, Budman, & Douglas, 2009).

- Dynamic optimization-based approaches: These approaches reduce the limitations of the previous mentioned methodology using nonlinear dynamic models and coupling this to the solution of a dynamic optimization problem. Strategies for reducing the larger computational load required for solving the problem are currently under study. For the optimization and to find the design and control optimal match the worst case scenario is evaluated as seed value (Luis A Ricardez-Sandoval et al., 2009).

Table 2 summarizes the main characteristics of the most relevant works related to methodologies for design-control integration having into account the kind of mathematical approach used, the main contribution of each work and the case study addressed (Sharifzadeh, 2013; P Vega, Lamanna, Revollar, & Francisco, 2014).

**Table 2 Recent Works on the Design- Control integration topic**

PAPER	DESIGN AND CONTROL INTEGRATION APPROACH	CONTRIBUTION	CASE STUDY
(2003) Parametric Controllers in Simultaneous Process and Control Design (Sakizlis, Perkins, & Pistikopoulos)	Incorporation of model-based parametric controllers into a simultaneous process and control design framework, using parametric programming and solving by MIDO.	Improvement in economic performance and guaranteed operability.	Binary distillation column
(2004) Recent advances in optimization-based simultaneous process and control design (Sakizlis, Perkins, & Pistikopoulos)	Simultaneous process and control design methodology based in MIDO algorithms, and advanced model-based predictive controllers.	A decomposition framework and incorporation of advanced optimizing controllers is presented. It solves the process and control design problem under uncertainty.	Simple binary distillation
(2005) A Robust and Efficient Mixed-Integer Non-Linear Dynamic Optimization Approach for Simultaneous Design And Control (Flores-Tlacuahuac & Biegler)	Discretization of the manipulated and controlled variables of the MIDO problem into a mixed-integer nonlinear programming (MINLP)	Efficient addressing in a systematic way the solution for simultaneous design a control problem	A system of two connected continuous stirred tank reactors, where a first order reaction takes place.
(2005) Metodología para la integración diseño - control en el espacio de estados (Ochoa, 2005)	Based on modern control theory, it evaluates the controllability in the state space, and uses phenomenological based models and, nonlinear constrained optimization	It defines the local practical controllability concept and it develops metrics to evaluate it.	A CSTR reactor and a Vaporizer.
(2006) Simultaneous process and control system design for grade transition in styrene polymerization (Asteasuain, Bandoni, Sarmoria, & Brandolin, 2006)	Multi objective optimization as a MIDO problem decomposed into a master problem and dynamic optimization problem.	It allows simultaneous selection of the polymerization equipment, the multivariable feedforward–feedback controller’s structure and tuning parameters.	Styrene polymerization in a CSTR.
(2007) Simultaneous mixed-integer dynamic	MIDO problem solved by transformation into MINLP with discretization using simultaneous	Better disturbance rejection and stabilization of control and profile variables.	Two CSTR in sequence with a single control loop

optimization for integrated design and control (Flores-Tlacuahuac & Biegler)	dynamic optimization approach, and development of three MINLP formulation (nonconvex, Big-M and Generalized disjunctive programming).		
(2008) Simultaneous design and control of processes under uncertainty: A robust modeling approach (Ricardez Sandoval, Budman, & Douglas)	Described as a linear state-space model complemented with uncertain model parameters the nonlinear behavior of the integrated design, optimization problem was solved in using Sequential Quadratic Programming	The integration of design and control problem is reduced to a nonlinear constrained optimization problem.	Mixing tank process
(2010) A Model-Based Methodology for Simultaneous Design and Control of a Bioethanol Production Process (Alvarado-Morales et al.)	Model-based methodology and the concepts of the attainable region (AR) and driving force (DF), are used to determine the optimal design-control of the process as well as to generate feasible alternatives	The implementation of the AR concept provides an optimal design with better dynamic performance	Bioethanol production process
(2011) A methodology for the simultaneous design and control of large-scale systems under process parameter uncertainty (Luis A Ricardez-Sandoval, Douglas, & Budman)	Structured Singular Value (SSV) analysis is proposed for the determination of the worst-case variability. The problem is formulated as a nonlinear constrained optimization problem.	Applied to a large-scale system	Tennessee Eastman process
(2012) Metodología de Diseño Simultáneo de Proceso y Control aplicada a un secado por atomización multiproducto para sustancias químicas naturales (Peña & Yurani)	Phenomenological Based Semiphysical Model (PBSM) is obtained and by Lie algebra the control matrix and parameter design are calculated simultaneously.	State space-based methodology. Results are applicable in a large region of state space.	Multiproduct spray dryer equipment for powder natural dyes production
(2012) Optimal design and control of dynamic systems under uncertainty: A	A distribution analysis on the worst-case variability is performed and the results were used for evaluating the process constraints, the	The methodology is computationally efficient, and it is a practical tool. Includes uncertainties analysis	Continuous stirred tank reactor

probabilistic approach (Luis A. Ricardez-Sandoval)	system's dynamic performance and the process economics			
(2014) An MPC-based control structure selection approach for simultaneous process and control design (Gutierrez, Ricardez-Sandoval, Budman, & Prada)	The cost function analyzed includes the worst-case closed-loop variability. Optimization is solved by NLP or MINLP formulations.	It considers both centralized and decentralized control schemes.	Wastewater industrial plant.	treatment
(2013) Integration of process design and control: A review (Sharifzadeh)	Integrated design and control methods: evolution, advantages, and disadvantages.	It suggests topics for future investigation.	--	
(2014) Simultaneous design and MPC-based control for dynamic systems under uncertainty: A stochastic approach (Bahakim & Ricardez-Sandoval)	A stochastic-based worst-case variability index is proposed for determining the dynamic feasibility under uncertainty and a multivariable model predictive control (MPC) is used for the control scheme.	It can maintain dynamic feasibility when the system is subject to single and multiple disturbances	Wastewater industrial plant	treatment
(2014) Integrated design and control of chemical processes – Part I: Revision and classification (P Vega et al.)	It presents a comprehensive classification of design and control integrated methods, integrated optimization methods, and mathematical algorithms for solving the problem.	It suggests topics for future investigation.	--	
(2016) Simultaneous design and control under uncertainty: A back-off approach using power series expansions (Rafiei-Shishavan, Mehta, & Ricardez-Sandoval, 2017)	It is proposed a new approach to simultaneous design and control of dynamic systems under uncertainty using Power Series Expansion (PSE) functions at lower computational costs.	It allowed to find operating conditions dynamically feasible, back-off of the steady-state approach.	Isothermal storage tank and wastewater treatment plant	
(2016) Integrated design and control of semicontinuous distillation systems utilizing	It was optimized both the structural and control tuning parameters by mean of integrated design and control applying using a mixed-integer	It shows the advantages and disadvantages of mixed-integer dynamic optimization	Semicontinuous distillation system for a ternary mixture	

<p>mixed-integer dynamic optimization (Meidanshahi &amp; Adams II, 2016)</p>	<p>dynamic optimization (MIDO) problem formulation for a semicontinuous distillation processes</p>	<p>(MIDO) front to particle swarm optimization (PSO) method</p>	
<p>(2017) Probabilistic uncertainty based simultaneous process design and control with iterative expected improvement model (Chan &amp; Chen, 2017)</p>	<p>The function cost is represented by a Gaussian Process (GP) model trained that depict the uncertainty in the input, and the expected improvement searches in simultaneous design and control the most probable operating condition.</p>	<p>For avoid the redundant data in the model was defined the representative data using the expected improvement optimization</p>	<p>Mixing tank</p>
<p>(2018) Integrated operation design and control of Organic Rankine Cycle systems with disturbances</p>	<p>Considering the fluctuations that occur in the Organic Rankine Cycle (ORC) the design of operating conditions is integrated with the closed-loop dynamic performance analysis based on the mechanistic nonlinear model</p>	<p>Safe process under disturbances is ensured while the waste heat recovery is increased</p>	<p>Organic Rankine Cycle (ORC)</p>
<p>(2019) Integrated design and control of full sorption chiller systems (Gibelhaus, Tangkrachang, Bau, Seiler, &amp; Bardow, 2019)</p>	<p>Integrated optimization of design and control with the total cost or electrical efficiency like objective function in the sorption chillers was developed.</p>	<p>Include the consumption of the chiller auxiliary equipments, that allows the optimization of the electrical demand</p>	<p>Solar-thermally-driven adsorption chiller system</p>

## 2. THEORETICAL FRAMEWORK

Ethyl lactate is a green solvent that is produced mainly by the esterification of lactic acid with ethanol. However, its production costs prevent the use of this green solvent in a wider manner. Therefore, recent studies have proposed to use Reactive Distillation Column (RDC) system to produce it, to reduce the capital and operating costs of the process, allowing higher selectivity and reducing the energy consumption (Daengpradab & Rattanaphanee, 2015; Mo, Shao-Tong, Li-Jun, Zhi, & Shui-Zhong, 2011). The importance of this work lies in the fact that implementing the simultaneous design and control approach incorporating the local practical controllability concept, will provide a basis for designing and building a reactive distillation column for ethyl lactate production, meeting safety, quality and environmental requirements being controllable and feasible from an economic point of view.

### 2.1. Ethyl Lactate production in Reactive Distillation (RD) Columns

The reactive distillation (RD) process integrates reaction and separation in multifunctional equipment. RD is related to problems or processes where chemical and phase equilibrium co-exist, and the products are separated in the top or/and the bottoms simultaneously as the reaction occurs (Kiss, 2013). Then, thermodynamic and diffusional coupling in the phases and at the interface are accompanied by complex chemical reactions. The process model of an RD column consists of sub-models for mass transfer, reaction, and hydrodynamics of various complexities (Boodhoo & Harvey, 2013). Some advantages of RD are: reduction of capital operating costs, higher selectivity, reduction of energy consumption, and smaller space used in the plant. RD columns are commonly employed in etherification and esterification (Mo et al., 2011).

An RD column (*Fig. 1*) consists of a rectifying zone at the top, a stripping zone in the bottom, and, in the middle, a reactive zone. The conversion of reagents using homogeneous or heterogeneous catalysts occurs in the reactive zone. When working with homogeneous catalysis it is possible to manipulate the concentration of catalyst to influence the process and obtain the desired reaction rate. Although, the flexibility of homogeneous catalysis provides a great advantage, it requires expensive additional steps, like separation processes for catalyst recovery,

which isn't necessary when working with heterogeneous catalysts. However, when using heterogeneous catalysis, usually a special arrangement is required to fix the catalytic particles in the reactive zone, for example packed catalyst in “tea bags” over trays, or sandwiched catalyst in structured packing like Sulzer Katapak (Kiss, 2013).

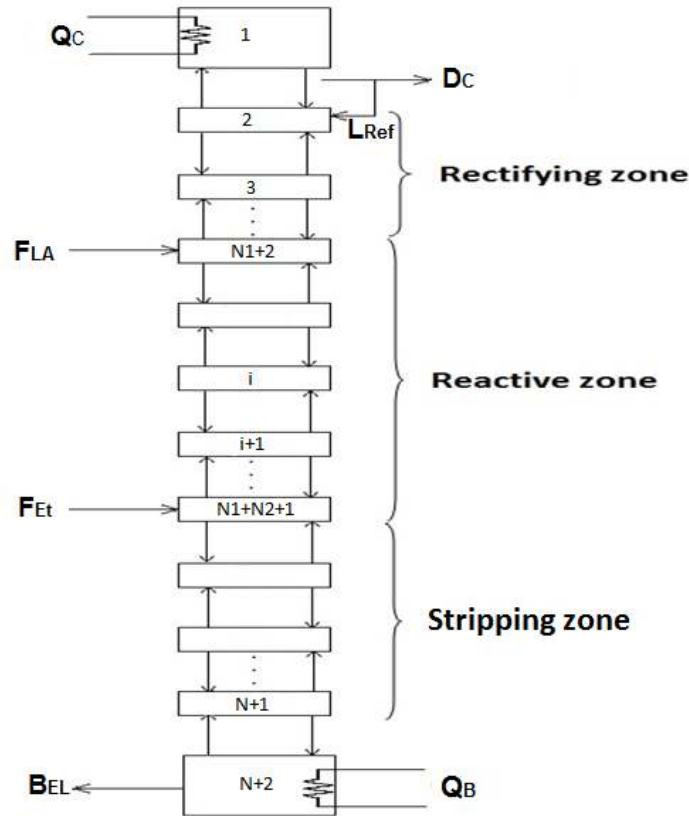


*Fig. 1 Internal distribution of a Reactive Distillation Column*

Characteristics that influence the capability of RD involves the reaction that occurs, the properties of the substances present, the concentration of the reactants, and the feed ratio, the catalysis used, the equipment configuration, among others. For this specific process, the order of relative volatilities from the most volatile to less volatile is  $\alpha_{Ethanol} > \alpha_{Water} > \alpha_{Ethyl Lactate} > \alpha_{Lactic Acid}$ , the reaction is reversible and it occurs in the liquid phase. In order to exploit the differences of volatility between the reactants and products, and seeking to improve the reaction yield forward, the countercurrent configuration could be a good option, since it generates more turbulence than in co-current (Gao et al., 2007; W. L. Luyben & Yu, 2009). In terms of concentration of reactants, usually 95%wt Ethanol and 88%wt Lactic Acid in aqueous solution are

used. Furthermore, it has been shown that oligomers and its esters concentration can be negligible when ethanol is used in excess (C. S. Pereira et al., 2011).

The equipment is divided in three sections (the non-reactive stripping, the reactive catalytic packed and the non-reactive enriching section). Lactic acid is fed at the top, and ethanol in excess is fed at the bottom of the reactive section. The heterogeneous catalyst (some super-fine solid super-acid) is packed in the reactive section. Ethyl Lactate product is recovered at the stripping section, whereas ethanol and water are recovered at the rectifying zone (Gao et al., 2007; C. S. Pereira et al., 2011). Amberlyst 15wet is the catalyst employed, and its behavior for this reaction has been studied in (Asthana, Kolah, Vu, Lira, & Miller, 2006; Delgado, Sanz, & Beltrán, 2007b; C. S. Pereira, Pinho, Silva, & Rodrigues, 2008), where the importance of catalyst loading, reactant molar ratio and reaction temperature were investigated. Furthermore it was found that intra-particle diffusion resistance can be normally neglected when this series of resins is used (Delgado et al., 2007b).

In order to model and simulate a distillation process for obtaining the equipment's design, it is necessary to know at least, a series of physicochemical properties for multicomponent systems such as vapor pressure, acentric factor, critical properties, solubility parameters, heat capacities and liquid-vapor equilibrium data. In a similar way, that information is required for reactive distillation column design with some additional considerations and prerequisites. For modeling in RD is assumed that the outlets of vapor flow and liquid flow in each stage are in thermodynamic equilibrium; furthermore, by using reaction equilibrium equations, or introducing reaction rate expressions in the mass and energy balances, the chemical reaction is considered (Kenig & Górak, 2007). Other important variables to take into account are the liquid holdup and the amount of catalyst available by stage in the reactive zone, since they are directly related to the reaction rate.

## **2.2. Traditional Design**

During the process design there are several constraints that must be fulfilled (for example mass and energy balances). Usually, designing a process involves solving an optimization problem for minimizing the total costs (including investment and operational costs). In this optimization problem, the decision variables are usually the dimensions of the equipment whereas the



constraints are typically the mass and energy balances as well as environmental and safety constraints.

The general steps for designing a process are (Mikleš & Fikar, 2007):

- a. Definition of the design objective, the statement of problem and the design requirements.
- b. Data collection, design organizations guidelines and the national and international standards can be used as sources.
- c. Proposal of possible design solutions, it can involve modifications, substitutions or additions into an existing plant.
- d. Selection of the best design option based on an economical objective function and the fulfillment of the constraints.
- e. Proposal of the control system, process control focuses in the fulfillment of the ranges of operability wished for a process, assuring stability, disturbance attenuation, and optimal process operation, in such a way that the desired product specifications are met.

The process control is distributed in four levels that describe the importance, impact and contribution in the engineering areas. The lowest level sets a constant value for the variables to be controlled. The second level proposes the type of controller. The third level determines the control structure (pairing of controlled and manipulated variables). Finally, the top-level deals with the proposal of the control system design, to obtain a controllable plant. Therefore, just at this point it is possible to know whether a process is feasible to be operated at the desired conditions or not (M. L. Luyben & Luyben). That is why the sequential design approach presents limitations, for example, unfeasible operating points, process overdesigning or under-performance. Therefore, it is stated that the traditional process design does not guarantee robustness (Mansouri, Sales-Cruz, Huusom, Woodley, & Gani, 2015).

### **2.3. Integrated Design and Control**

The integration of Design and Control provides a structure developed for taking into account simultaneously the design issues and the dynamic behavior of the chemical processes, contrary to the traditional design paradigm, which is based on stationary assumptions, assuming an ideal behavior, and based mostly on the experience of the engineers in charge of the decision-making process. The simultaneous design–control approach considers control concepts from the beginning

of the design, allowing assuring the design of a controllable plant, by including some controllability considerations into the optimization step. Therefore, solution of the optimization problem could be more expensive and increase the time consuming but would lead to better results (M. L. Luyben & Luyben, 1997; Peña & Yurani, 2012).

The Design and control integration problem is usually solved through iterative methods, considering an economic and some controllability-related objective function, to be solved in the optimization problem. Furthermore, constraints are also included in the optimization problem (i.e. safety, quality, environmental and in some cases control-related constraints). This methodology, involves the definition of the optimization problem (decision variables, objective function, operation and controllability constraints), solution of optimization problem (optimization strategies and convergence criteria), and validations by simulations (Francisco Sutil, 2011). In some cases the simultaneous design-control problem is handled as a mixed-integer dynamic optimization (MIDO) problem, where the focus is to find the best design configuration, to select the control structure and the controller tuning parameters so that the disturbances are rejected in a short time (Flores-Tlacuahuac & Biegler, 2007). By these approaches, the operability and controllability are simultaneously considered in the process design.

In this work, the methodology presented in (Ochoa, 2005) will be used for the design-control integration of an ethyl lactate reactive distillation column, where the decision variables of the optimization problem could be: the number of stages by zone, column diameter, feed ratio and catalyst weight.

Unlike other methodologies that use input-output controllability metrics, the methodology proposed by Ochoa (2005) faces the design and control integration by using the state controllability concept, since the state variables represent the dynamic behavior of the nonlinear system. The concept of practical controllability was introduced as *"A system is locally controllable in practice in an equilibrium state  $x = x^*$  if state  $x^*$  is reachable from an initial point  $x_0$  belonging to a neighborhood of  $x^*$ , in a finite time, using a set of control actions  $u(t)$  belonging to the available space  $U$  of bounded control actions among manipulated inputs"*. Four indexes that can be used to determine whether a system is controllable (in the sense of practical controllability) were proposed.

It must be noticed that practical non-controllability formulations are stated here for dynamic systems represented by an input affine nonlinear system of differential equations as reported by Isidori (1995) (Isidori, 1995):

$$\dot{x} = f(x) + \sum_{i=1}^m g_i(x)u_i \quad (Eq. 1)$$

Where  $x$  is the state vector,  $u_i$  is the manipulated inputs or control actions vector,  $f(x)$  is a nonlinear vector-valued function associated with the natural response of the system,  $g_i(x)$  is a nonlinear a nonlinear vector-valued function of the states but linear with respect to manipulated input (input affine system). This function is associated with the forced response of the system. In the case of systems with only one input ( $m = 1$ ),  $g_i(x)$  is a forcing action vector; whereas for multiple inputs case,  $u_i$  is a vector of  $m$  inputs  $m > 1$  and  $g_i(x)$  is a  $n * m$  matrix that further on will be written as  $G(x)$ , and (Eq. 1) must be re-written. The controllability indexes proposed are four, summarized as follows:

**a. Rank of Controllability Matrix:** This formulation takes into account the physical possibility of reaching the desired state. The rank condition for being used as controllability constraint is:

$$rank(W_c) = n \quad (Eq. 2)$$

Where  $W_c$  is the controllability matrix and  $n$  the number of system states. The general expression for nonlinear controllability matrix of a single input nonlinear system affine to the input is

$$W_c = |g_1(x) \dots g_m(x) \quad ad_f g_1(x) \quad ad_f g_m(x) \dots \quad ad_f^{n-1} g_1(x) \dots \quad ad_f^{n-1} g_m(x)|_{n \times (n+m)} \quad (Eq. 3)$$

Where  $ad_f g_1(x) \quad ad_f g_m(x)$  is the Lie brackets defined as:

$$ad_f g(x) = [f, g](x) = \frac{\partial g}{\partial x} f(x) - \frac{\partial f}{\partial x} g(x) \quad (Eq. 4)$$

The terms  $ad_f^{n-1} g_1(x) \dots \quad ad_f^{n-1} g_m(x)$  are the lie brackets applied recursively (Henson & Seborg, 1997)

**b. Determinant of Matrix  $G(x)$  Associated with Forced Response:** If an input affine nonlinear dynamic system is composed by  $n$  states,  $n > 1$  and equal number of manipulated variables,

the term associated to the forced response is a matrix  $G(x)$  and not a vector  $g(x)$ . This way, the general dynamic system affine with the input described previously can be re-written as:

$$\dot{x} = f(x) + G(x)u \quad (\text{Eq. 5})$$

Where the vectors  $\dot{x}$ ,  $u$  and  $f(x)$  are given by:

$$\dot{x} = \begin{bmatrix} \dot{x}_1 \\ \dot{x}_2 \\ \vdots \\ \dot{x}_i \\ \vdots \\ \dot{x}_n \end{bmatrix}_{n \times 1} \quad u = \begin{bmatrix} u_1 \\ u_2 \\ \vdots \\ u_i \\ \vdots \\ u_n \end{bmatrix}_{n \times 1} \quad f(x) = \begin{bmatrix} f_1 \\ f_2 \\ \vdots \\ f_i \\ \vdots \\ f_n \end{bmatrix}_{n \times 1} \quad (\text{Eq. 6})$$

The matrix  $G(x)$  associated to the forced response is:

$$G(x) = \begin{bmatrix} g_{11}(x) & g_{12}(x) & \dots & g_{1j}(x) & \dots & g_{1n}(x) \\ g_{21}(x) & g_{22}(x) & \dots & g_{2j}(x) & \dots & g_{2n}(x) \\ \vdots & \vdots & \dots & \vdots & \dots & \vdots \\ g_{i1}(x) & g_{i2}(x) & \dots & g_{ij}(x) & \dots & g_{in}(x) \\ \vdots & \vdots & \dots & \vdots & \dots & \vdots \\ g_{n1}(x) & g_{n2}(x) & \dots & g_{nj}(x) & \dots & g_{nn}(x) \end{bmatrix}_{n \times n} \quad (\text{Eq. 7})$$

In the local practical controllability concept, it is stated that the desired final point to be reached, whose controllability is evaluated, is a forced equilibrium point  $x^*$  such that in absence of disturbances none of the system states changes with time ( $\dot{x} = 0$ ) when the control action applied is the forcing control action  $u^*$  given by:

$$u^* = -[G(x^*)]^{-1}f(x^*) \quad (\text{Eq. 8})$$

It was concluded that if the inverse of matrix  $G(x)$  does not exist, it would not be possible to guarantee the practical controllability of the system. Therefore, in order to assure controllability, it must be satisfied that

$$\text{Det}(G(x)) \neq 0 \quad (\text{Eq. 9})$$

**c. Forcing Control Action ( $u^*$ ) belonging to the Available Interval of Control Actions ( $U$ ):** To maintain the equilibrium point  $x^*$ , it is required that the forcing control action  $u^*$  belongs to the available interval of the control actions  $U$ , which is denoted by (Eq. 10).

$$U = \left\{ u = \begin{bmatrix} u_1 \\ u_2 \\ \vdots \\ u_i \\ \vdots \\ u_n \end{bmatrix}, \text{ such that } \begin{cases} u_{1 \min} \leq u_1 \leq u_{1 \max} \\ u_{2 \min} \leq u_2 \leq u_{2 \max} \\ \vdots \\ u_{i \min} \leq u_i \leq u_{i \max} \\ \vdots \\ u_{n \min} \leq u_n \leq u_{n \max} \end{cases} \right\} \quad (\text{Eq. 10})$$

Where  $u_{i \min}$  and  $u_{i \max}$  are respectively the minimum and maximum available values for  $i$ -th manipulated variable. If control action  $u^*$  (Eq. 8) that forces the system to remain in the equilibrium point  $x^*$  does not belong to the available interval of control actions  $U$  (Eq. 10), the system will not be controllable in this point. Therefore, for a system to be controllable in practice, it must fulfill that:

$$u^* \in U \quad (\text{Eq. 11})$$

**d. Existence of a linear reachability trajectory:** This metrics evaluates the existence of linear trajectories that allow to reach the desired equilibrium point ( $x^*$ ), when the system starts at an initial point ( $x_0$ ) located within its vicinity. It is related to the existence of at least one linear trajectory of reachability. In this metric, the set of control actions  $U_T$  that allow the state variables vector to move in a straight line from its initial state  $x_0$  towards the final desired state  $x^*$  (equilibrium point) is calculated, as

$$U_T = \left\{ u_T \mid u_T = u_0^* + \frac{G^{-1}(x_0) \cdot (x^* - x_0)}{\Delta t_T}; \Delta t_T > 0 \right\} \quad (\text{Eq. 12})$$

Therefore, it must be determined if at least any of the vectors  $u_T$  belongs to the set  $U_T$  and belongs to the available rank for the manipulated variables  $U$ . Then, the fourth constraint is:

$$u_{i \min} \leq u_{T,i} \leq u_{i \max} \quad i = 1, 2, \dots, n \quad (\text{Eq. 13})$$

Which guarantees that there is at least one vector of control actions  $u_T \in U$  and that also belongs to  $U$ .

To determine the controllability of a dynamic system, all the practical controllability formulations stated here (Eq. 2, Eq. 9, Eq. 11 and Eq. 13) must be evaluated together because they are necessary

but not sufficient conditions. If after evaluating all formulations, the system is controllable in practice, then such a system is declared as practical locally controllable in the evaluated equilibrium point.

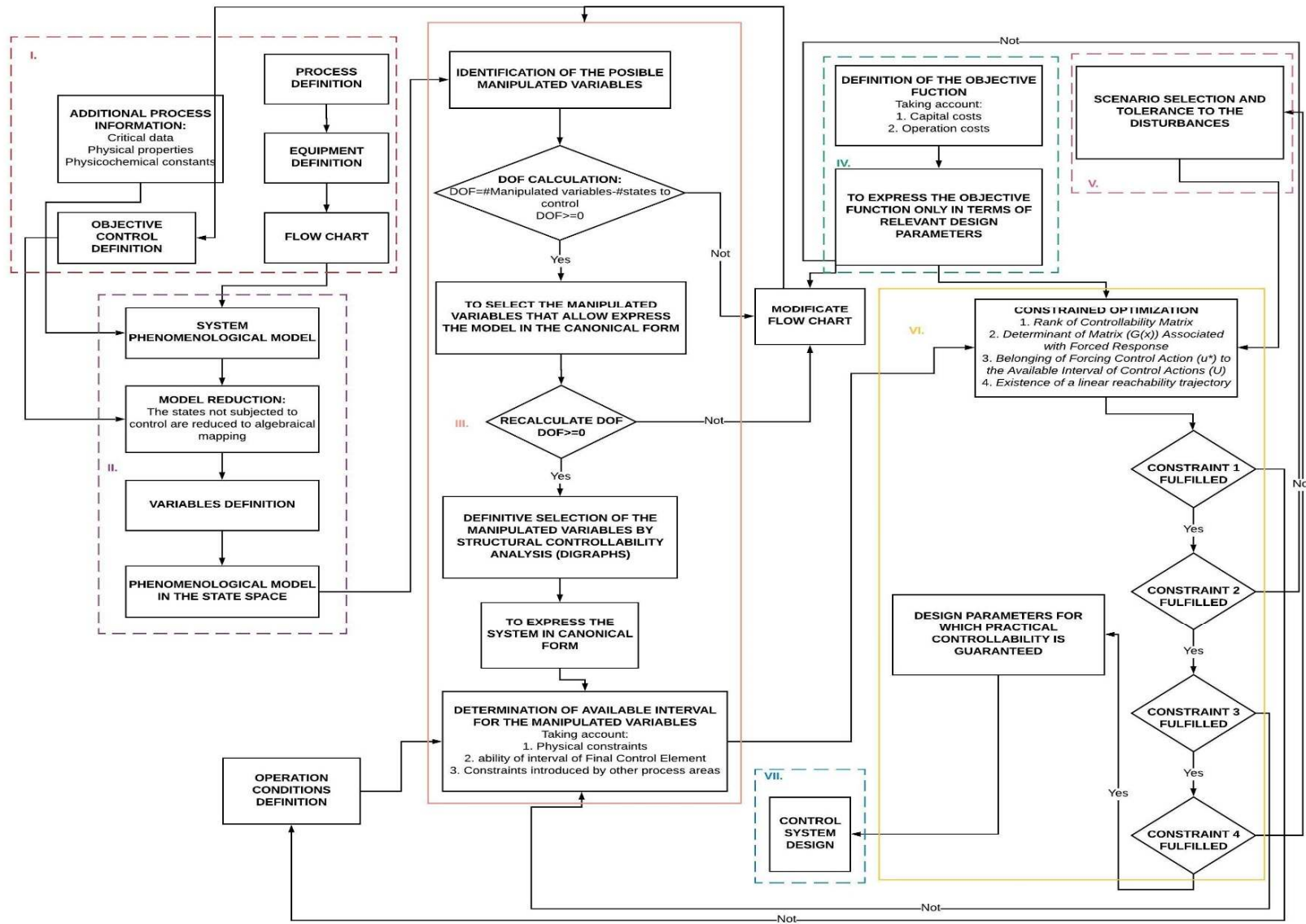


Fig. 2 Design and Control Methodology proposed by Ochoa [8]

*Fig. 2* shows the Design-Control Integration methodology proposed by Ochoa [8], which will be used as a guide for the simultaneous process and control system design of a reactive distillation column for ethyl lactate production. The core of such methodology is composed by the controllability metrics for verifying practical local controllability, which are presented as constraints within the optimization procedure. In this methodology, practical controllability is guaranteed no matter the control strategy to be used. The methodology consists of seven principal stages that go from problem definition up to control system design for the considered system. The stages of this methodology are described in the following.

### **2.3.1. Problem Definition**

Here, some important basic characteristics of the process to be designed are defined: the desired products, raw material, the production technology, equipment in which the process will take place, Process Flow Diagram (PFD), desired installed capacity, additional process data and the desired controlled variables of the system (control objectives).

### **2.3.2. Obtaining of a Phenomenological Based Semiphysical Model (PBSM)**

This stage consists on developing a model in the state space based on a Phenomenological Based Semiphysical Model (PBSM). The task begins with one or more Process Systems (PS) definition on the PFD, all in accordance with the level of detail necessary in the model for answering the design questions. Next, mass, energy and momentum (if required) balances formulation are stated for each previously defined PS. The model variables must be classified as states, inputs (disturbances and possible manipulated variables) and parameters. Furthermore, a set of constitutive equations are written, in order to complement the model.

### **2.3.3. Selection of Manipulated Variables and Determination of the Available Interval**

In this stage, the criterion of the Control Degrees of Freedom for the control (CDOF) must be reviewed. The CDOF show the number of variables that can be controlled in the process, by means of SISO loops. If the CDOF are lower than zero, this means that there were stated more control objectives (e.g. variables to be controlled) than manipulated variables. In that case, it is necessary



to include new manipulated variables. Therefore, new inputs to be used as manipulated variables must be defined. For this reason, it is necessary:

- To evaluate the input variables (not considered as disturbances in this stage) that allows expressing the model in the affine form

$$\dot{x} = f(x) + G(x)u \quad (Eq. 5)$$

The inputs that do not allow such representation will be discarded as manipulated variables since proposed controllability formulations were developed for systems that can be described by (Eq. 5). Finishing this stage, the *DOF* must be.

- If  $CDOF > 0$  (once performed the previous stage), it is necessary to use a selection criteria to choose only one set of  $n$  manipulated variables. That is because controllability formulations were developed assuming matrix  $G(x)$  as squared. Some of the most common criteria used to select the manipulated variables are: Singular Value Analysis (*SVA*), Relative Gain Array (*RGA*), Condition Number (*CN*), and sensibility analysis by using process simulators as Aspen, Chemcad, Hysys Plant, etc.

Once the set of  $n$  manipulated variables is selected (for controlling  $n$  variables), the model must be expressed as in (Eq. 5), in order to continue applying the methodology of integrated design. The available interval for manipulated variables must be determined considering physical constraints, rangeability of final control elements and all constraints resulting from current equipment interaction with other process equipment.

#### **2.3.4. Definition of the Objective Function**

The objective function must consider capital costs, written as correlations between design parameters which characterize equipment and operating costs which mostly are costs of utilities. Once the objective function is determined, it must be expressed in terms of the most relevant design parameters, with the aim of reducing the number of variables to be optimized and the computational demand for solving the problem.

### **2.3.5. Scenarios Selection**

Due to the different disturbances that can affect the process, it is necessary to define some possible scenarios ( $x_0$ ) from which it will be desirable to reach the final desired state ( $x^*$ ) and evaluate the capability to do it through lineal trajectories. For selecting the scenarios, some tolerances to disturbance must be defined.

### **2.3.6. Constrained Optimization**

In this stage, the formulation for verifying practical controllability are introduced as constraints within the optimization problem stated by the objective function selected.

### **2.3.7. Control System Design**

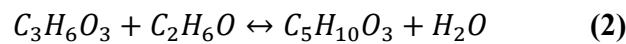
After finding the optimum design parameters, the final control system design for the process is addressed. For this, the following steps are considered: selection of the control algorithm, controller tuning, evaluation of closed loop stability, and assessment of closed loop process performance.

### 3. MODELING AND SIMULATION OF THE ETHYL LACTATE PROCESS BY REACTIVE DISTILLATION

One of the main steps in the methodology for simultaneous design-control integration that will be applied to the ethyl lactate case study is the developing of a Phenomenological Based Semiphsical Model (PBSM). In this chapter, a PBSM is developed for ethyl lactate production from lactic acid esterification with ethanol by reactive distillation. This chapter is divided in four parts. The system to be modeled is described in section 3.1. The model equations are derived in section 3.2. Model simulation results are presented in section 0. Finally, model validation using a state of the art software simulator of chemical processes is presented in section 3.4.

#### 3.1. Description of the system to be modeled

Production of Ethyl Lactate (EL) from esterification of Lactic Acid (LA) with Ethanol (Et) catalyzed by Acid Ion-Exchange Resin (Amberlyst 15wet) is carried out in a reactive distillation column, where the following reaction takes place:



The equipment is divided into three sections: rectifying, reactive and stripping zones in that order from top to the bottom, respectively. Lactic acid is fed in the upper tray of reactive zone and the Ethanol is fed in the lower tray of that zone (*Fig. 4*).

The data for the calculation of thermodynamic properties and equilibrium, kinetic model and the reaction rate, dimensions of column, and other parameters and conditions necessities for solving the problem were taken from literature (Albright, 2008; Delgado, Sanz, & Beltrán, 2007a; Gao et al., 2007; Lunelli et al., 2011; W. L. Luyben & Yu, 2009; C. S. Pereira et al., 2008; C. S. Pereira et al., 2011).

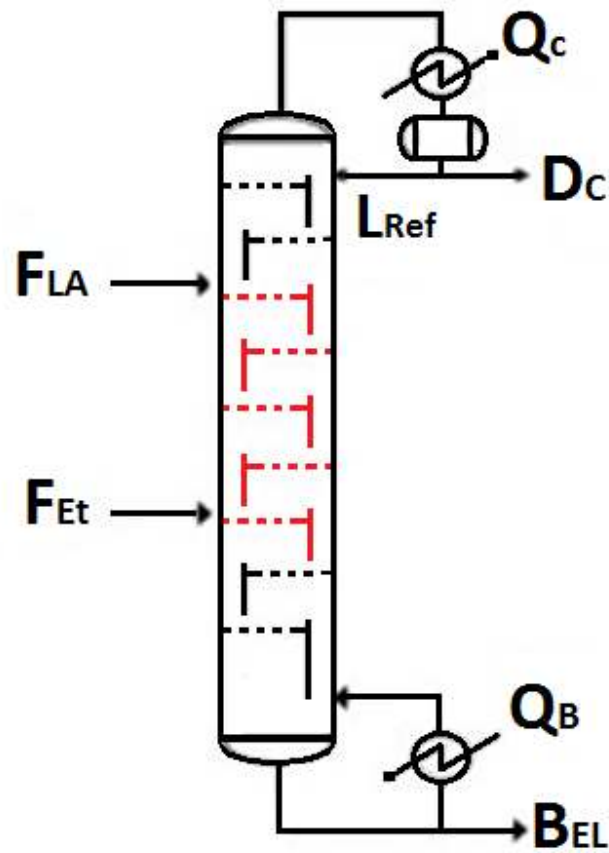


*Fig. 3 Reactive Distillation column for Ethyl Lactate production*

### 3.2. Phenomenological Based Semiphsical Model (PBSM)

The PBSM model for the reactive distillation column is developed from writing for each tray the total material balance, the material balances per component, and the energy balance. These balances are applied for the three column zones, the condenser and the reboiler.

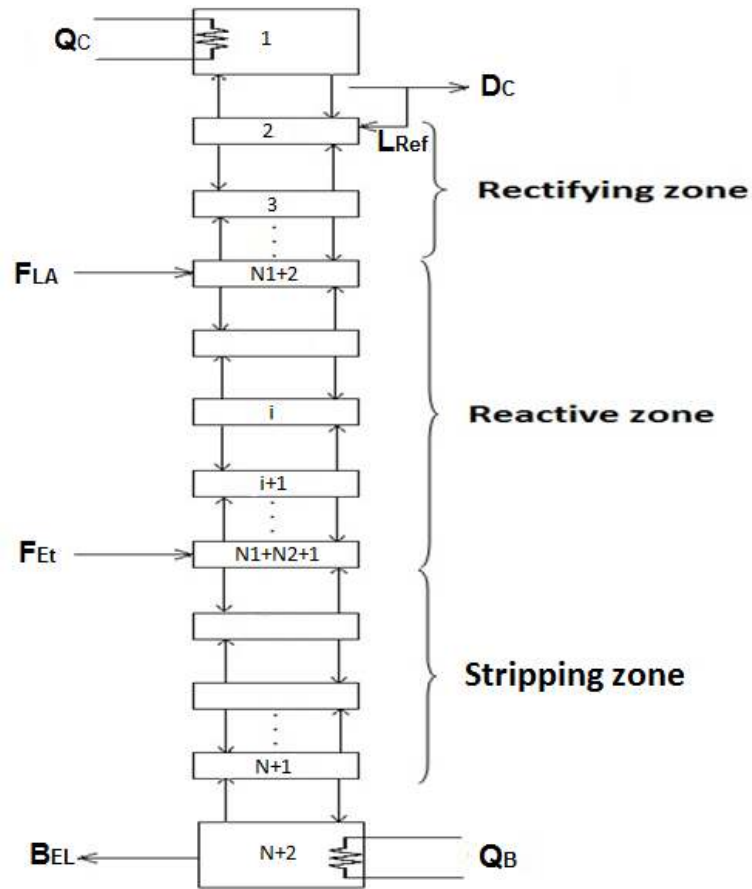


Fig. 4 Internal distribution of a Reactive Distillation Column

**a. Assumptions:**

- Fugacity coefficients of components in vapor phase are taken as the unity, due to the low pressure (atmospheric)
- Presence of oligomers is neglected (C. S. Pereira et al., 2011)
- Reboiler and condenser are modeled as trays
- Kinetic and potential energy are neglected.
- Feeds are saturated liquids
- The Langmuir-Hinshelwood model has been considered for the reaction between lactic acid and ethanol, because it takes into account the adsorption of both reactants on the surface, where the reaction takes place (Delgado et al., 2007b; C. S. Pereira et al., 2008). This kinetic model is represented in (Eq. 49) following the reaction mechanism (4) to (8).



- *Equations for general rectifying or stripping zone trays (different from the reboiler, condenser or top tray), with  $2 < i \leq N_1 + 1$  and  $N_1 + N_2 + 2 \leq i \leq N + 1$*

**Total Material balance:**

$$\frac{dZ_i}{dt} = L_{i-1} + V_{i+1} - L_i - V_i \quad (\text{Eq. 14})$$

**Molar balance per component:**

$$\frac{dx_{i,n}}{dt} = \frac{\left( x_{i-1,n}L_{i-1} + y_{i+1,n}V_{i+1} - x_{i,n}L_i - y_{i,n}V_i - x_{i,n} \frac{dZ_i}{dt} \right)}{Z_i} \quad (\text{Eq. 15})$$

**Energy balance:**

$$\frac{dT_i}{dt} = \frac{h_{i-1}L_{i-1} + H_{i+1}V_{i+1} - h_iL_i - H_iV_i - h_i \frac{dZ_i}{dt}}{Z_i * C_{pmix,i}} \quad (\text{Eq. 16})$$

- *Equations for reactive trays, with  $N_1 + 2 < i < N_1 + N_2 + 1$*

**Total Mass balance:**

$$\frac{dZ_i}{dt} = L_{i-1} + V_{i+1} - L_i - V_i \quad (\text{Eq. 17})$$

**Molar balance per component:**

$$\frac{dx_{i,n}}{dt} = \frac{\left( x_{i-1,n}L_{i-1} + y_{i+1,n}V_{i+1} - x_{i,n}L_i - y_{i,n}V_i + R_{n,i} - x_{i,n} \frac{dZ_i}{dt} \right)}{Z_i} \quad (\text{Eq. 18})$$

**Energy balance:**

$$\frac{dT_i}{dt} = \frac{h_{i-1}L_{i-1} + H_{i+1}V_{i+1} - h_iL_i - H_iV_i + Q_{r,i} - h_i \frac{dZ_i}{dt}}{Z_i * C_{pmix,i}} \quad (\text{Eq. 19})$$

- *Equations for feed trays (In reactive zone), with  $i = N_1 + 2$  and  $i = N_1 + N_2 + 1$*

**Total Mass balance:**

$$\frac{dZ_i}{dt} = L_{i-1} + V_{i+1} - L_i - V_i + F_i \quad (\text{Eq. 20})$$

**Molar balance per component:**

$$\frac{dx_{i,n}}{dt} = \frac{\left( x_{i-1,n}L_{i-1} + y_{i+1,n}V_{i+1} - x_{i,n}L_i - y_{i,n}V_i + (x_{F,n})_i q_{F,i}F_i + R_{n,i} - x_{i,n} \frac{dz_i}{dt} \right)}{Z_i} \quad (\text{Eq. 21})$$

**Energy balance:**

$$\frac{dT_i}{dt} = \frac{h_{i-1}L_{i-1} + H_{i+1}V_{i+1} - h_iL_i - H_iV_i + h_{F,i}q_{F,i}F_i + Q_{r,i} - h_i \frac{dz_i}{dt}}{Z_i * C_{pmix,i}} \quad (\text{Eq. 22})$$

- *Equations for reboiler*

**Total Mass balance:**

$$\frac{dZ_B}{dt} = L_{N+1} - B_{EL} - V_B \quad (\text{Eq. 23})$$

**Molar balance per component:**

$$\frac{dx_{B,n}}{dt} = \frac{x_{N+1,n}L_{N+1} - x_{B,n}B_{EL} - y_{B,n}V_B - x_{B,n} \frac{dz_i}{dt}}{Z_B} \quad (\text{Eq. 24})$$

**Energy balance:**

$$\frac{dT_B}{dt} = \frac{h_{N+1}L_{N+1} - h_B B_{EL} - H_B V_B + Q_B - h_B \frac{dz_B}{dt}}{Z_B * C_{pmix,B}} \quad (\text{Eq. 25})$$



- *Equations for Top tray*

**Total Mass balance:**

$$\frac{dZ_2}{dt} = L_{Ref} + V_3 - L_2 - V_2 \quad (Eq. 26)$$

**Molar balance per component:**

$$\frac{dx_{2,n}}{dt} = \frac{x_{Ref,n}L_{Ref} + y_{3,n}V_3 - x_{2,n}L_2 - y_{2,n}V_2 - x_{2,n}\frac{dZ_2}{dt}}{Z_{2,n}} \quad (Eq. 27)$$

**Energy balance:**

$$\frac{dT_2}{dt} = \frac{h_{Ref}L_{Ref} + H_3V_3 - h_2L_2 - H_2V_2 - h_2\frac{dZ_2}{dt}}{Z_2 * C_{pmix,2}} \quad (Eq. 28)$$

- *Equations for condenser*

**Total Mass balance:**

$$\frac{dZ_c}{dt} = V_2 - L_{Ref} - D_c \quad (Eq. 29)$$

**Molar balance per component:**

$$\frac{dx_{c,n}}{dt} = \frac{y_{2,n}V_2 - x_{Ref,n}L_{Ref} - x_{Ref,n}D_c - x_{c,n}\frac{dZ_c}{dt}}{Z_{c,n}} \quad (Eq. 30)$$

**Energy balance:**

$$\frac{dT_c}{dt} = \frac{H_2V_2 - Q_c - h_{Ref}L_{Ref} - h_{Ref}D_c - h_{Ref}\frac{dZ_c}{dt}}{Z_c C_{pmix,c}} \quad (Eq. 31)$$

### c. Constitutive Equations

For complementing the model, the following constitutive equations were used.

Equation	Name	Number
▪ $A_n = A_{tray} * \frac{x_n a_n}{\sum_{k=1}^{NC} x_k a_k}$	Area covered by component	(Eq. 32)
▪ $h_i = \sum x_{i,n} C_{p,n} \Delta T$	Enthalpy in the liquid phase	(Eq. 33)
▪ $H_i = h_i + \Delta H_{vap,i}$	Enthalpy in the vapor phase	(Eq. 34)
▪ $\Delta H_{rxn} = \sum \vartheta_n * H_{f,n,i}$	Enthalpy reaction	(Eq. 35)
▪ $\Delta H_{vap,i} = \sum x_{i,n} * \Delta H_{vap,n}$	Vaporization enthalpy	(Eq. 36)
▪ $k_c = k_{o,c} e^{-\frac{E_a}{RT_i}}$	Kinetic constant	(Eq. 37)
▪ $K_{eq} = \exp\left(2.9625 - \frac{515.13}{T_i}\right)$	Equilibrium constant	(Eq. 38)
▪ $K_s = k_{o,s} e^{-\frac{\Delta H_s}{RT_i}}$	Adsorption constant	(Eq. 39)
▪ $l_B = \frac{Z_B * (MW_{mix})_B}{(\rho_{mix})_B * A_w}$	Reboiler level	(Eq. 40)
▪ $l_C = \frac{Z_C * (MW_{mix})_C}{(\rho_{mix})_C * A_w}$	Condenser level	(Eq. 41)
▪ $L_i = 0.215 \frac{\rho_{mix,i}}{MW_{mix,i}} \left( \frac{Z_i * MW_{mix,i}}{\rho_{mix,i}} - v_{weir} \right)^{1.5}$	Francis-weir formula	(Eq. 42)
▪ $MW_{mix} = \sum_n x_{i,n} MW_n$	Mixture molecular weight	(Eq. 43)
▪ $P_{t_i} = P + (i - 1) * \Delta P$	Total pressure by tray	(Eq. 44)

- $P_{vap,n} = 100 * \exp\left(A - \frac{B}{T_i+C} + D * T_i + E * \ln T_i + F * T_i^G\right)$  Vapor pressure per compound (Eq. 45)
- $Q_B = UA(T_{Hot} - T_{N+2})$  Reboiler heat (Eq. 46)
- $Q_C = \Delta H_{vap-mix,2} V_2$  Condenser heat (Eq. 47)
- $Q_r = w_{cat} * r * \Delta H_{rxn}$  Reaction heat (Eq. 48)
- $r = k_c \frac{a_{Et} a_{LA} - \frac{a_{EL} a_W}{K_e}}{(1 + \sum_n K_{s,n} a_n)^2}$  Specific reaction rate (Eq. 49)
- $r_{evap,i} = 1000 * \sum_n \left( A_n * \sqrt{\frac{1}{2\pi * MW_n RT_i}} (P_{vap,n,i} - P_{t,i}) \right)$  Evaporation rate (Eq. 50)
- $R_n = \vartheta_n * w_{cat} * r$  Reaction rate (Eq. 51)
- $w_{cat} = \frac{m_{cat}}{N_2}$  Catalyst loading by tray (Eq. 52)
- $\sum x_{n,i} = 1$  Sum of fractions (Eq. 53)
- $y_{i,n} P_{t,i} = (\gamma_n x_n P_{vap})_i$  Thermodynamic equilibrium (Eq. 54)
- $\sum y_{n,i} = 1$  Sum of fractions (Eq. 55)
- $\rho_{mix,i} = \frac{1}{\sum_n \left( \frac{x_{i,n}}{\rho_{i,n}} \right)}$  Mixture density (Eq. 56)

#### d. Definition of Variables

The variables and subscripts used for the integrated design and control, model simulation and validation, and traditional design are described in Table 3 and Table 4, respectively.

Table 3 Classification of variables

Variable	Description	Dimension	Variable kind
$A, B, C$	Antoine equation coefficients	--	--
$a_{ij}, a_{ji}$	UNIQUAC binary interaction parameters	--	--
$a_n$	Activity of the component	--	--
$A_k$	Area	$m^2$	Design parameter
$B_{EL}$	Flow of bottoms	$kmol/sec$	Possible manipulated variable or disturbance
$b_{ij}, b_{ji}$	UNIQUAC binary interaction parameters	--	--
$C_{operation}$	Operations Cost	\$COP	
$C_p$	Heat capacity of the liquid	$\frac{kJ}{kmol * K}$	System parameter
$C_{Total}$	Total Cost	\$COP	--
$d$	Step size	--	--
$Diam$	Column diameter	$m$	Design parameter
$D_C$	Flow of Distillate	$kmol/sec$	possible manipulated variable or disturbance
$\Delta H_S$	Adsorption Enthalpy	$kJ/kmol$	System parameter
$E$	Cost per unity of substance or energy	$\frac{\$COP}{Unity}$	--
$E_{ae}$	Reaction activation energy	$kJ/kmol$	System parameter
$F$	Feed stream	$kmol/sec$	Controlled by $F_{LA}$ ratio
$\gamma$	Activity coefficient	--	System parameter
$h$	Liquid phase enthalpy	$kJ/kmol$	System parameter
$H$	Vapor phase enthalpy	$kJ/kmol$	System parameter
$H_{f,n}$	Enthalpy of formation of component	$kJ/kmol$	System parameter
$H_{vap}$	Heat vaporization	$kJ/kmol$	System parameter
$H_T$	Column Height	$m$	Design parameter
$H_w$	weir Height	$m$	Design parameter
$k_c$	kinetic constant	$\frac{kmol}{kg * sec}$	System parameter
$k_{0,c}$	Pre-exponential Arrhenious factor	$\frac{kmol}{kg * sec}$	System parameter
$K_{eq}$	Thermodynamic equilibrium constant	--	System parameter
$K_{os}$	Pre-exponential for $K_s$	--	System parameter
$K_S$	Adsorption equilibrium constant	--	System parameter
$L$	Liquid flow rate	$kmol/sec$	State
$l_B$	Reboiler Level	$m$	State

$l_c$	Colector Level	$m$	State
$m_{cat}$	Total catalyst loading	$kg$	Design parameter
$MW$	Molecular weight	$kg/kmol$	System parameter
$N$	Total number of trays	--	Design parameter
$N_1$	Number of trays in rectifying zone	--	Design parameter
$N_2$	Number of trays in reactive zone	--	Design parameter
$NC$	Number of components	--	Model input
$P$	Pressure of column	$kPa$	State
$P_c$	Critical pressure	$kPa$	System parameter
$P_t$	Total pressure	$kPa$	--
$P_{vap}$	Vapor pressure per compound	$kPa$	System parameter
$Q$	Heat duty	$kJ/sec$	possible manipulated variable or disturbance
$q$	liquid fraction	--	Disturbance
$r$	Specific reaction rate	$\frac{kmol}{kg_{cat} * sec}$	System parameter
$R$	Gas constant	$\frac{kJ}{kmol * K}$	Constant
$Rat$	Feed molar ratio	$\frac{F_{Et}}{F_{LA}}$	Design parameter
$reb$	Boil up ratio	--	Design parameter
$ref$	Reflux ratio	--	Design parameter
$r_{evap}$	Evaporation rate	$kmol/sec$	State
$R_n$	Reaction rate	$kmol/sec$	--
$\rho$	Density	$kg/m^3$	System parameter
$T_i$	Temperature in the tray i (Rectifying, reactive and stripping zone)	$K$	State
$T_b$	Normal boiling temperature	$K$	System parameter
$T_c$	Critical temperature	$K$	System parameter
$t$	Time	$sec$	Design parameter
$V$	Vapor flow rate	$kmol/sec$	State
$V_k$	Volume	$m^3$	Design parameter
$\omega$	Acentric factor	[–]	System parameter
$w_{cat}$	Catalyst loading by tray	$kg$	System parameter
$x$	Liquid molar fraction in the present time	[–]	State
$y$	Vapor molar fraction in the present time	[–]	--
$Z$	Molar liquid holdup in the tray i	$kmol$	State
%w	Mass percent	[–]	--
%A <sub>a</sub>	Percentage active area	[–]	--

**Table 4 Description of subscripts**

<b>Subscript</b>	<b>Meaning</b>
<i>bt</i>	Between trays
<i>B</i>	Reboiler
<i>C</i>	Condenser
<i>Cold</i>	Cold fluid
<i>EL</i>	Ethyl Lactate
<i>Et</i>	Ethanol
<i>F</i>	Feed
<i>Hot</i>	Hot fluid
<i>L</i>	Liquid phase
<i>LA</i>	Lactic Acid
<i>mix</i>	Mixture
<i>n</i>	Component
<i>r</i>	Reaction
<i>Ref</i>	Reflux
<i>rf</i>	Rectifying zone
<i>rxn</i>	Reaction zone
<i>serv</i>	Service fluid
<i>st</i>	Stripping zone
<i>v</i>	Vapor phase
<i>w</i>	Weir
<i>W</i>	Water

For summarizing, the model is a DAE system that includes ordinary differential equations (see *Eq. 14 – 31*) and algebraic equations (see *Eq. 32 – 56*). The total number of equations will depend on the actual number of trays. As it will be seen in section 4, the total number of trays is  $N + 2$ , which means that such number of trays is not fixed, but it is a result of the optimization carried out during the process design.

### **3.3. Model Simulation**

The complete model was simulated using an explicit numerical method for the solution in MATLAB, specifically for representing the dynamic behavior of a reactive distillation column for Ethyl Lactate production using Lactic Acid esterification with Ethanol. Data required for running the simulation (properties of pure substances, system parameters and some required initial data) are shown in sub-section 3.3.1. These data were taken from the literature and from the Aspen database. In order to validate the model built from the mass and energy balances shown in section

3.2 a three-step strategy was followed. First, dynamic simulation of a distillation column (without reaction) was run (see sub-section 3.3.2). Second, the reactive zone was “coupled” to the simple distillation model (see sub-section 3.3.3). Third, in the next section 3.4, validation was carried out by comparing the simple distillation column model and the complete reactive distillation model against results obtained when using the corresponding Aspen model.

### **3.3.1. Data required for Simulation**

Table 5 shows the feed conditions, kinetic and design parameters used for the simulation. These data were taken from literature. Kinetic studies for lactic acid esterification over a catalyst Amberlyst 15wet are available in the literature. Asthana et al (2006) proposed a kinetic power law due to the uncertainty in the liquid-phase environment within the Amberlyst 15 cation-exchange resin (Asthana et al., 2006). On the other hand, Delgado et al (2007) and Pereira et al (2008) proposed a Langmuir Hinshelwood mechanism for describing the kinetics, because the reaction occurs on the catalyst surface, and this mechanism considers the adsorption over surface (Delgado et al., 2007b; C. S. Pereira et al., 2008). However, in the work by Pereira et al (2008) only stronger adsorption (Water and Ethanol) is taken into account (C. S. Pereira et al., 2008). Therefore, in this work we used the consideration and data proposed by Pereira et al (2008).

In order to define the purity and feed molar ratio (between the ethanol and lactic acid) some works (Asthana et al., 2006; Figueroa et al., 2015; C. S. Pereira et al., 2011; C. S. M. Pereira, 2009) have reported the presence of oligomers at high lactic acid concentrations. Furthermore, it has been observed an inversely proportional relation with the feed molar ratio, also, it has been reported (C. S. Pereira et al., 2011) that for ethanol/lactic acid feeding ratios slightly larger than 1, oligomers are practically absent. Finally, it has been reported that feeding temperatures close to 75°C are more suitable, because this is near to the theoretical temperature for the esterification reaction, which is around 90 °C - 110°C (Gao et al., 2007; Kiss, 2013). For the purpose of simulating the model, the column dimensions were taken from a similar reactive distillation process to ensure that the initial data belong to an equipment with suitable results (W. L. Luyben & Yu, 2009). Additionally, some practical recommendations were applied to calculate the active area (Albright, 2008).

Table 6 summarizes the properties of pure components used in the dynamic simulation of the proposed model; furthermore, this table includes the UNIQUAC binary interaction and Van der Waals parameters for vapor-liquid equilibrium in the quaternary system Water-Ethanol-Ethyl Lactate-Lactic Acid.

**Table 5 Kinetic parameters, design parameters and feed conditions**

<b>Kinetic parameter for Langmuir Hinshelwood Mechanism(C. S. Pereira et al., 2008)</b>					
$k_{0,c}$	$E_{ae}$	$K_{os,W}$	$\Delta H_{S,W}$	$K_{os,Et}$	$\Delta H_{S,Et}$
450000	49980	15.19	-99.85	1.22	-2995
<b>Feed and initial conditions (Gao et al., 2007; W. L. Luyben &amp; Yu, 2009; C. S. Pereira et al., 2008)</b>					
$\%W_{LA}$	$\%W_{Et}$	$F_{LA} \left[ \frac{kmol}{sec} \right]$	$Rat \left( \frac{F_{Et}}{F_{LA}} \right)$	$T_F [K]$	$\%m_{cat}$
88	95	0.0134	4	348.15	6
<b>Design parameter (Albright, 2008; Lunelli et al., 2011; W. L. Luyben &amp; Yu, 2009)</b>					
$Diam [m]$	$\%A_a$	$H_w [m]$	$N$ (total number of trays)	$N_1$ (Number of trays in rectifying zone)	$N_2$ (Number of trays in reactive zone)
1.78	88.18	0.1016	27	2	18

**Table 6 Properties of pure substances and system parameter**

	<b>Water</b>	<b>Ethanol</b>	<b>Ethyl Lactate</b>	<b>Lactic Acid</b>
<b>Basic properties(C. S. Pereira et al., 2011)</b>				
$MW \left[ \frac{kg}{kmol} \right]$	18.0150	46.0690	118.1330	90.0790
$\rho_L \left[ \frac{kg}{m^3} \right]$	1027	789	1031	1209
$\rho_V \left[ \frac{kg}{m^3} \right]$	0.7354	1.8805	4.8222	3.677
$C_p \left[ \frac{kJ}{kmol * K} \right]$	74.2	121	202	308
$T_b [K]$	373.15	351.44	427.65	490
$P_c [kPa]$	22064	6137	3740.1	5960
$v_c [m^3]$	0.055947	0.168	0.354	0.251
$T_c [K]$	647.13	516.25	588	616

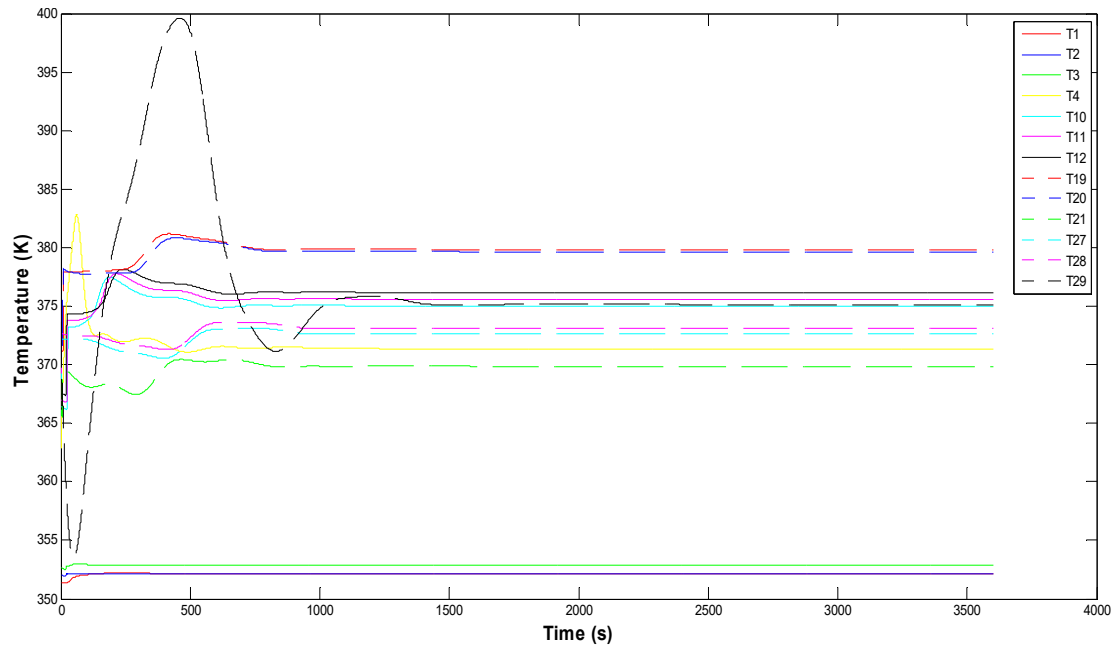


$\omega$	0.34486	0.64356	0.60323	1
$H_{vap} \left[ \frac{kJ}{kmol} \right]$	40693.6	39185.1	43316.63	62400.07
$H_f \left[ \frac{kJ}{kmol} \right]$ (C. S. Pereira et al., 2008)	-241814	-234950	-695084	-682960
<b>Antoine equation coefficients</b>				
<i>A</i>	62	62	61	214
<i>B</i>	-7258.2	-7122.3	-8249.7	-18757
<i>C</i>	0	0	0	0
<i>D</i>	0	0	0	0
<i>E</i>	-7	-7	-7	-29
<i>F</i>	4.17E-06	2.89E-06	7.55E-18	1.30E-05
<i>G</i>	2	2	6	2
<b>Van der Waals parameters (Delgado et al., 2007a)</b>				
$r_n$	0.9200	2.1055	4.4555	3.1648
$q_n$	1.4000	1.9720	3.9280	2.8800
<b>UNIQUAC binary interaction parameters(Delgado et al., 2007a)</b>				
<b><math>a_{ij}</math></b>				
<i>W</i>	0	-765.95	64.53	-39.61
<i>Et</i>	728.97	0	-148.67	191.28
<i>EL</i>	99.80	341.77	0	52.64
<i>LA</i>	155.18	-43.32	125.29	0
<b><math>b_{ij}</math></b>				
<i>W</i>	0	2.4936	0	0
<i>Et</i>	-2.0046	0	0	0
<i>EL</i>	0	0	0	0
<i>LA</i>	0	0	0	0

### 3.3.2. Dynamic simulation of the distillation column

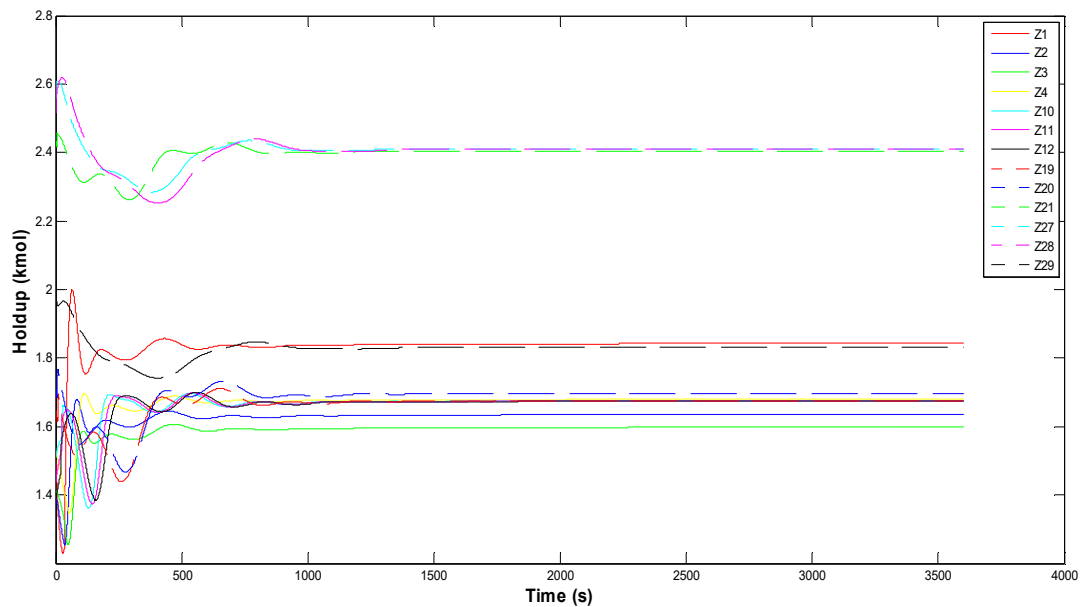
The PBSM model described in section 3.2 was simulated but deleting the terms corresponding to the reaction. The purpose of this was to run the model but for a distillation column without reaction. Results obtained from doing so were compared against Aspen results, to validate the proposed model. Unfortunately, there was not a way to compare directly the results of the model for the reactive distillation column against Aspen. However, it is considered that validation of a “simple” (no reactive) distillation column was required for validating the model of the complete reactive distillation column.

Fig. 6 to Fig. 9 show the dynamic behavior of important state variables (Temperature, Holdup, Ethanol and Lactic Acid mole fractions), at some trays in the column.



**Fig. 6 Dynamic behavior of the Temperature at some stages in the distillation column**

**T1: Condenser, T2: Top tray, T4: Feed LA tray, T21: Feed Et tray, T29: Reboiler, T2, T3, T10, T11, T12, T19, T20, T27, and T28: Internal trays**



**Fig. 7 Dynamic behavior of the Holdup at some stages in the distillation column**

**Z1: Condenser, Z2: Top tray, Z4: Feed LA tray, Z21: Feed Et tray, Z29: Reboiler, Z2, Z3, Z10, Z11, Z12, Z19, Z20, Z27, and Z28: Internal trays**

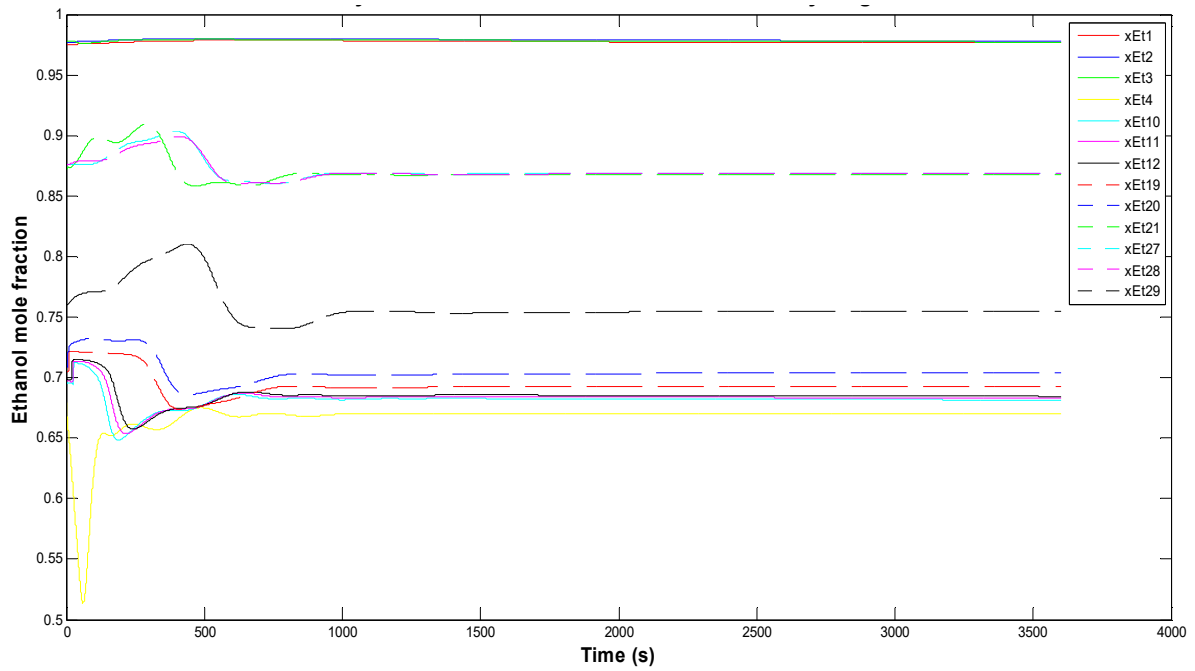


**Fig. 8 Dynamic behavior of the Ethanol mole fraction at some stages in the distillation column.**

*xEt1: Condenser, xEt2: Top tray, xEt4: Feed LA tray, xEt21: Feed Et tray, xEt29: Reboiler, xEt2, xEt3, xEt10, xEt11, xEt12, xEt19, xEt20, xEt27, and xEt28: Internal trays*

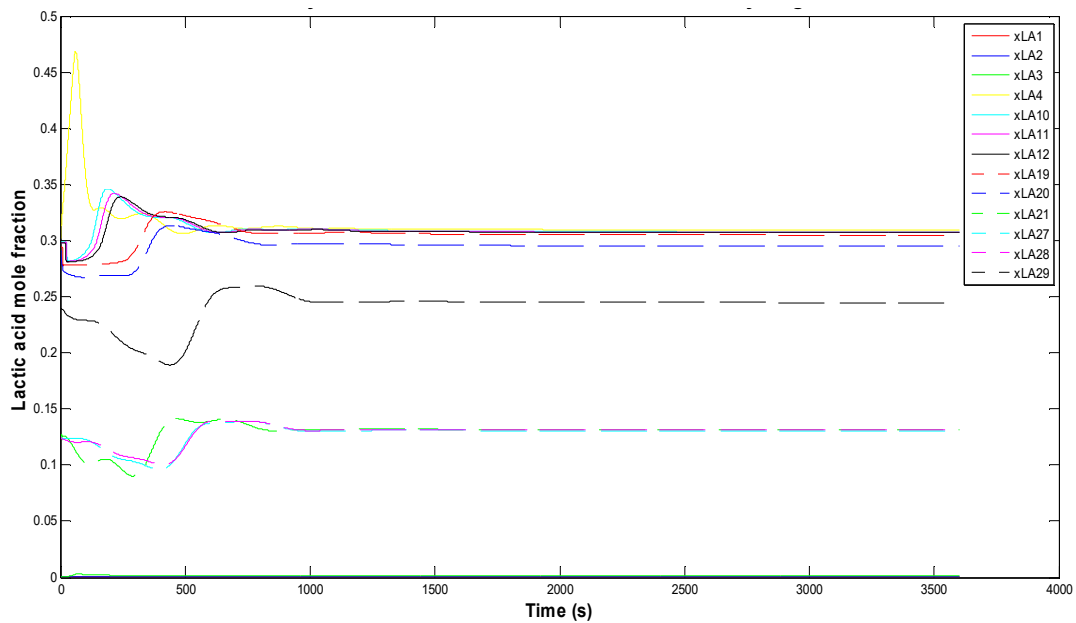


**Fig. 9 Dynamic behavior of the Lactic Acid mole fraction at some stages in the distillation column.**

*xLA1: Condenser, xLA2: Top tray, xLA4: Feed LA tray, xLA21: Feed Et tray, xLA29: Reboiler, xLA2, xLA3, xLA10, xLA11, xLA12, xLA19, xLA20, xLA27, and xLA28: Internal trays*

The model simulation was carried out starting at an initial condition defined by a vector of 145 components. There are 29 trays, at each tray we have the initial condition for the temperature (29 values) and the mass of liquid (29 values). Furthermore, at each tray the mole fraction of Ethanol, Lactic acid and Ethyl Lactate in the liquid phase are required (87 values). The initial conditions vector is available at the APPENDIX. Data to define such initial condition were obtained from (Albright, 2008; Gao et al., 2007; Lunelli et al., 2011; W. L. Luyben & Yu, 2009; C. S. Pereira et al., 2008). The simulation results shown that from the starting point, by using the developed model, it was possible to reach a steady state.

### 3.3.3. Dynamic simulation of a reactive distillation column

In this sub-section, simulation results for the reactive distillation column are presented. At the initial condition, it was assumed that the column was filled with Ethanol. *Fig. 10* to *Fig. 14* show the dynamic behavior of the main state variables and the steady state reached. Simulation was run for three hours.

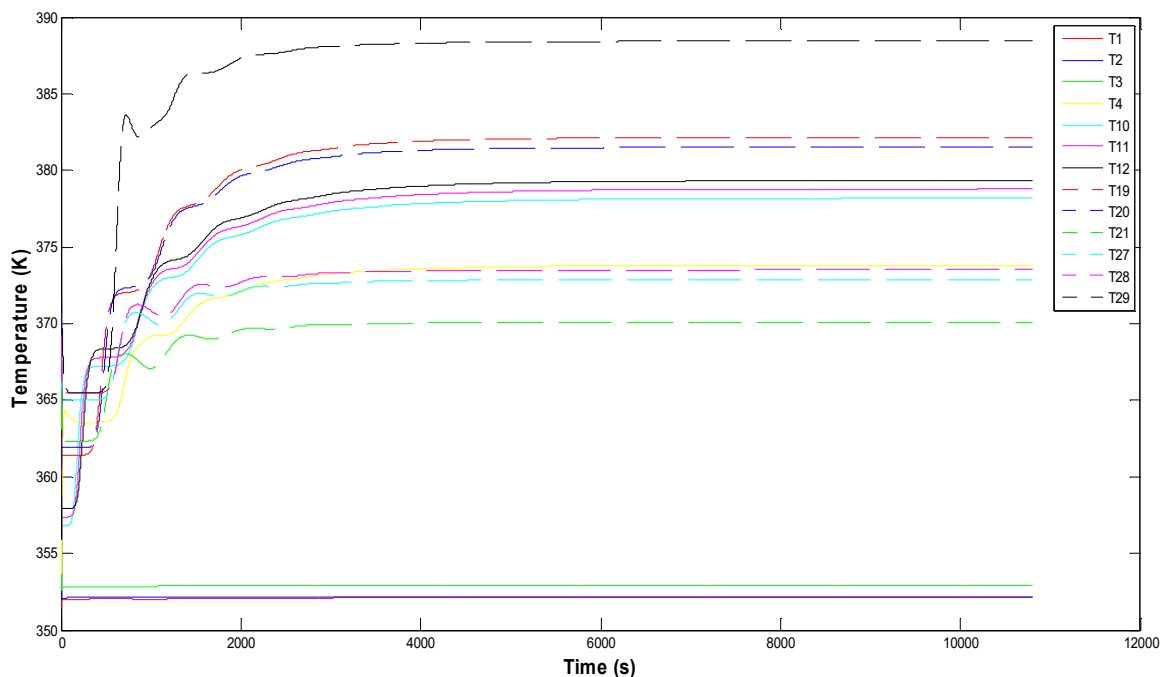


*Fig. 10 Dynamic behavior of the Temperature at some stages in reactive distillation column*

*T1: Condenser, T2: Top tray, T4: Feed LA tray, T21: Feed Et tray, T29: Reboiler, T2, T3, T10, T11, T12, T19, T20, T27, and T28: Internal trays*

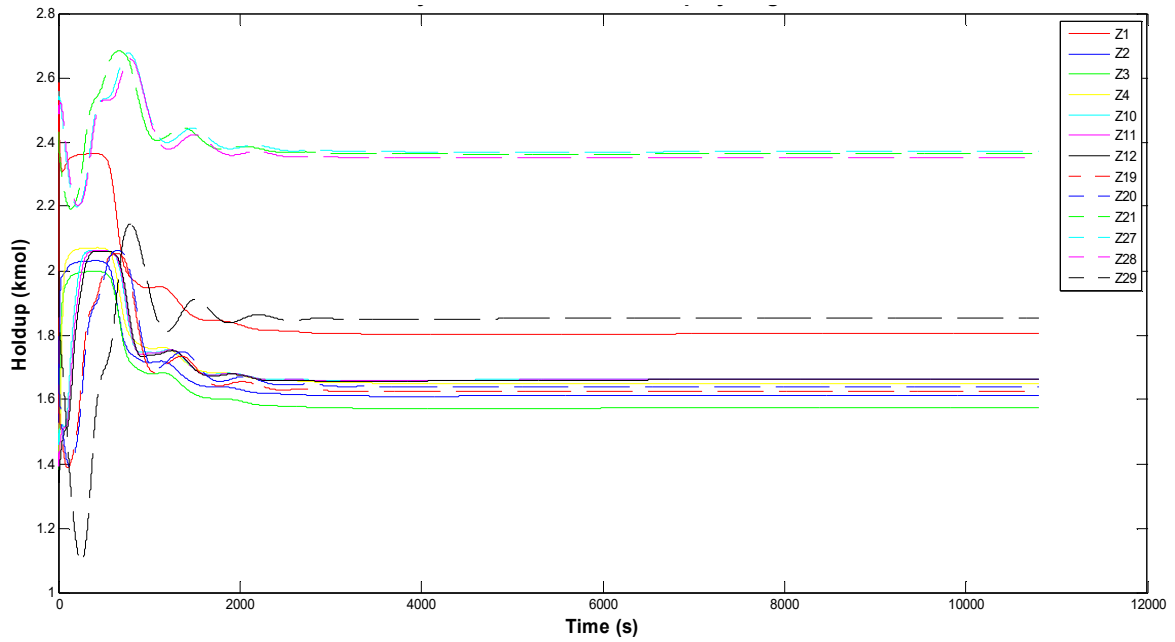


**Fig. 11** Dynamic behavior of the Holdup at some stages in reactive distillation column

Z1: Condenser, Z2: Top tray, Z4: Feed LA tray, Z21: Feed Et tray, Z29: Reboiler, Z2, Z3, Z10, Z11, Z12, Z19, Z20, Z27, and Z28: Internal trays

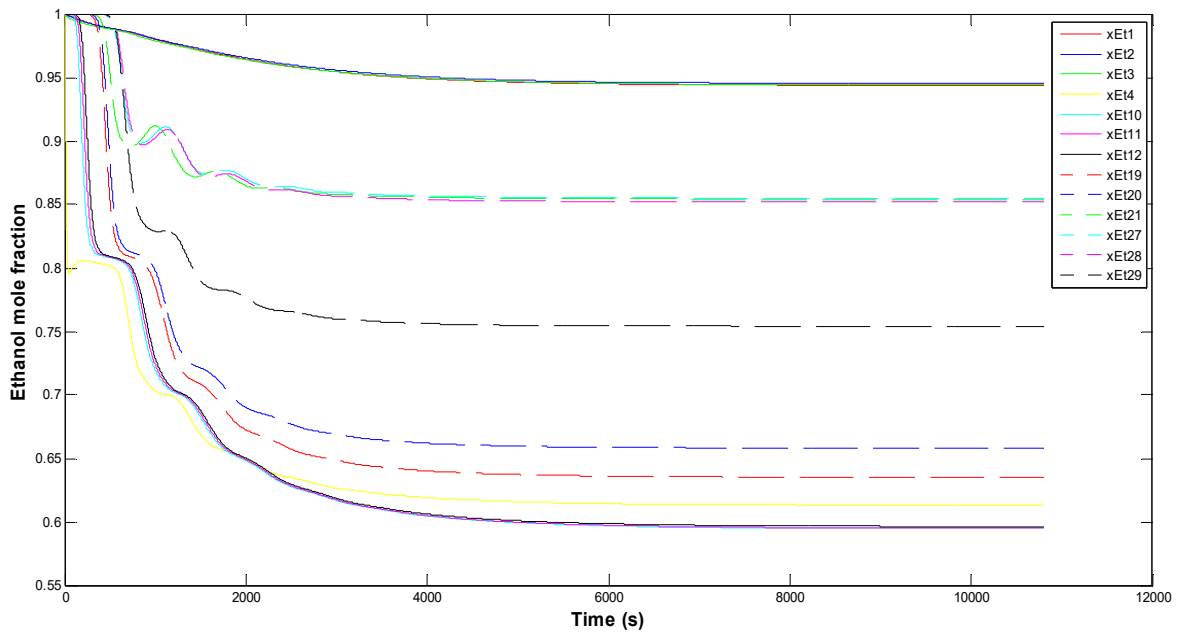


**Fig. 12** Dynamic behavior of the Ethanol mole fraction at some stages in reactive distillation column

xEt1: Condenser, xEt2: Top tray, xEt4: Feed LA tray, xEt21: Feed Et tray, xEt29: Reboiler, xEt2, xEt3, xEt10, xEt11, xEt12, xEt19, xEt20, xEt27, and xEt28: Internal trays

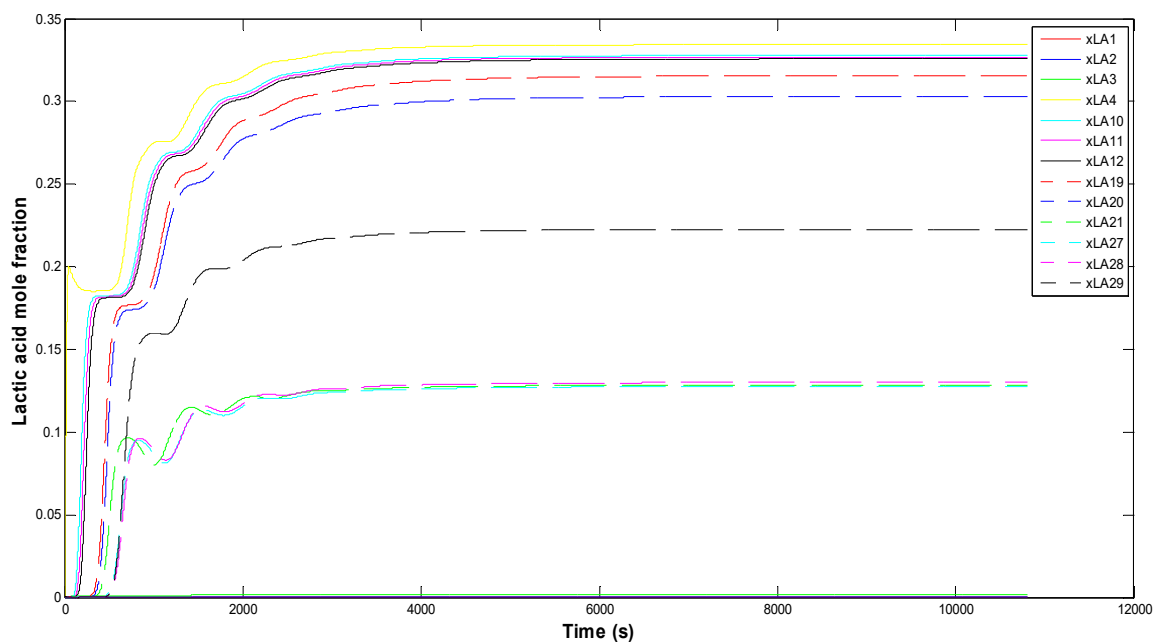


**Fig. 13 Dynamic behavior of the Lactic Acid mole fraction at some stages in reactive distillation column**  
*xLA1: Condenser, xLA2: Top tray, xLA4: Feed LA tray, xLA21: Feed Et tray, xLA29: Reboiler, xLA2, xLA3, xLA10, xLA11, xLA12, xLA19, xLA20, xLA27, and xLA28: Internal trays*

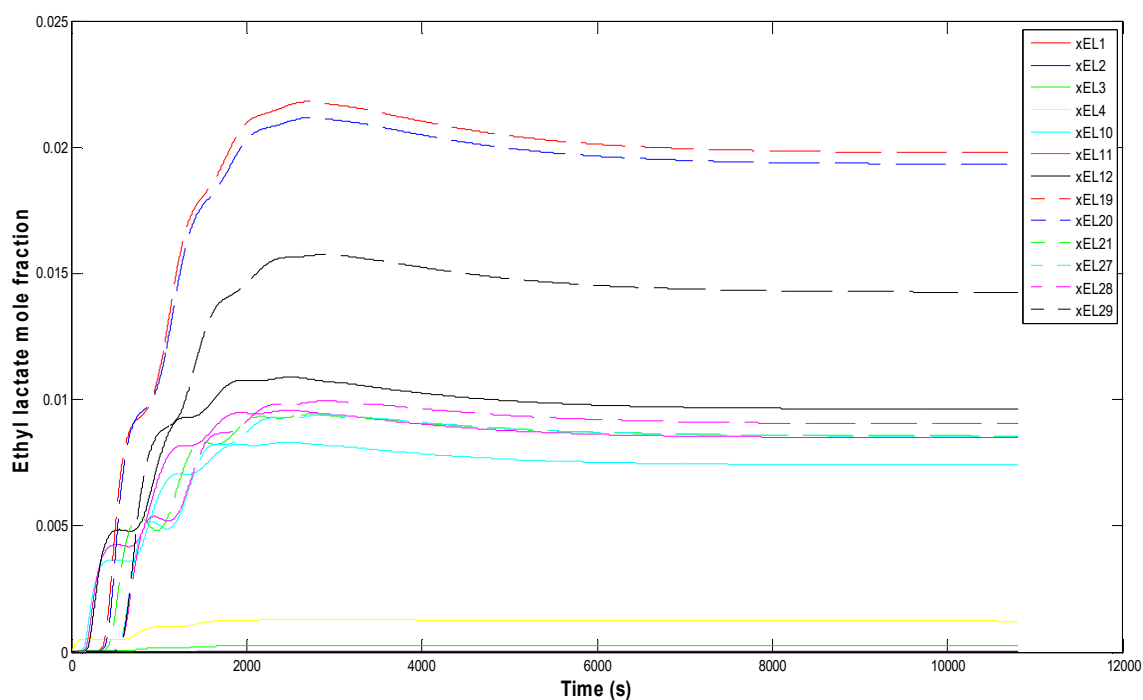


**Fig. 14 Dynamic behavior of the Ethyl Lactate mole fraction at some stages in reactive distillation column**  
*xEL1: Condenser, xEL2: Top tray, xEL4: Feed LA tray, xEL21: Feed Et tray, xEL29: Reboiler, xEt2, xEL3, xEL10, xEL11, xEL12, xEL19, xEL20, xEL27, and xEL28: Internal trays*

For the process conditions run in the simulation (including the pre-defined design parameters, see sub-section 3.3.1) it is possible to observe that the system tends to a steady state. However, such steady state is not a desired operating point, mainly because the Ethyl Lactate mole fraction reached at this point is too low.

### 3.4. Model validation

In the two previous sub-sections the models (for the distillation and reactive distillation columns) were run from a given set of initial conditions until a steady state was reached. In this section, both models will be validated against results obtained when using the commercial software Aspen, using the *Radfrac* module.

The validation was carried out by simulating both models (with and without reaction) in MATLAB and Aspen, using the same conditions. Before showing the validation results, it is important to notice that the following special assumptions and considerations were done:

- The UNIQUAC solution model was selected with the prediction of the binary interaction coefficients using UNIFAC for all simulations.
- Equal feed conditions ( $F, x_F, T_F$ ) are supplied in both simulations
- $Q_B$  and *ref* are operating specifications for Radfrac simulation. The same values were used for the MATLAB simulation.

For the sake of a fair comparison against Aspen, the following assumptions were considered for both simulations:

- As Radfrac module in Aspen only allows using a power law mechanism for the reaction, it was necessary to use the power law reaction mechanism also in the MATLAB model (for the sake of comparing).
- As Radfrac calculates the reaction rate based on the volume. For this reason, in the MATLAB model the reaction rate must be calculated by multiplying the specific reaction rate by the molar liquid holdup.

It is important to notice that these two assumptions were just considered in this section, for the sake of comparison. This means that in the upcoming chapters, indeed the Langmuir Hinshelwood mechanism was used, as well as a reaction rate based on the catalyst weight

Steady state profiles for the MATLAB and Aspen distillation column models are compared from *Fig. 15* to *Fig. 18*. The following variables were graphically compared along the column stages: Temperature, Mole fraction in the liquid phase (for water, ethanol and lactic acid), Mole fraction in the vapor phase (for the same compounds as in the liquid), and the liquid and vapor flowrates. Results for the MATLAB model are presented as a solid line, while Aspen results are marked with an asterisk. *Fig. 15* compares the Temperature profiles. Although both models (Aspen and Matlab) result in the same trend, the proposed model in this work (MATLAB model) predicts a higher temperature in the reactive zone than the Aspen predictions. This might suggest some differences in the thermodynamic models, which unfortunately were not detected, since a part of internal programming of Aspen is not accessible to the user.

An important difference is that the MATLAB model is a dynamic model, while the Aspen simulation is at steady state, for that reason each program finds different steady state values, although very close and (most importantly) within a physically possible range. On the other hand, the similarity in the results for the mole fractions and internal flows (liquid and vapor) is illustrated in *Fig. 16* to *Fig. 18*. From these figures it can be concluded that the PBSM model developed and simulated in MATLAB, represents adequately the variables behavior in a distillation column.



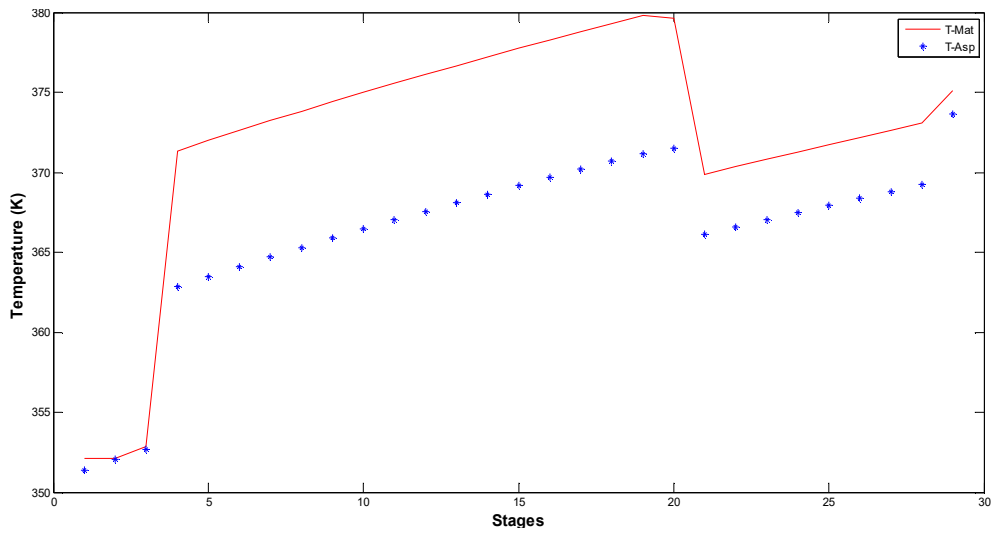


*Fig. 15 Temperature profile in the distillation column*

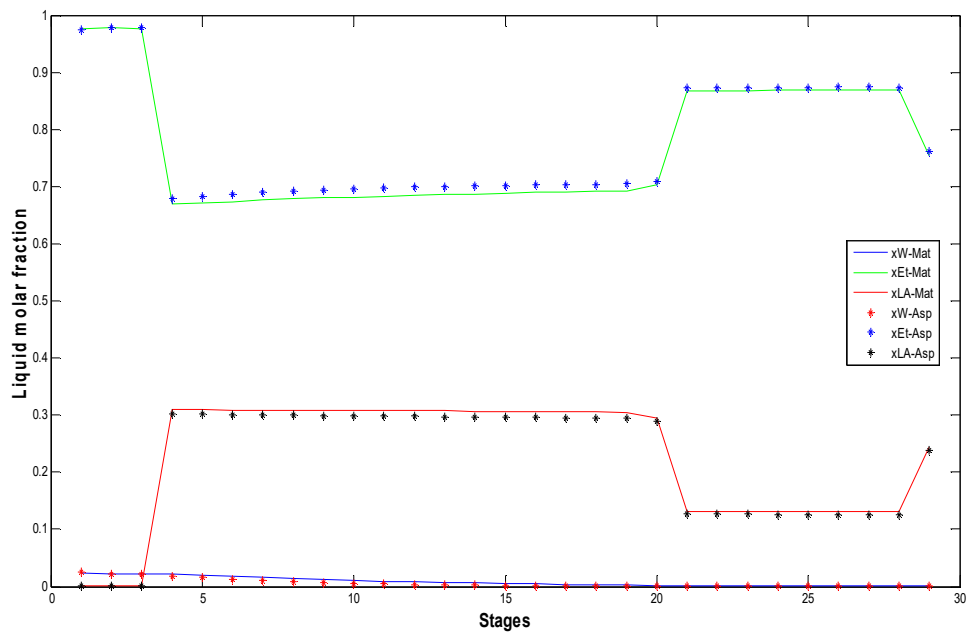


*Fig. 16 Liquid molar fraction profile in the distillation column*

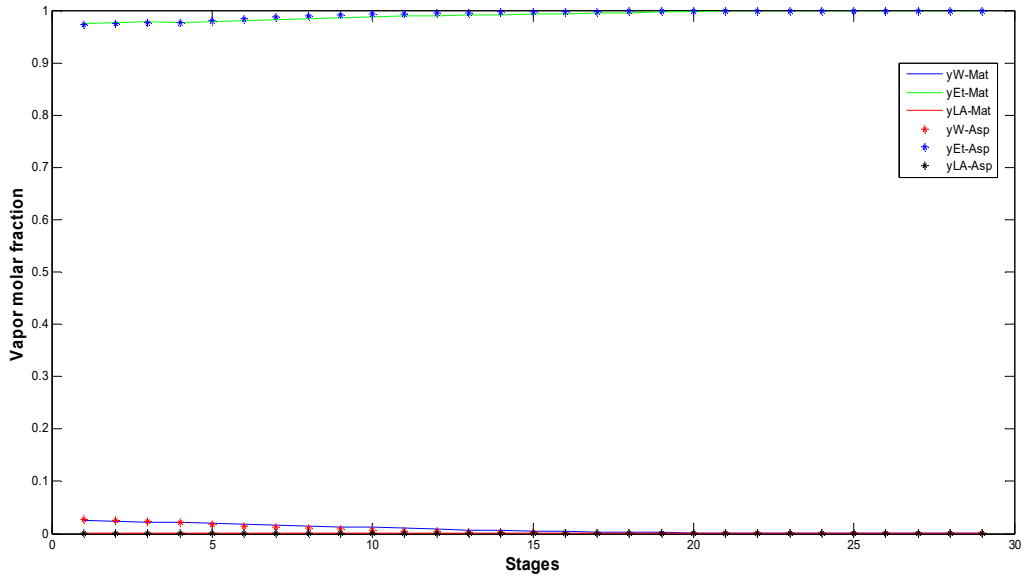


**Fig. 17 Vapor molar fraction profile in the distillation column**

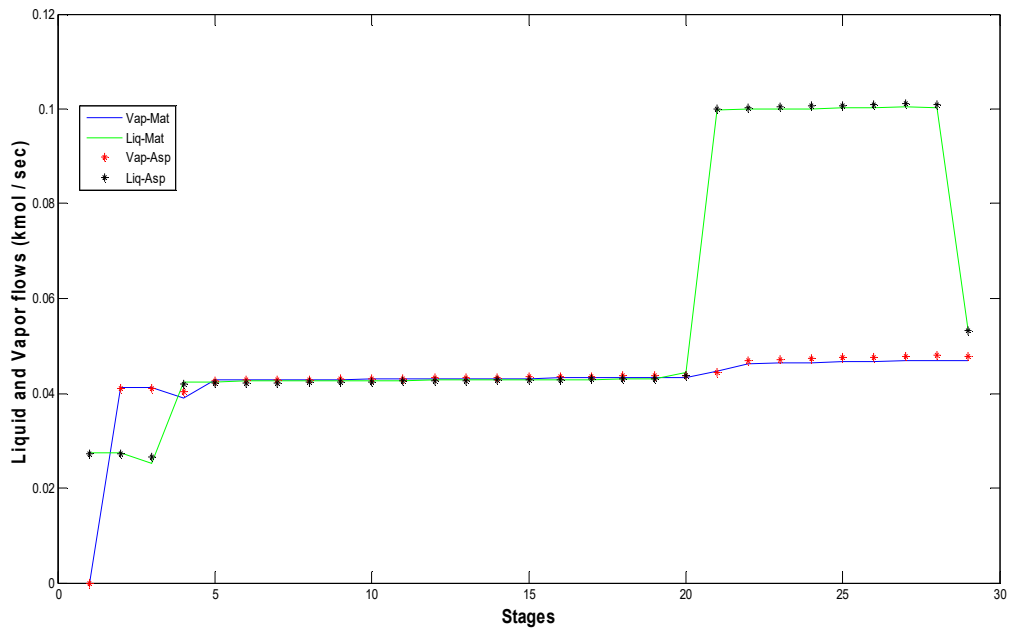


**Fig. 18 Internal flows profile in the distillation column**

Key results obtained for the input (feed streams) and output (bottoms stream and distillate) column streams are summarized in Table 7. These results allow evidencing quantitatively that the MATLAB model results are very close to the Aspen model results, with most of the errors in the order of  $10^{-4}$  and lower except for temperature.

Table 7 Summary streams, Aspen vs MATLAB simulation in distillation column

	Bottoms (BEL)			Distillate (Dc)			Ethanol Feed (F <sub>Et</sub> )		Lactic Acid Feed (F <sub>LA</sub> )	
	ASPEN	MATLAB	Error	ASPEN	MATLAB	Error	ASPEN	MATLAB	ASPEN	MATLAB
	LIQUID			LIQUID			LIQUID		LIQUID	
<b>Mole Flow [kmol/sec]</b>										
Water	2.20E-05	4.42E-05	2.22E-05	3.38E-04	3.22E-04	1.60E-05	2.15E-05	2.10E-05	3.38E-04	3.57E-04
Ethanol	4.04E-02	4.05E-02	1.00E-04	1.33E-02	1.33E-02	0.00E+00	5.38E-02	5.38E-02	0	0
Lactic Acid	1.27E-02	1.31E-02	4.00E-04	1.49E-11	2.18E-10	2.03E-10	0.00E+00	0	1.27E-02	1.31E-02
	--									
Total Flow [kmol/sec]	0.0531	0.0536	5.00E-04	0.0137	0.0136	1.00E-04	0.0538	0.0538	0.013	0.0134
Total Flow [kg/sec]	3.004	3.0434	3.94E-02	0.6196	0.6188	8.00E-04	2.4769	2.4769	1.1467	1.1853
Total Flow [cum/sec]	3.59E-03	3.50E-03	9.00E-05	8.43E-04	7.80E-04	6.30E-05	--	--	--	--
Temperature [K]	373.663	376.664	3.00E+00	351.3925	352.1299	7.37E-01	348.15	348.15	348.15	348.15
Pressure [N/sqm]	1.74E+05	1.74E+05	0.00E+00	1.01E+05	1.01E+05	0.00E+00	--	--	--	--
Reflux [kmol/sec]	--	--	--	0.0273	0.0275	2.00E-04	--	--	--	--
Boilup vapor flow	0.0477	0.0468	9.00E-04	--	--	--	--	--	--	--
Molar reflux ratio	--	--	--	2	2	0.00E+00	--	--	--	--
Molar boilup ratio	0.8731	0.8731	0.00E+00	--	--	--	--	--	--	--
Condenser heat duty [Kw]	--	--	--	-1609.16	-1617.6	8.44E+00	--	--	--	--
Reboiler heat duty [kW]	1864.9	1864.9	0.00E+00	--	--	--	--	--	--	--

In the following, validation of the developed model for the reactive distillation column implemented in MATLAB is carried out by comparing the obtained results against the Aspen model results. As it can be seen in *Fig. 19* to *Fig. 22* the profiles observed have very similar trends, however, higher differences are found when the reactive zone is included in the models (higher than those observed in *Fig. 15* to *Fig. 18* for the validation of a non-reactive distillation column model). The observed differences are possibly due to the fact that the parameters for the thermodynamic models in ASPEN and MATLAB are different. Parameters for MATLAB model were taken from the literature whereas ASPEN parameter were taken from the ASPEN Data Base. Additionally, the ASPEN model is a steady state model whereas the MATLAB is a dynamic model. Despite the observed differences it was decided to accept the proposed model in MATLAB as valid for the purposes of investigating the design–control integration for ethyl lactate production in a reactive distillation column. It is important to notice that the production of Ethyl Lactate by esterification of Lactic Acid with Ethanol in RDC presents complex interactions leading to multiple steady-states and complex dynamics (Kiss, 2013). Additionally, the Radfrac module doesn't allow to use a reaction mechanism different to the power law (the suggested mechanism in literature and the one used in the upcoming sections for the MATLAB model is a Langmuir-Hinshelwood). Finally, the Radfrac module doesn't consider either that the reaction rate might be a function of the mass of catalyst. These two mentioned points have been reported in the literature as disadvantages (W. L. Luyben & Yu, 2009). Precisely, the model developed and simulated in this work eliminates those disadvantages, and therefore, might be more suitable for being used for predicting the dynamic behavior of the analyzed system.

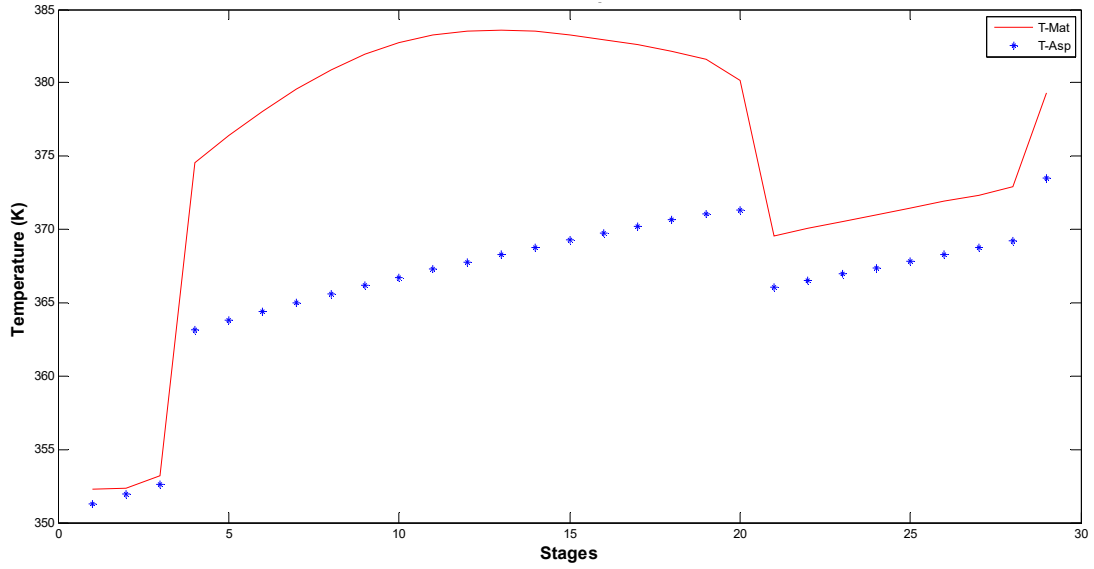


*Fig. 19 Temperature profile in the reactive distillation column*

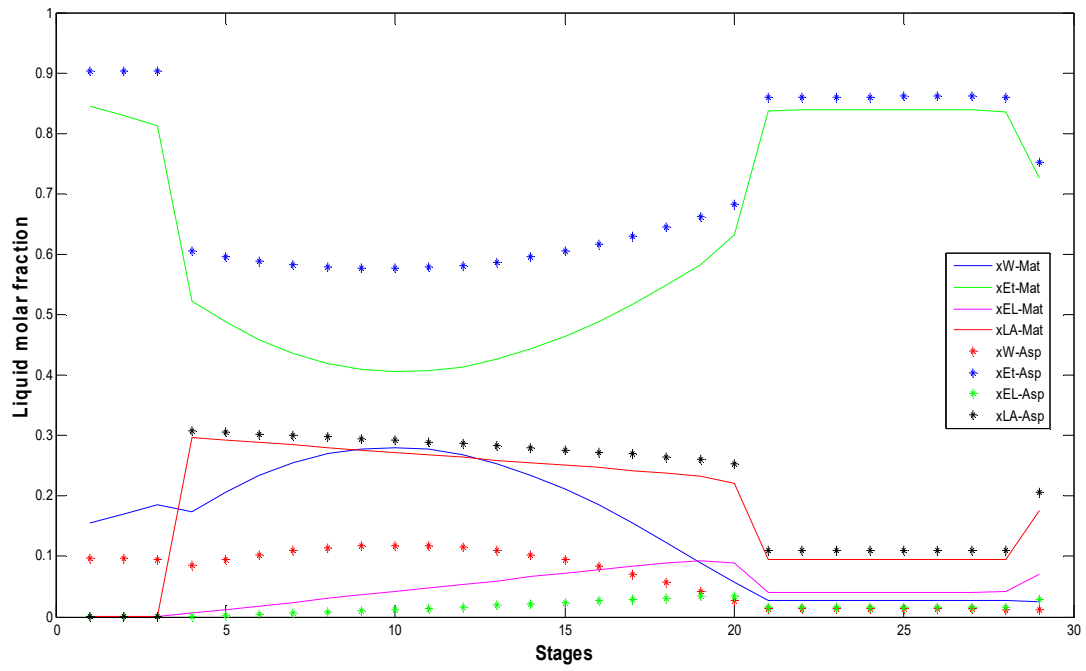


*Fig. 20 Mole fraction profile at the liquid in the reactive distillation column*

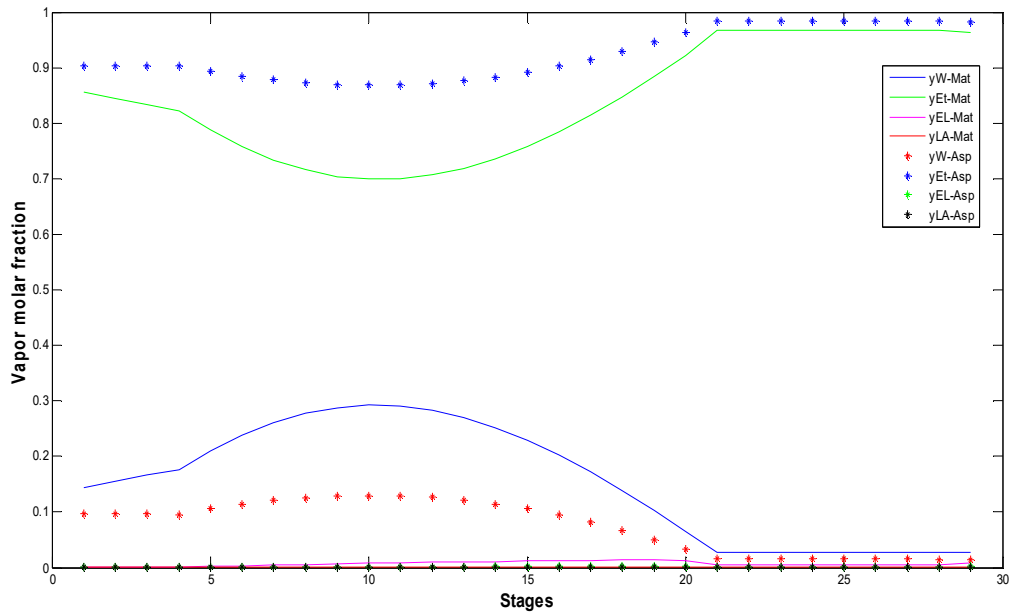


**Fig. 21 Mole fraction profile at the vapor in the reactive distillation column**

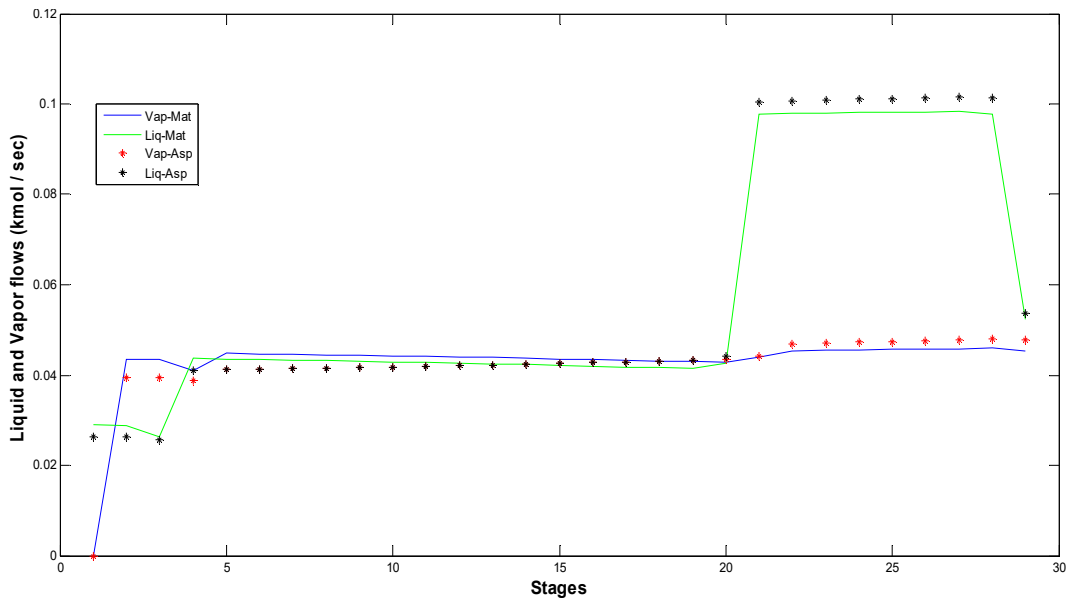


**Fig. 22 Internal flows (Liquid and vapor) profiles in the reactive distillation column**

Key results obtained for the input (feed streams) and output (bottoms stream and distillate) streams are summarized in Table 8. These results allow to observe that the MATLAB model results are very close to the Aspen model results.

Table 8 Summary streams, Aspen vs MATLAB simulation in reactive distillation column

	Bottoms (BEL)			Distillate (DC)			Ethanol Feed (F <sub>Et</sub> )		Lactic Acid Feed (F <sub>LA</sub> )	
	ASPEN	MATLAB	Error	ASPEN	MATLAB	Error	ASPEN	MATLAB	ASPEN	MATLAB
	LIQUID			LIQUID			LIQUID		LIQUID	
<b>Mole Flow [kmol/sec]</b>										
Water	6.40E-04	1.30E-03	6.60E-04	1.28E-03	2.30E-03	1.02E-03	2.15E-05	2.10E-05	3.38E-04	3.57E-04
Ethanol	4.03E-02	3.81E-02	2.20E-03	1.19E-02	1.22E-02	3.00E-04	5.38E-02	5.38E-02	0	0
Ethyl Lactate	1.56E-03	3.70E-03	2.14E-03	1.13E-08	2.30E-07	2.19E-07	0.00E+00	0	0.00E+00	0
Lactic Acid	1.11E-02	9.30E-03	1.80E-03	1.23E-11	1.50E-10	1.38E-10	0.00E+00	0	1.27E-02	1.31E-02
	--									
Total Flow [kmol/sec]	0.0536	0.0524	1.20E-03	0.0132	0.0145	1.30E-03	0.0538	0.0538	0.013	0.0134
Total Flow [kg/sec]	3.0524	3.0549	2.50E-03	0.5711	0.6049	3.38E-02	2.4769	2.4769	1.1467	1.1853
Total Flow [cum/sec]	3.66E-03	3.50E-03	1.60E-04		7.39E-04	7.39E-04	--	--	--	--
Temperature [K]	373.474	379.3185	5.84E+00	351.302	352.2836	9.82E-01	348.15	348.15	348.15	348.15
Pressure [N/sqm]	1.74E+05	1.74E+05	0.00E+00	1.01E+05	1.01E+05	0.00E+00	--	--	--	--
Reflux [kmol/sec]	--	--	--	0.0263	0.029	2.70E-03	--	--	--	--
Boilup vapor flow	0.0477	0.0452	2.50E-03	--	--	--	--	--	--	--
Molar reflux ratio	--	--	--	2	2	0.00E+00	--	--	--	--
Molar boilup ratio	0.8632	0.8632	0.00E+00	--	--	--	--	--	--	--
Condenser heat duty [kW]	--	--	--	-1558.63	-1715.5	1.57E+02	--	--	--	--
Reboiler heat duty [kW]	1864.9	--	--	--	1864.9	--	--	--	--	--

### 3.5. Sensitivity Analysis

A sensitivity analysis was carried out for evaluating the relative importance of different selected input factors on the Ethyl Lactate concentration obtained at the bottom of the distillation column ( $x_{EL}$ ) and in the conversion ( $X_C$ ). The procedure was divided in two stages. In the first stage, the change in ( $x_{EL}$ ) and ( $X_C$ ) when a 50% of variation is applied to each one (one at each time) of the selected input factors from its nominal value is assessed. The input factors tested were selected from a priori knowledge. **¡Error! No se encuentra el origen de la referencia.** Table 9 **¡Error! No se encuentra el origen de la referencia.** shows (in the second column) the nominal values used for varying the selected input factors. These nominal data were taken from the results obtained in the model validation for the reactive distillation column.

Table 9 Sensitivity analysis applying 50% of change to the nominal value

Variable	Nominal	$x_{EL}$	$m(x_{EL})$	$X_C$	$m(X_C)$
<i>Diam</i> [m]	1.7857	0.81	0.1635	0.32	0.1458
$reb \left( \frac{V(N+2)}{B_{EL}} \right)$	0.4358	0.69	0.1279	0.49	0.2226
$Rat \left( \frac{F_{Et}}{F_{LA}} \right)$	1.00	0.73	0.1348	0.37	0.1434
$ref \left( \frac{L_R}{D_C} \right)$	2.00	0.61	0.0520	0.38	0.0647
$m_{cat}$ [kg]	246.60	0.69	0.0002	0.47	0.0002
$UA \left[ \frac{kW}{s} \right]$	4250	0.66	0.0000	0.44	0.0000
$P$ [kPa]	101.325	0.68	0.0003	0.45	0.0001

Where *Diam*, *reb*, *Rat*, *ref*,  $m_{cat}$ ,  $P$  and  $UA$  are the diameter, boil-up ratio, feed molar ratio, reflux ratio, total catalyst loading, column pressure and the global heat transfer coefficient for the reboiler, respectively. The effect of each input factor on  $x_{EL}$  and  $X_C$  was evaluated as the rate of change (slope) between them, in absolute value. Table 9 shows the results for the slope for  $x_{EL}$  ( $m(x_{EL})$ ) and the slope for  $X_C$  ( $m(X_C)$ ). Analyzing the results, it was decided to select the first five input factors as most sensitive parameters to be taking into account during the process design. This, because they have the higher effect on both, the conversion and the product quality.



The second stage of this sensitivity analysis was sequential in such a way that one input factor was varied while the others were kept constant, but then, the best result was used as an initial point to assess the effect on the next input. Table 10 shows the simulated design of experiments used for the second stage of the sensitivity analysis.

Table 10 Simulated Experimental Design and Results for Sensitivity Analysis

Experiment Number	Fraction or % varied from the nominal value	Diam [m]	$\frac{reb}{\left(\frac{V(N+2)}{B_{EL}}\right)}$	$\frac{Rat}{\left(\frac{F_{Et}}{F_{LA}}\right)}$	$\frac{ref}{\left(\frac{L_{Ref}}{Diam}\right)}$	$m_{cat}$ [kg]	$X_C$	$x_{EL}$
1	0.33Diam	0.5893	0.4358	1	2	246.6041	0.66	0.44
2	0.5Diam	0.8929	0.4358	1	2	246.6041	0.67	0.44
3	0.75Diam	1.3393	0.4358	1	2	246.6041	0.65	0.40
4	Diam	1.7857	0.4358	1	2	246.6041	0.66	0.45
5	1.5Diam	2.6786	0.4358	1	2	246.6041	0.81	0.32
6	2Diam	3.5714	0.4358	1	2	246.6041	1.00	0.32
7	0.5reb	Best*	0.2179	1	2	246.6041	0.60	0.36
8	1,5reb	Best	0.4358	1	2	246.6041	0.71	0.53
9	2reb	Best	0.6536	1	2	246.6041	0.75	0.60
10	3reb	Best	0.8715	1	2	246.6041	0.79	0.70
11	4reb	Best	1.3073	1	2	246.6041	0.80	0.75
12	Rat	Best	Best	1	2	246.6041	0.80	0.75
13	2Rat	Best	Best	2	2	246.6041	0.87	0.57
14	3Rat	Best	Best	3	2	246.6041	0.80	0.37
15	4Rat	Best	Best	4	2	246.6041	0.74	0.26
16	0.5Ref	Best	Best	Best	1	246.6041	0.88	0.86
17	Ref	Best	Best	Best	2	246.6041	0.80	0.75
18	1.5Ref	Best	Best	Best	3	246.6041	0.70	0.59
19	0.4 $m_{cat}$	Best	Best	Best	Best	98.6416	0.85	0.82
20	0.6 $m_{cat}$	Best	Best	Best	Best	147.9625	0.87	0.84
21	0.8 $m_{cat}$	Best	Best	Best	Best	197.2833	0.88	0.85
22	$m_{cat}$	Best	Best	Best	Best	246.6041	0.88	0.86

\* Best is the corresponding value for the parameter which resulted in the highest values for  $X_C$  and  $x_{EL}$

Sensitivity results for the Lactic acid conversion and ethyl lactate concentration obtained at the bottom of the column when varying the selected variables, are shown in Fig. 23 to Fig. 27. The results show evidence that:

- All variables selected for sensitivity analysis affect the Lactic acid conversion and Ethyl Lactate purity at the bottoms; however, the process was more sensitive to the changes in the Boilup (*reb*), reflux (*ref*) and feed ratios (*Rat*).
- The Ethyl Lactate molar fraction at the bottoms is directly proportional to the boilup ratio (*reb*) and catalyst loading ( $m_{cat}$ ). On the other hand,  $x_{EL}$  is inversely proportional to the reflux ratio (*ref*) and feed molar ratio (*Rat*).

It is important to bear in mind that this analysis will serve as a guide for the selection of the decision variables, and its operating limits, in order to carry out the optimization. The objective will be finding the best combination of these values that maximizes an economic objective function while keeping the product quality above a certain defined value.

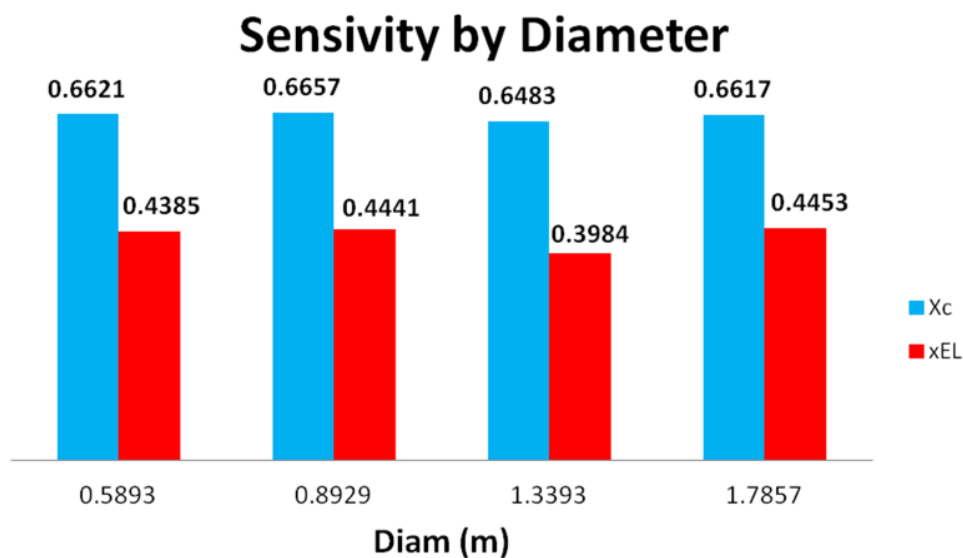


*Fig. 23 Effect of Diameter in the conversion and Ethyl Lactate molar fraction at Bottoms*

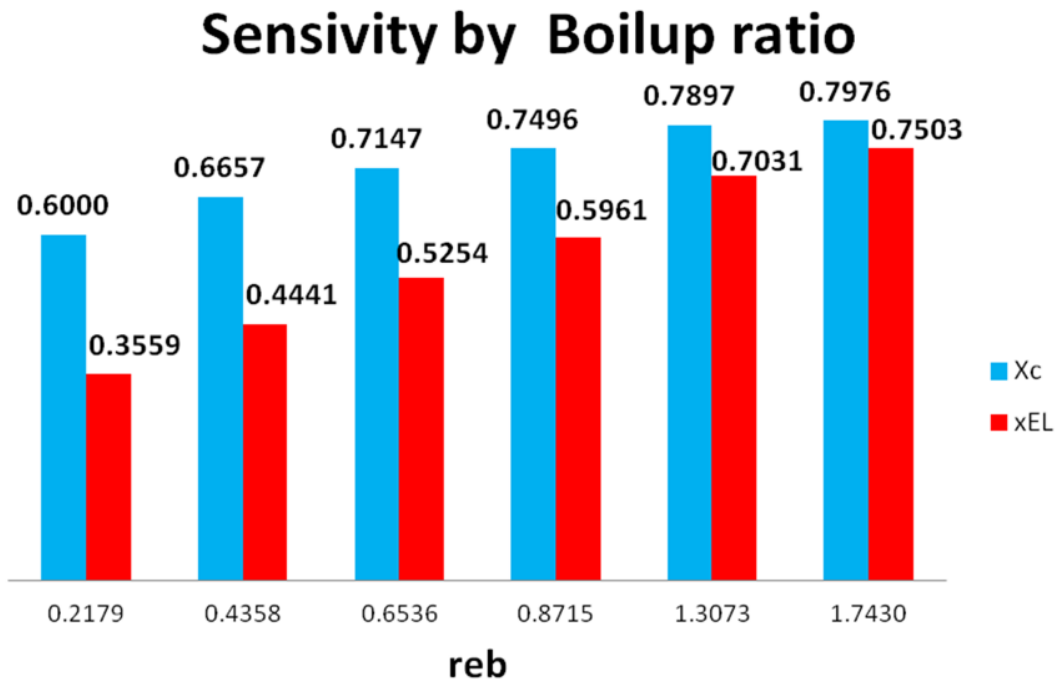


Fig. 24 Effect of Boilup ratio in the conversion and Ethyl Lactate molar fraction at Bottoms

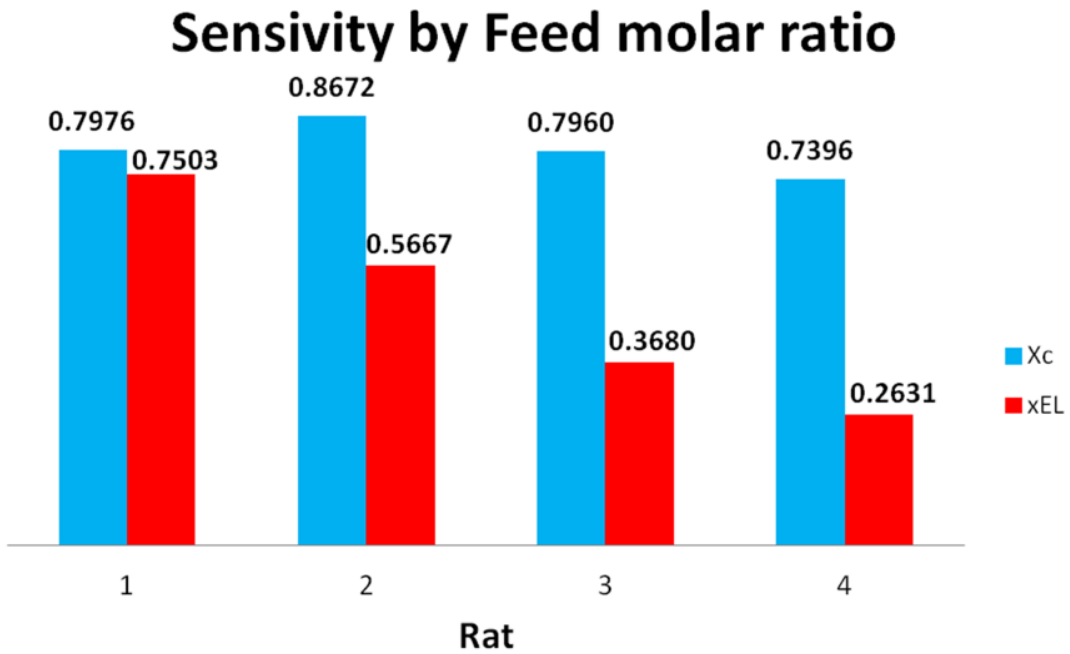


Fig. 25 Effect of Feed molar ratio in the conversion and Ethyl Lactate molar fraction at Bottoms

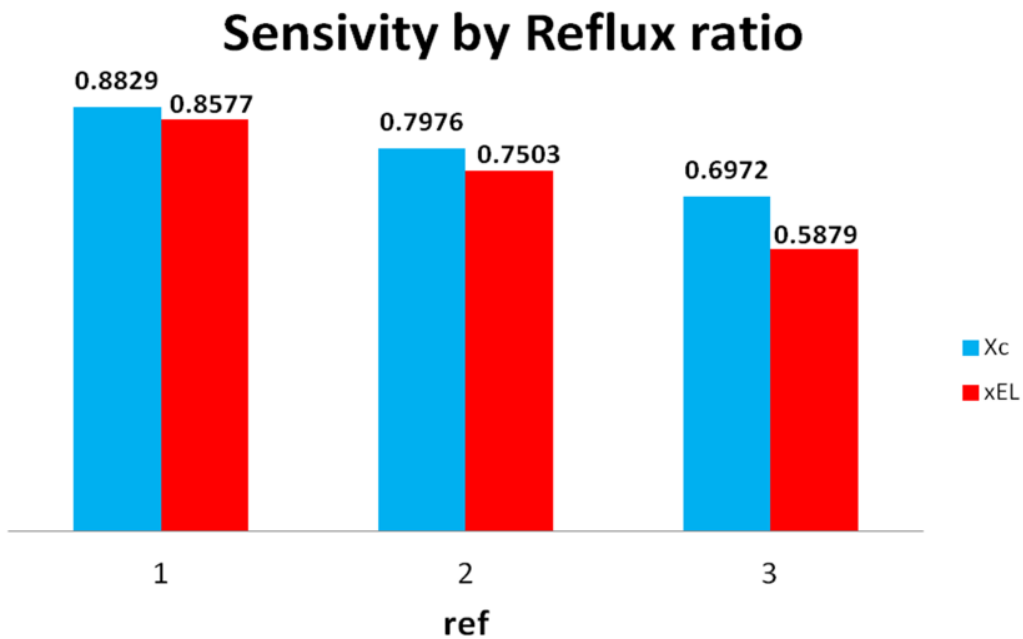


Fig. 26 Effect of Reflux ratio in the conversion and Ethyl Lactate molar fraction at Bottoms

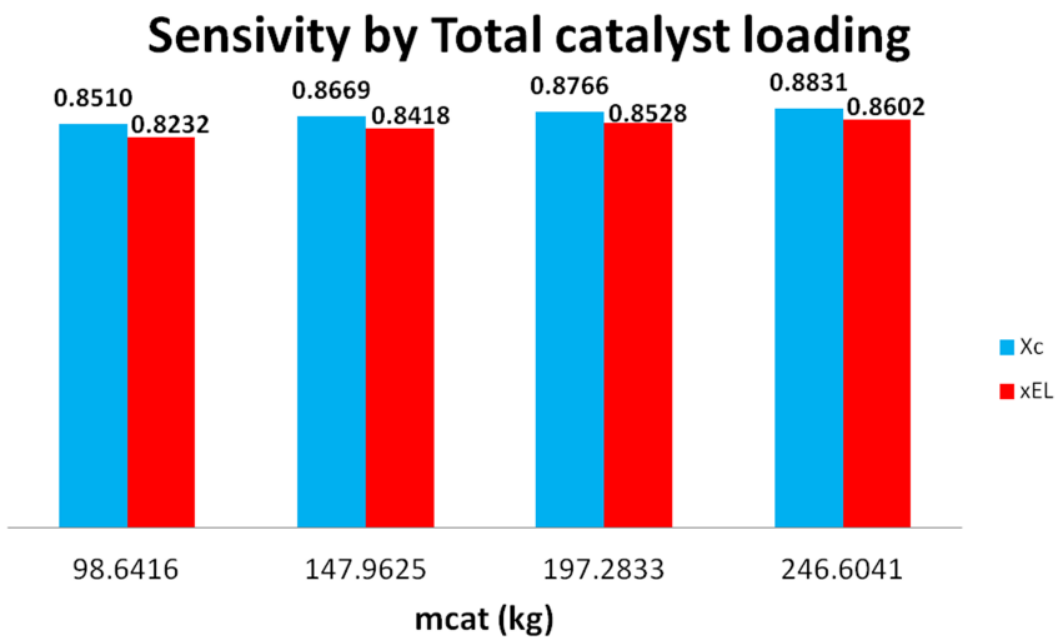


Fig. 27 Effect of Total catalyst loading in the conversion and Ethyl Lactate molar fraction at Bottoms

## **4. DESIGN AND CONTROL INTEGRATION OF A REACTIVE DISTILLATION COLUMN FOR ETHYL LACTATE PRODUCTION**

In this chapter, the methodology for design – control integration proposed by Ochoa (2005) is applied step by step to the reactive distillation column case, taking as example the ethyl lactate production (Section 4.1).

### **4.1. Application of the methodology**

#### **4.1.1. Problem Definition**

The problem is stated as the design of a reactive distillation column system for the ethyl lactate production by the esterification of lactic acid with ethanol, as mentioned in Section 3.1. For defining the desired installed capacity, the projected demand for ethyl lactate to year 2020 was taken into account [42]. In this projections, it was taken into account: the Colombia demand for solvents, the demand of green solvents worldwide in 2013 (as well as its participation in the total solvents market) and the annual growth of green solvents market worldwide (Arroyave Restrepo, Correa Moreno, & Duque Lozano, 2015). Using such projections, a desired capacity of 9000 ton/year was settled.

#### **4.1.2. Obtaining of a Phenomenological Based Semiphsical Model (PBSM)**

The model developed and detailed at section 3.2 is the PBSM used in the application of the design-control integration methodology. Some model characteristics worthy of being mentioned here for the sake of clarity are:

- Langmuir-Hinshelwood was selected as kinetic model.
- Condenser and reboiler are modeled as “trays”.
- Feeding point for the lactic acid and ethanol are fixed and were decided to be the first and the last tray of the reactive zone, respectively.

It is also important to notice that for optimization purposes, the total number of trays is taken as  $N + 2$ , which means that such number of trays is not fixed but is a result of the optimization. This is different from the simulation developed in section 0, where the number of trays was fixed.

#### 4.1.3. Selection of Manipulated Variables and Determination of the Available Interval

- a. **Identification of the manipulated variables:** Table 11 shows the input variables to the process, which can be classified into manipulated variables or disturbances and were selected from Table 3 and the Phenomenological Based Semiphysical Model (PBSM).

Table 11 Input variables classification

Variable	Description	Dimension	Type of Variable
$B_{EL}$	Flow of bottoms	$kmol/sec$	manipulated
$D_C$	Flow of Distillate	$kmol/sec$	Manipulated
$F_{LA}$	Lactic Acid Feed stream	$kmol/sec$	manipulated
$L_{Ref}$	Reflux flow rate	$kmol/sec$	manipulated
$Q_B$	Reboiler heat duty	$kJ/sec$	manipulated
$T_F$	Temperature at the feed flow rate	$K$	Disturbance
$x_{Et,F}$	Et mol fraction on the Et feed stream	--	Disturbance
$x_{LA,F}$	LA mol fraction on the LA feed stream	--	Disturbance

- b. **Degrees of freedom calculation for the control:** The control degrees of freedom are calculated as:

$$CDOF = N.M.V. - N.C.V. \quad (Eq.57)$$

Where  $N.M.V.$  is the number of available manipulated variables (control actions) and  $N.V.C.$  is the number of variables to control (output variables to be controlled). From Table 11, there are five input variables classified as manipulated. The number of controlled variables for this system is also five, including: the temperature at a tray in the rectification section ( $T_{rf}$ ), the temperature at a tray located in the reaction section ( $T_{rxn}$ ), the temperature at a tray

located in the stripping section ( $T_{st}$ ), the level at the condenser ( $l_C$ ) and at the reboiler ( $l_B$ )

$$CDOF. = 5 - 5 = 0$$

- c. ***Selection and pairing of the manipulated variables that allow expressing the system in the canonical form:*** As it was shown in Table 11, there are five manipulated variables available for controlling the five state variables mentioned above. Once the control degrees of freedom are met, the next step is to pair the available manipulated variables and the controlled variables. For choosing the “best” pairing, the evaluation procedure of structural controllability by means of digraphs reported in [43,44] is used. The digraphs analysis was preferred because it is based only in structural information, it doesn't require neither linearization procedures nor the definition of design parameters (i.e. the latter will be just available after finishing the process design).

In the following, the methodology based on digraphs analysis used for the pairing manipulated–controlled variables are applied to the case study. First, the vector of available manipulated variables and the vector of the defined controlled variables is defined, as shown in Eq. 58 and Eq. 59, respectively.

$$\dot{x} = \begin{bmatrix} x_1 \\ x_2 \\ x_3 \\ x_4 \\ x_5 \end{bmatrix} = \begin{bmatrix} T_{rf} \\ T_{rxn} \\ T_{st} \\ l_C \\ l_B \end{bmatrix} \quad (Eq. 58)$$

$$u = \begin{bmatrix} u_1 \\ u_2 \\ u_3 \\ u_4 \\ u_5 \end{bmatrix} = \begin{bmatrix} B_{EL} \\ D_C \\ F_{LA} \\ L_{Ref} \\ Q_B \end{bmatrix} \quad (Eq. 59)$$

The digraph for this system is composed by 15 nodes: 5 nodes corresponding to the manipulated variables, 5 to the state variables to be controlled, and finally, the 5 outputs

impacted by the states. The digraph built for the system is shown in *Fig. 28*. The connecting lines between nodes represent the relationship between the variables.

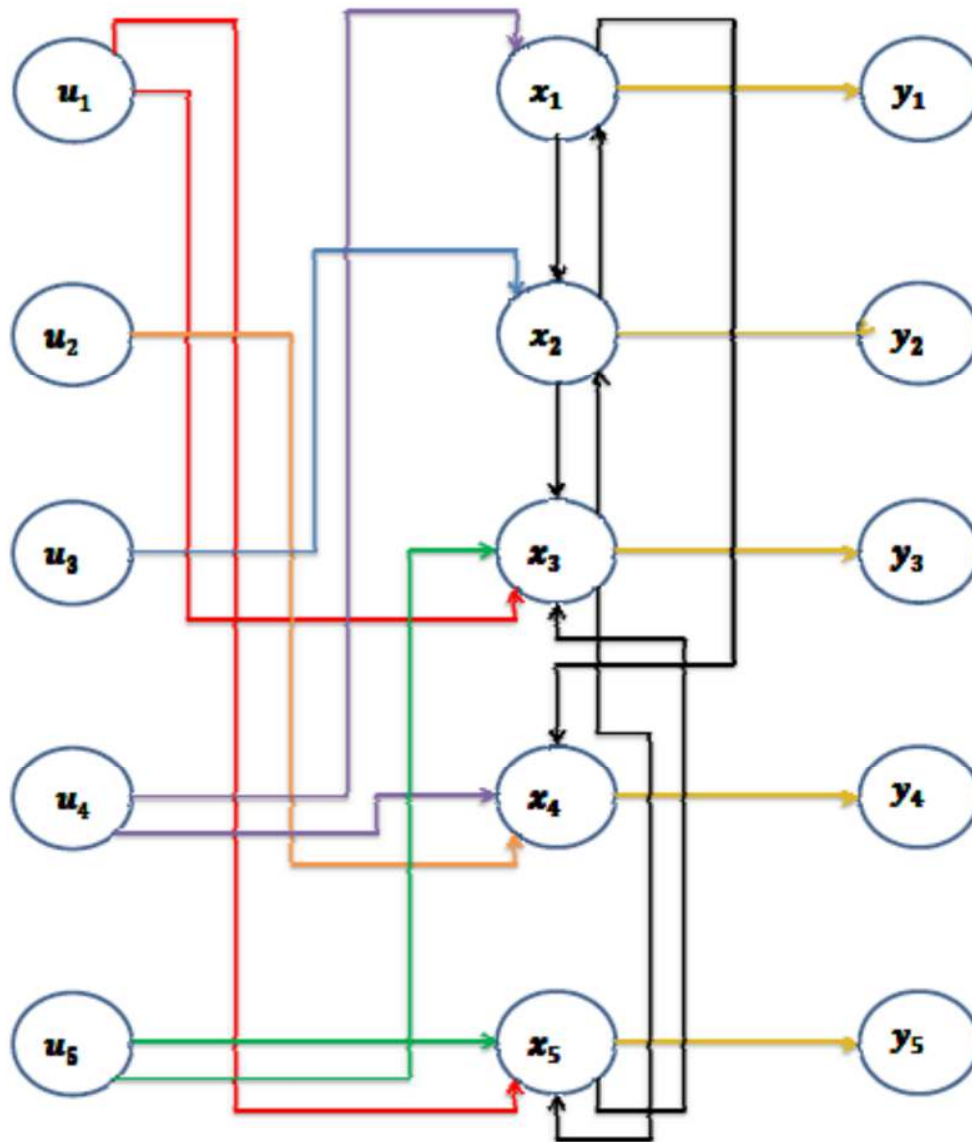


*Fig. 28 Digraph*

The next step in the procedure is obtaining the relative order matrix  $M_r$ , for the resulting digraph. In general, the relative order matrix is written as:



$$M_r = \begin{bmatrix} r_{11} & r_{12} & \dots & r_{1n} \\ r_{21} & r_{22} & \dots & r_{2m} \\ \dots & \dots & \dots & \dots \\ r_{n1} & r_{n2} & \dots & r_{nm} \end{bmatrix}$$

Where  $m$  is the number of manipulated variables, and  $n$  is the number of states to be controlled. Each  $r_{ij}$  is the relative order of the state  $i$  ( $i=1, 2, \dots, n$ ) with respect to the input  $j$  ( $j=1, 2, \dots, m$ ). The relative order quantifies how direct is the effect of each input variable over the output variable. This order is determined by counting the number of nodes that can be encountered in the shortest path possible that connects the node  $j$  with the output  $i$ . When there is not a path connecting the nodes  $i$  and  $j$ , the relative order is taken as infinite ( $\infty$ ). For the case study here, following the connecting lines for the digraph shown in *Fig. 28*, the resulting  $M_r$  is given by *Eq. 60*.

$$M_r = \begin{bmatrix} 3 & \infty & 2 & 1 & 3 \\ 2 & \infty & 1 & 2 & 2 \\ 1 & \infty & 2 & 3 & 1 \\ 4 & 1 & 3 & 1 & 4 \\ 1 & \infty & 3 & 4 & 5 \end{bmatrix} \quad (\text{Eq. 60})$$

According to the results for the relative order matrix, it is found that the best possible pairing for the manipulated and controlled variables (shown in *Eq. 58* and *Eq. 59*, respectively) is:

$$\begin{array}{llll} u_4 & \rightarrow & x_1 & L_{Ref} \rightarrow T_{rf} \\ u_3 & \rightarrow & x_2 & F_{LA} \rightarrow T_{rxn} \\ u_5 & \rightarrow & x_3 & \rightarrow Q_B \rightarrow T_{st} \\ u_2 & \rightarrow & x_4 & D_C \rightarrow l_C \\ u_1 & \rightarrow & x_5 & B_{EL} \rightarrow l_B \end{array}$$

In order to keep the nomenclature simple, the vector of available manipulated variables is reorganized as:

$$u = \begin{bmatrix} u_1 \\ u_2 \\ u_3 \\ u_4 \\ u_5 \end{bmatrix} = \begin{bmatrix} L_{Ref} \\ F_{LA} \\ Q_B \\ D_C \\ B_{EL} \end{bmatrix} \quad (\text{Eq. 61})$$

**d. Canonical expression for the system:** In order to apply the design-control methodology detailed in section 2.3, it is necessary to write the model equations (presented in section 3.2) in the canonical form (Eq. 5), using the selected controlled variables (Eq. 58) and the manipulated variables (Eq. 61). For the sake of clarity, the canonical form is recalled, as:

$$\dot{x} = f(x) + G(x)u$$

The desired controlled variables are the following:

- $T_{rf}$  is the temperature at tray 2 (rectification zone), and it will be denoted by  $x_1$ .
- $T_{rxn}$  is the temperature at tray  $N_1 + N_2 - 1$  (reactive zone) and it will be denoted by  $x_2$
- $T_{st}$  is the temperature at tray  $N + 1$  (stripping zone) and it will be denoted by  $x_3$
- $l_C$  is the level at tray 1 (condenser) and it will be denoted by  $x_4$
- $l_B$  is the level at tray  $N + 2$  (reboiler) and it will be denoted by  $x_5$

The model in the canonical form for the case study is:

$$\frac{dx_1}{dt} = \frac{H_3V_3 - H_2V_2 - h_2(V_3 - V_2)}{Z_2C_{pmix,2}} + \frac{(h_{Ref} - h_2)}{Z_2C_{pmix,2}}u_1 \quad (Eq. 62)$$

$$\begin{aligned} \frac{dx_2}{dt} = & \frac{h_{(N_1+1)}L_{(N_1+1)} + H_{(N_1+N_2)}V_{(N_1+N_2)} - H_{(N_1+2)}V_{(N_1+2)} + Q_{r,(N_1+N_2-1)}}{Z_{(N_1+N_2-1)} * C_{pmix,(N_1+N_2-1)}} - \frac{h_{(N_1+N_2-1)}(L_{(N_1+1)} + V_{(N_1+N_2)} - V_{(N_1+2)})}{Z_{(N_1+N_2-1)} * C_{pmix,(N_1+N_2-1)}} \\ & + \frac{h_{F,(N_1+2)} * q_{F,(N_1+2)} - h_{(N_1+N_2-1)}}{Z_{(N_1+N_2-1)} * C_{pmix,(N_1+N_2-1)}}u_2 \end{aligned} \quad (Eq. 63)$$

$$\frac{dx_3}{dt} = \frac{h_N L_N - H_{N+1} V_{N+1} - h_{N+1} (L_N - V_{N+1})}{Z_{N+1} * C_{pmix,N+1}} + \frac{h_{N+1}}{Z_{N+1} * C_{pmix,N+1}}u_5 + \frac{1}{Z_{N+1} * C_{pmix,N+1}}u_3 \quad (Eq. 64)$$

$$\frac{dx_4}{dt} = \frac{(MW_{mix})_c}{A_w(\rho_{mix})_c}V_2 - \frac{(MW_{mix})_c}{A_w(\rho_{mix})_c}u_4 - \frac{(MW_{mix})_c}{A_w(\rho_{mix})_c}u_1 \quad (Eq. 65)$$

$$\frac{dx_5}{dt} = (L_{N+1} - V_B) * \frac{(MW_{mix})_B}{A_w(\rho_{mix})_B} - \frac{(MW_{mix})_B}{A_w(\rho_{mix})_B}u_5 \quad (Eq. 66)$$

The vector  $f(x)$  associated to the natural response, and the matrix  $G(x)$  associated to the forced response, are given by Eq. 67 and Eq. 68

$$f(x) = \begin{bmatrix} \frac{H_3V_3 - H_2V_2 - h_2(V_3 - V_2)}{Z_2 C_{pmix,2}} \\ \frac{h_{(N_1+1)}L_{(N_1+1)} + H_{(N_1+N_2)}V_{(N_1+N_2)} - H_{(N_1+2)}V_{(N_1+2)} + Q_{r,(N_1+N_2-1)}}{Z_{(N_1+N_2-1)} * C_{pmix,(N_1+N_2-1)}} - \frac{h_{(N_1+N_2-1)}(L_{(N_1+1)} + V_{(N_1+N_2)} - V_{(N_1+2)})}{Z_{(N_1+N_2-1)} * C_{pmix,(N_1+N_2-1)}} \\ \frac{h_N L_N - H_{N+1} V_{N+1} - h_{N+1} (L_N - V_{N+1})}{Z_{N+1} * C_{pmix,N+1}} \\ \frac{(MW_{mix})_c}{A_w (\rho_{mix})_c} V_2 \\ (L_{N+1} - V_B) * \frac{(MW_{mix})_B}{A_w (\rho_{mix})_B} \end{bmatrix} \quad (Eq. 67)$$

$$G(x) = \begin{bmatrix} \frac{h_{Ref} - h_2}{Z_2 C_{pmix,2}} & 0 & 0 & 0 & 0 \\ 0 & \frac{h_{F,(N_1+2)} * q_{F,(N_1+2)} - h_{(N_1+N_2-1)}}{Z_{(N_1+N_2-1)} * C_{pmix,(N_1+N_2-1)}} & 0 & 0 & 0 \\ 0 & 0 & \frac{1}{Z_{N+1} * C_{pmix,N+1}} & 0 & \frac{h_{N+1}}{Z_{N+1} * C_{pmix,N+1}} \\ -\frac{(MW_{mix})_c}{A_w (\rho_{mix})_c} & 0 & 0 & -\frac{(MW_{mix})_c}{A_w (\rho_{mix})_c} & 0 \\ 0 & 0 & 0 & 0 & -\frac{(MW_{mix})_B}{A_w (\rho_{mix})_B} \end{bmatrix} \quad (Eq. 68)$$

Once the canonical form is obtained, the next step is applying the design-control methodology proposed in (Ochoa, 2005), by performing the economic optimization using the practical controllability metrics as constraints.

- **Available interval for the manipulated variables:** For defining the available interval in which each manipulated variable is allowed to vary, actual physical constraints were taken into account (i.e. negative flows are not allowed), therefore, the vector  $u_{min}$  that defines the lower bounds for the manipulated variables set, is given by:

$$u_{min} = \begin{bmatrix} u_1 \\ u_2 \\ u_3 \\ u_4 \\ u_5 \end{bmatrix}_{min} = \begin{bmatrix} 0 \\ 0 \\ 0 \\ 0 \\ 0 \end{bmatrix} \quad (Eq. 69)$$

Selection of the upper bounds for the available interval was carried out analyzing the highest peaks reached during the model validation carried out in section 3.4. The vector  $u_{max}$  that defines the upper bounds for the manipulated variables set is given by:

$$u_{max} = \begin{bmatrix} u_1 \\ u_2 \\ u_3 \\ u_4 \\ u_5 \end{bmatrix}_{max} = \begin{bmatrix} 71.05 \text{ kmol/h} \\ 29.92 \text{ kmol/h} \\ 50000 \text{ kW} \\ 25.19 \text{ kmol/h} \\ 59.83 \text{ kmol/h} \end{bmatrix} \quad (Eq. 70)$$

#### 4.1.4. Definition of the Objective Function

The objective function is shown in *Fig. 29*. This function represents the revenues obtained per year and it is calculated as the difference between the annualized building costs  $C_{RDC_{Bu}}$  and the operating costs  $C_{RDC_{Op}}$ . In the operating costs term considered in this thesis, many terms were considered, as described in the following:

- Profits due to the selling of the product (Ethyl Lactate).
- Expenses due to the raw material used (Lactic acid and Ethanol)
- Expenses due to the utilities use (steam, cooling water).

In the objective function definition, it was considered that the process will operate 24 hours per day during 330 days per year. The remaining days per year will be used for equipment maintenance, catalyst replacement, between other activities that allow a correct performance of the process. Given the unit of time handled in the model (seconds), the term  $C_{RDC_{op}}$  must be multiplied by the conversion factor  $2.8512e7$

For the annualized building costs, four terms were included:

- Costs due to the column shell.
- Costs due to the column internals.
- Costs due to the use of the catalyst.
- Expenses generated due to replacement of the catalyst.

For the first two points, correlations for estimating the costs and the Guthrie method for correcting the costs per size and materials of construction were used (Albright, 2008). These costs were deferred to 20 years (defined useful life). For the third term (costs due to the use of the catalyst), the mass of catalyst charged to the column is multiplied by a “renovation factor”. Such “renovation factor” was determined as 2 (which means that the catalyst will be replaced twice a year to avoid catalyst deactivation). For determining such factor, the data sheet for the selected catalyst (Amberlyst 15wet), for both, the Dow Chemical Company and Rohm and Haas Company (Company, 2018) was consulted, as well as the review carried out by Pal et al. (2012). In those references, it is stated that one of the advantages of this catalyst is that it could be regenerated several times, by using acid washing (with hydrochloric acid 4-10% or sulfuric acid 1-5%).

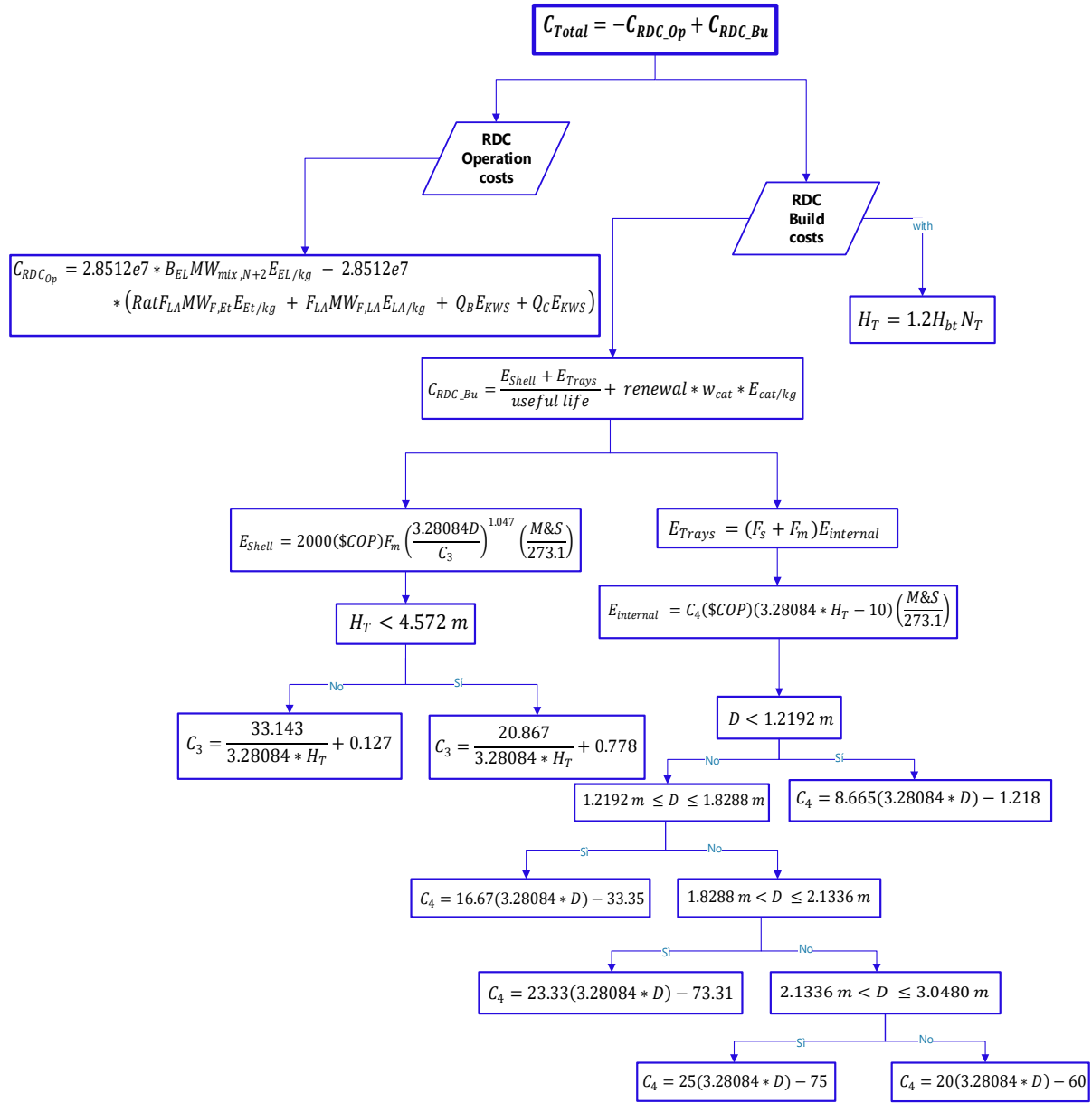


Fig. 29 Definition of the Objective function (Albright, 2008; W. L. Luyben & Yu, 2009; Treybal & García Rodríguez, 1988)

For selecting the materials for building the column, Table 12, which presents a table of chemical compatibility, was used as a guide. As it can be seen in the Table 12, the materials that have a better compatibility to the chemical substances present during the process are: The stainless steel AISI 316, and Teflon. However, it must be taken into account that during catalyst regeneration, hydrochloric acid must be avoided due to its incompatibility with stainless steel.

Table 12 Chemical compatibility for building materials (ARGENTINA, 2014)

Substance		MATERIAL								
		SHELL				DIAPHRAGM-VALVES				
DESCRIPTION	CHEMICAL FORMULA	Aluminum	Cast Iron	Stainless steel AISI 316	Polypropylene	Neoprene (CR)	Buna-N (NBR)	Nordel (EPDM)	Viton (FPM)	Teflon (PTFE)
Lactic Acid	$CH_3CHOHCOOH$	D	M	E	E	D	B	B	E	E
Ethanol	$CH_3CH_2OH$	B	E	E	E	E	E	E	E	E
Water	$H_2O$	E	B	E	E	B	E	E	E	E
Sulfuric Acid (<10%)	$H_2SO_4$	M	M	B	E	B	B	E	E	E
Hydrochloric Acid (20%)	$HCl$	M	M	M	E	M	D	E	E	E
E complete compatibility B acceptable compatibility D appreciable effects M incompatibility - no data		<b>Is recommended not to use</b>								

Additionally, it was required to define the type of column internals as well as the placement of the catalyst in the reactive zone. As variations on temperature and pressure are much more significant in reactive distillation columns (Kiss, 2013), it was decided to work with a trays column configuration. Furthermore, in order to decide the type of trays, some considerations presented by Coulson & Richardson's (2005) (Beresford, 2005), were taken into account. A comparative matrix of the performance of the different types of trays is given in Table 13. As it can be seen, sieve trays type shows more advantages, and therefore, this type of tray was selected.

Table 13 Comparison of principal factors for selection tray type

FACTOR	TRAY PERFORMANCE		
	Bubble-cap	Sieve	Valve plates
Cost	More expensive	Cheapest	Moderate cost
Capacity	Less capacity	More capacity	Medium capacity
Operating range	Less flexibility	More flexibility	Medium flexibility
Efficiency	Equal behavior	Equal behavior	Equal behavior
Pressure drop	Highest	Lowest	Medium

According to the selected type of tray, there were two options for the catalyst placement: directly on the tray or in the weir. However, in this case, the first option was selected with an array for packing the catalyst in the flow direction, as it is shown in Fig. 30. The main reasons for



selecting this option are: a more suitable contact between the reactants and the catalyst and lower pressure drop. Furthermore, if the catalyst were to be placed on the weir, it would be a more limited volume, which will restrict the reaction at each tray (Montoya Sánchez; Subawalla & Fair, 1999; Taylor & Krishna, 2000).

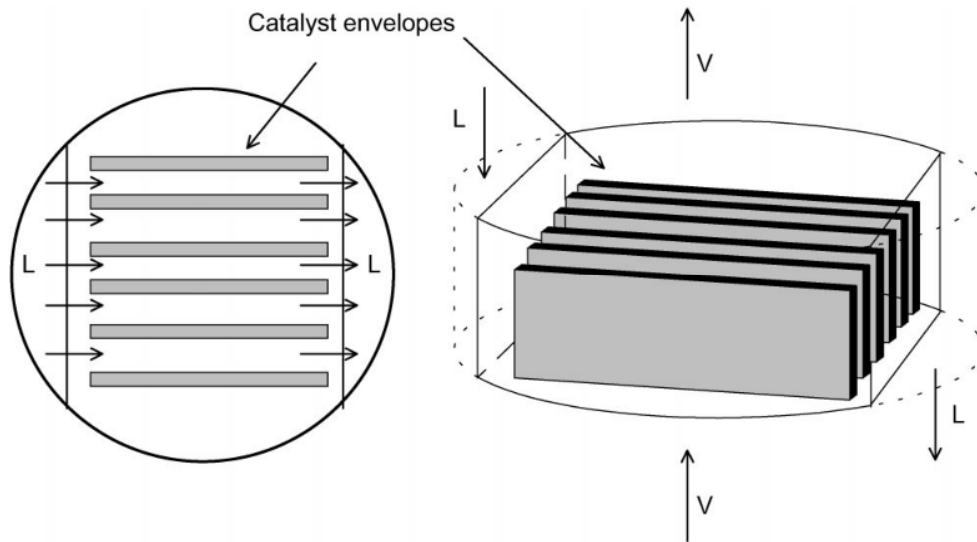


Fig. 30 Catalyst placed on the tray (Taylor & Krishna, 2000)

Table 14 shows a summary of the factors and their respective values used for the design and objective function calculation, according to the selected materials, the column diameter, the average market representative exchange rate and the Marshall and Swift cost index. Furthermore, the costs for the raw materials, catalyst, product (selling cost) and energy, are included.

Table 14 Factors and values for Objective Function calculation (Albright, 2008; República-Colombia; Treybal & García Rodríguez, 1988)

Variable	Name	Value	Units
$F_s$	Spacing factor	1	--
$F_{m\_shell}$	Material factor for column	1.7	--
$F_{m\_internal}$	Material factor for internal	8.9	--
$M\&S$	Marshall and Swift index	1200	--
$H_{bt}$	Height between trays	$\begin{cases} 0.5 \text{ m} & \text{if } Diam < 1 \\ 0.6 \text{ m} & \text{if } 1 \leq Diam < 3 \\ 0.75 \text{ m} & \text{if } 3 \leq Diam < 4 \\ 0.9 \text{ m} & \text{if } Diam \geq 4 \end{cases}$	m

$\$COP$	Average market representative exchange rate 2018	2939.22	$COP/US$
$E_{Et/kg}$	Ethanol Price	2198.75	$COP/kg$
$E_{EL/kg}$	Ethyl Lactate Price	5742	$COP/kg$
$E_{LA/kg}$	Lactic Acid Price	3239.50	$COP/kg$
$E_{cat/kg}$	Catalyst Price	184832	$COP/kg$
$E_{KWS}$	Energy Price	505.9/3600	$COP/kws$

#### 4.1.5. Scenarios Selection

During process operation different disturbances can take place. However, for selecting the scenarios to evaluate controllability, only two disturbances were taken account: i) variations on the purity of the ethanol fed to the column, and ii) variations on the purity of the lactic acid fed to the column. In order to check how such disturbances, affect the process in open loop, simulations were run where the purity of lactic acid and the ethanol feed streams were changed. In a first disturbance case, the purity of lactic acid was decreased in 8% (with respect to the nominal case) at time  $t=0$ . The second disturbance case considered the reduction of the ethanol purity in 4% at time  $t=0$ . Each disturbance case was run independently, and each simulation was run for three hours of process to check whether or not such variations on the raw material quality perturbed the dynamic behavior of the main process variables. Simulation results are shown in *Fig. 31* to *Fig. 35*. *Fig. 31* shows the effect of the disturbances on the rectifying zone, mainly, the dynamic behavior of  $T_{rf}$ , which is the temperature at tray 2, when the ethanol concentration (*Fig. 31a*) and the lactic acid concentration (*Fig. 31b*) decreased on their respectively feed streams.

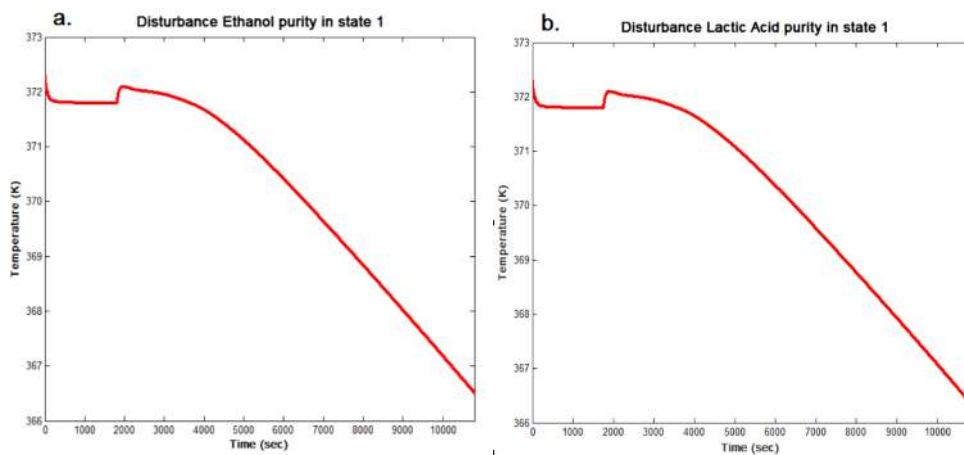


*Fig. 31 Disturbances effects in Rectifying zone*

*a.  $F_{Et_{low\ purity}}$ , b.  $F_{LA_{low\ purity}}$*

Fig. 32 shows the effect of the disturbances on the reactive zone, mainly, the dynamic behavior of  $T_{rxn}$ , which is the temperature at tray  $N_1 + N_2 - 1$  (reactive zone), where the ethanol concentration (Fig. 32a) and the lactic acid concentration (Fig. 32b) decreased on their respectively feed streams.

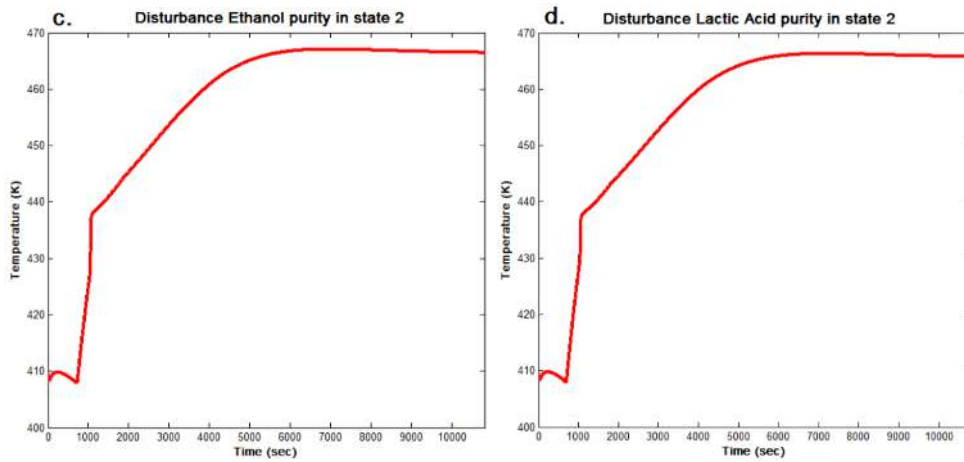


Fig. 32 Disturbances effects in Reactive zone

c.  $F_{Et_{low\ purity}}$ , d.  $F_{LA_{low\ purity}}$

Fig. 33 shows the effect of the disturbances on the stripping zone, mainly, the dynamic behavior of  $T_{st}$ , which is the temperature at tray  $N + 1$ , when the ethanol concentration (Fig. 33a) and the lactic acid concentration (Fig. 33b) decreased on their respectively feed streams.

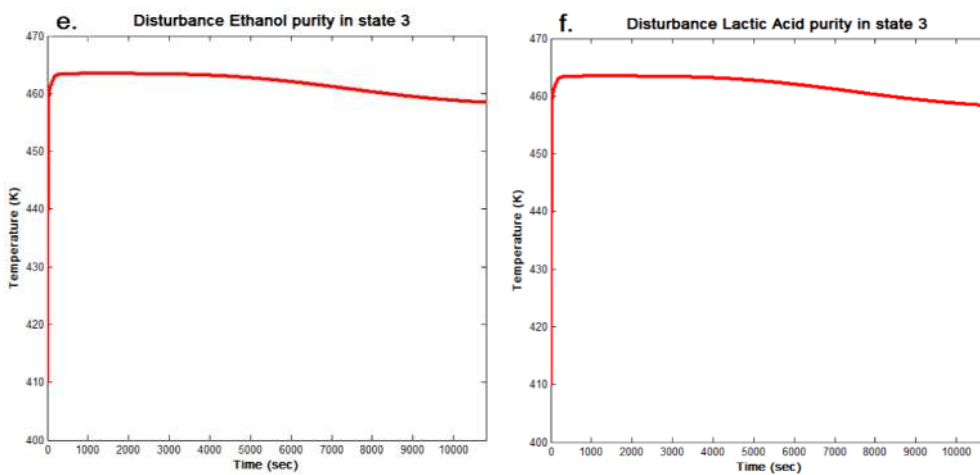


Fig. 33 Disturbances effects in Stripping zone

e.  $F_{Et_{low\ purity}}$ , f.  $F_{LA_{low\ purity}}$

Fig. 34 shows the effect of the disturbances on the condenser level (the level at tray 1), for the ethanol concentration (Fig. 34a) and the lactic acid concentration (Fig. 34b) for the two disturbance cases analyzed.

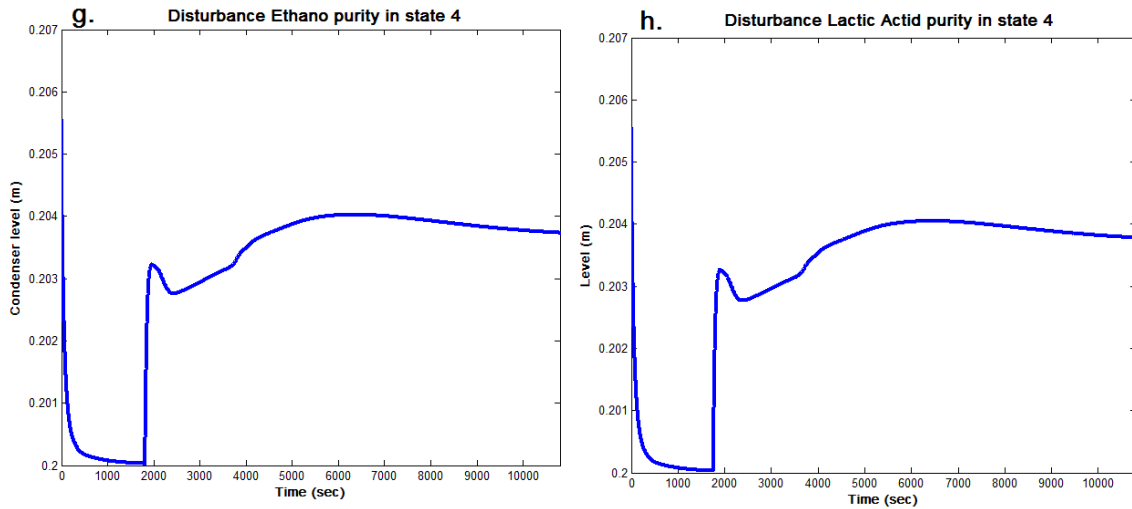


Fig. 34 Disturbances effects in Condenser

g.  $F_{Et_{low\ purity}}$ , h.  $F_{LA_{low\ purity}}$

Fig. 35 shows the effect of the disturbances on the reboiler level (the level at tray  $N + 2$ ), for the ethanol concentration (Fig. 35a) and the lactic acid concentration (Fig. 35b) disturbances on their respectively feed streams.

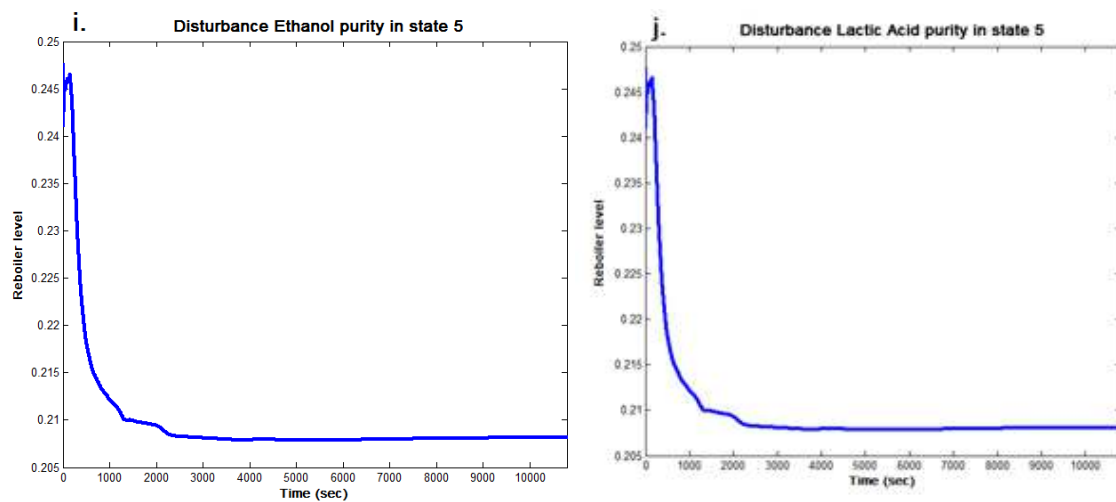


Fig. 35 Disturbances effects in Reboiler

i.  $F_{Et_{low\ purity}}$ , j.  $F_{LA_{low\ purity}}$

After analyzing the simulation results, two scenarios  $E_i$  were selected from which it will be desirable to reach the final desired state and evaluate the capability to do it through lineal trajectories. The scenarios selected are shown in Table 15.

The values reported at the table are those to which the controlled variables  $\mathbf{x}=[T_{rf} T_{rxn} T_{st} l_C l_B]$  converged 10800 s after the system faced the two disturbance analyzed (one at each time), while the process run in open loop.

**Table 15 Scenarios selected for trajectories**

Variable	$F_{Et_{low\ purity}} (E_1)$	$F_{LA_{low\ purity}} (E_2)$
$T_{rf} [K]$	367.72	367.28
$T_{rxn} [K]$	432.97	431.62
$T_{st} [K]$	448.05	447.58
$l_C [m]$	0.2055	0.2055
$l_B [m]$	0.2061	0.2061

#### 4.1.6. Constrained optimization

The constrained optimization problem that will be solved in order to find the solution to the integrated design for the reactive distillation column is stated as follows:

$$\min_{d.v} C_{Total} \quad (Eq. 71)$$

$$s. to \mathbf{d.v}_{lb} < \mathbf{d.v} < \mathbf{d.v}_{ub} \quad (Eq. 72)$$

$$L, V, F > 0 \quad (Eq. 73)$$

$$x_{EL,N+2} \geq 0.85 \quad (Eq. 74)$$

$$B_{EL} \leq 18000 \frac{ton}{year} \quad (Eq. 75)$$

$$M1: D.O.F. \geq 0 \quad (Eq. 76)$$

$$M2: Rank(W_c) = 5 \quad (Eq. 77)$$

$$M3: \quad |Det(G(x))| > 0 \quad (Eq. 78)$$

$$M4: \quad \begin{bmatrix} u_1 \\ u_2 \\ u_3 \\ u_4 \\ u_5 \end{bmatrix}_{min} \leq \begin{bmatrix} u_1^* \\ u_2^* \\ u_3^* \\ u_4^* \\ u_5^* \end{bmatrix} \leq \begin{bmatrix} u_1 \\ u_2 \\ u_3 \\ u_4 \\ u_5 \end{bmatrix}_{max} \quad (Eq. 79)$$

$$M5: \text{Existence of a linear reachability trajectory} \quad (Eq. 80)$$

Where  $\mathbf{d.v}$  is the vector of decision variables (i.e. the solution of the optimization problem). In this case,

$$\mathbf{d.v} = \begin{bmatrix} Diam \\ reb \\ Rat \\ ref \\ m_{cat} \\ N \end{bmatrix} \quad (Eq. 81)$$

Where  $Diam, reb, Rat, ref, m_{cat}$  and  $N$  are the Column diameter, Boilup ratio, Feed molar ratio, Reflux ratio, Total catalyst loading and Total number of trays, respectively.

$C_{Total}$  is the objective function defined in Fig. 29.  $\mathbf{d.v}_{lb}$  and  $\mathbf{d.v}_{ub}$  (Eq. 72) are the lower and upper bounds defined for each decision variable. On the other hand, constraints described by (Eq. 73) are actual physical constraints imposed on the flows of liquid ( $L$ ), vapor ( $V$ ) and the feed ( $F$ ) streams, which can't take negative values. Eq. 74 acts as a constraint for assuring a minimal required quality of the ethyl lactate obtained. For settling such quality constraint, a common reference was taken, which is the purity in which the ethyl lactate is mostly commercialized worldwide. Such reference is the number CAS 687-47-8 (Organics, 2009; Scientific, 2018).

Constraint represented by (Eq. 75) is related to the amount of ethyl lactate per year that will be demanded in Colombia by year 2021. According to Arroyave et al. (2015) in year 2014 the total demand of solvents in Colombia was around 41812 *ton/year* and it is expected that the green solvents demand worldwide increases about 8.3% (Arroyave Restrepo et al., 2015). Furthermore, assuming that the plant will cover a maximum of the 25% of the Colombian requirements, the projected demand to be supplied at year 2021 is:

$$B_{EL} = 41812 \frac{\text{ton}}{\text{year}} * (1 + 0.083) * 0.25 = 18266 \frac{\text{ton}}{\text{year}} \quad (\text{Eq. 82})$$

The last five constraints denoted as  $M1$  to  $M5$  (Eq. 76 to Eq. 80) are the controllability metrics which are included as constraints of the optimization problem. In the following a brief mention about them is given.

### 1. *M1: fulfilling of the Degrees of Freedom*

With the purpose of confirming that the number of available manipulated variables is equal or higher than the number of state variables to be controlled, the control Degrees of Freedom are calculated. In order to fulfill this first metric of practical controllability, such CDOF must be equal or higher than zero. Therefore, metric  $M1$  (constraint Eq. 76) is:

$$M1: \quad CDOF. \geq 0$$

### 2. *M2: Rank of Controllability Matrix*

This controllability metric intends to verify the capacity for reaching the desired states (control objectives), however, this metric doesn't have into account neither the time nor the available interval for the control actions. Therefore, other metrics are included for having these topics into account. Due to the fact that for the case study 5 state variables were selected to be controlled, the second controllability metric  $M2$ , is written as:

$$M2: \quad \text{Rank}(W_c) = 5$$

### 3. *Determinant of Matrix (G(x)) Associated with Forced Response:*

Analyzing the general canonical form (Eq. 5) at a forced equilibrium point  $x^*$  where the states do not change ( $\dot{x} = 0$ ) at least a disturbance takes place, and given the relationship between the states to be controlled and the matrix  $G$  associated with the force response:

$$u^* = -[G(x^*)]^{-1}f(x^*) \quad (\text{Eq. 83})$$

As it can be seen from Eq.83, the  $G$  matrix (associated to the forced response) must be invertible in order to keep the system at the desired equilibrium state. This is evaluated by the third controllability metric,  $M3$ , written as:

$$M3. \quad |Det(G(x))| > 0$$

#### 4. **Forcing Control Action ( $u^*$ ) belonging to the Available Interval of Control Actions ( $U$ )**

The previous metric evaluates the existence of a control action  $u^*$  for allowing keeping the states at a forced equilibrium point. Now, it is necessary to check if the values of the manipulated variables required for keeping that equilibrium point, belong to the available interval defined for the manipulated variables. Therefore, the fourth metric is:

$$M4: \quad \begin{bmatrix} u_1 \\ u_2 \\ u_3 \\ u_4 \\ u_5 \end{bmatrix}_{min} \leq \begin{bmatrix} u_1^* \\ u_2^* \\ u_3^* \\ u_4^* \\ u_5^* \end{bmatrix} \leq \begin{bmatrix} u_1 \\ u_2 \\ u_3 \\ u_4 \\ u_5 \end{bmatrix}_{max}$$

#### 5. **Existence of a linear reachability trajectory:**

When the system is subject to disturbances, the vector of state variables will be forced to move from one operating point to another. To assure that the vector of states variables can be taken back to the original desired state, it must be certified that there exists at least, a trajectory for going back, trajectory that should be driven by the manipulated variables. Therefore, it is imperative to know at least a set of control finite actions that can be used for reaching back the desired equilibrium state  $x^*$  from the starting point  $x_0$ , where the states were “placed” due to the occurrence of a disturbance. Considering that the “shortest path” will be a linear trajectory, and that as mentioned, the control actions that must be taken for going back, must belong to the available interval of control actions, the fifth controllability metric,  $M5$  is given by Eq. 80, fulling he next constraints:

$$u_{2min} \leq u_{T2min1,E} \leq u_{2max} \quad \text{and} \quad u_{3min} \leq u_{T3min1,E} \leq u_{3max} \quad \text{and} \quad u_{4min} \leq u_{T4min1,E} \leq u_{4max} \quad \text{and}$$

$$u_{5min} \leq u_{T5min1,E} \leq u_{5max} \quad \text{and} \quad \Delta t_T > 0$$



Or

$$u_{2min} \leq u_{T2max1,E} \leq u_{2max} \text{ and } u_{3min} \leq u_{T3max1,E} \leq u_{3max} \text{ and } u_{4min} \leq u_{T4max1,E} \leq u_{4max} \text{ and}$$

$$u_{5min} \leq u_{T5max1,E} \leq u_{5max} \text{ and } \Delta t_T > 0$$

Or

$$u_{1min} \leq u_{T1min2,E} \leq u_{1max} \text{ and } u_{3min} \leq u_{T3min2,E} \leq u_{3max} \text{ and } u_{4min} \leq u_{T4min2,E} \leq u_{4max} \text{ and}$$

$$u_{5min} \leq u_{T5min2,E} \leq u_{5max} \text{ and } \Delta t_T > 0$$

Or

$$u_{1min} \leq u_{T1max2,E} \leq u_{1max} \text{ and } u_{3min} \leq u_{T3max2,E} \leq u_{3max} \text{ and } u_{4min} \leq u_{T4max2,E} \leq u_{4max} \text{ and}$$

$$u_{5min} \leq u_{T5max2,E} \leq u_{5max} \text{ and } \Delta t_T > 0$$

Or

$$u_{1min} \leq u_{T1min3,E} \leq u_{1max} \text{ and } u_{2min} \leq u_{T2min3,E} \leq u_{2max} \text{ and } u_{4min} \leq u_{T4min3,E} \leq u_{4max} \text{ and}$$

$$u_{5min} \leq u_{T5min3,E} \leq u_{5max} \text{ and } \Delta t_T > 0$$

Or

$$u_{1min} \leq u_{T1max3,E} \leq u_{1max} \text{ and } u_{2min} \leq u_{T2max3,E} \leq u_{2max} \text{ and } u_{4min} \leq u_{T4max3,E} \leq u_{4max} \text{ and}$$

$$u_{5min} \leq u_{T5max3,E} \leq u_{5max} \text{ and } \Delta t_T > 0$$

Or

$$u_{1min} \leq u_{T1min4,E} \leq u_{1max} \text{ and } u_{2min} \leq u_{T2min4,E} \leq u_{2max} \text{ and } u_{3min} \leq u_{T3min4,E} \leq u_{3max} \text{ and}$$

$$u_{5min} \leq u_{T5min4,E} \leq u_{5max} \text{ and } \Delta t_T > 0$$

Or

$$u_{1min} \leq u_{T1max4,E} \leq u_{1max} \quad \text{and} \quad u_{2min} \leq u_{T2max4,E} \leq u_{2max} \quad \text{and} \quad u_{3min} \leq u_{T3max4,E} \leq u_{3max} \quad \text{and}$$

$$u_{5min} \leq u_{T5max4,E} \leq u_{5max} \quad \text{and} \quad \Delta t_T > 0$$

Or

$$u_{1min} \leq u_{T1min5,E} \leq u_{1max} \quad \text{and} \quad u_{2min} \leq u_{T2min5,E} \leq u_{2max} \quad \text{and} \quad u_{3min} \leq u_{T3min5,E} \leq u_{3max} \quad \text{and}$$

$$u_{4min} \leq u_{T4min5,E} \leq u_{4max} \quad \text{and} \quad \Delta t_T > 0$$

Or

$$u_{1min} \leq u_{T1max5,E} \leq u_{1max} \quad \text{and} \quad u_{2min} \leq u_{T2max5,E} \leq u_{2max} \quad \text{and} \quad u_{3min} \leq u_{T3max5,E} \leq u_{3max} \quad \text{and}$$

$$u_{4min} \leq u_{T4max5,E} \leq u_{4max} \quad \text{and} \quad \Delta t_T > 0$$

Where,

$$u_{Timinj,E} = u_{0i}^* + (u_{minj} - u_{0j}^*) \frac{du_i}{du_j} \quad (\text{Eq. 84})$$

$$u_{Timaxj,E} = u_{0i}^* + (u_{maxj} - u_{0j}^*) \frac{du_i}{du_j} \quad (\text{Eq. 85})$$

$$\Delta t_T = \frac{du_i}{u_{Ti} - u_{0i}^*} \quad (\text{Eq. 86})$$

#### 4.1.7. Control system Design

The control system design was developed according to what is usually proposed in the literature for reactive distillation columns, specially by references (W. L. Luyben & Yu, 2009; Sundmacher & Kienle, 2006). An important variation to the typical control scheme is that the override control strategy is included here. Such strategy is used for:

- Keeping the level in the condenser between a desired range (max-min) while controlling the optimal reflux ratio (*ref*).
- Keeping the level at the bottom between a desired range (max-min) while controlling the optimal boil-up ratio (*reb*).

In both cases, the nominal control loop (e.g. the control of the reflux ratio and the boil-up ratio) is overridden when the level goes outside the pre-defined limits.

The control loops defined are feedback PI. For controller tuning, open loop identification was used in order to obtain the process gain ( $K_p$ ), the time constant ( $\tau$ ) and dead time ( $\theta$ ). Then, Ciancone correlations for disturbance response were used for finding the controller gain ( $K_c$ ) and the integral time ( $T_I$ ) (Marlin, 2015; Smith & Corripio, 2012). The general PI equation implemented in the simulations is given by Eq. 87

$$u_i = u_{sp,i} + K_{c_i} * Error_i + \frac{K_{c_i}}{T_{I,i}} * Ercum_i \quad (\text{Eq. 87})$$

$$Error_i = x_{sp,i} - x_i \quad (\text{Eq. 88})$$

$$Ercum_i = \sum_{t=0} Error_i(t) \quad (\text{Eq. 89})$$

Where  $Error_i$  and  $Ercum_i$  are the error and cumulative error respectively.

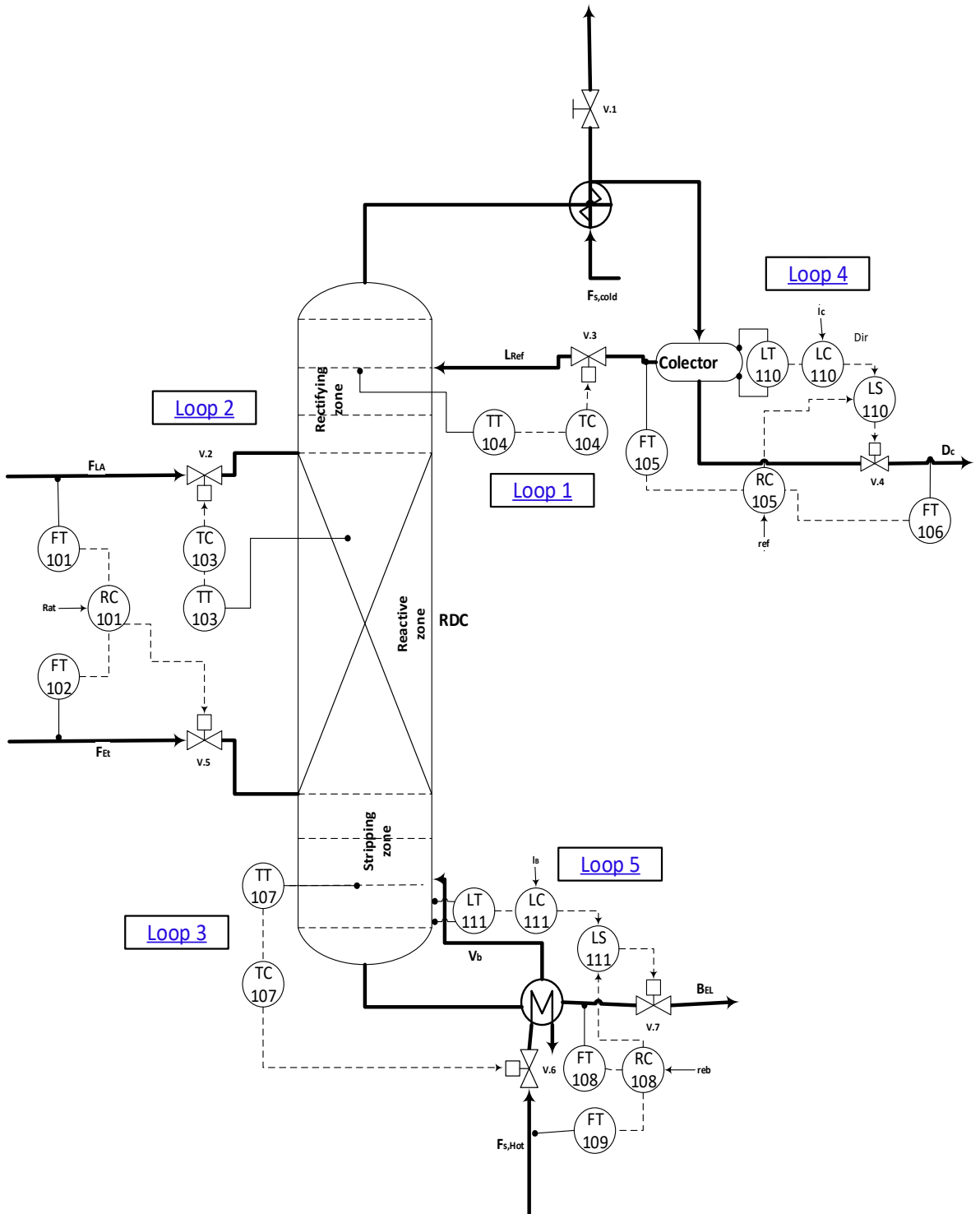


Fig. 36 Control loops for the Reactive Distillation Column

## 4.2. Results

### 4.2.1. Constrained optimization problem

The optimization problem was solved using the simulated annealing algorithm. Each optimization was repeated several times to obtain a near-global optimum, starting from different seed values. The solution reporting the minimal cost (maximal utility) was taken as the actual problem solution (e.g. the optimal values for the decision variables). Table 16 shows the optimal results, the corresponding value for the objective function resulted in a profit, this optimal value was reached considering a ratio of three to one between the number of trays in the rectification and the stripping sections ( $R_{zone} = 3/1$ ). It is important to mention that even though a common heuristic used in the design of distillation columns is to predefine a ratio between the diameter and the column height, the optimal results found here didn't consider such kind of heuristics. The reason for that is that when such constraint was considered, it was not possible to meet the quality constraint on the ethyl lactate purity; this will be shown in

Table 18.

Table 16 Optimal decision variables

<b><i>Diam</i> [m]</b>	<b><i>reb</i></b>	<b><i>Rat</i></b>	<b><i>ref</i></b>	<b><i>m<sub>cat</sub></i> [kg]</b>	<b><i>N</i></b>
0.97	2.39	1.27	1.94	719.48	29

It is important to mention that the optimal point presented in Table 16 fulfills all the constraints (operability, purity and controllability) described by Eq. 71 – 80. The above-mentioned ratio between the number of trays in the rectification and the stripping sections is denoted as  $R_{zone}$ , which is mathematically expressed as:

$$R_{zone} = \frac{N_{rf}}{N_{st}} \quad (Eq. 90)$$

Prior to find the optimal results shown in Table 16, different optimization runs were evaluated in order to find a suitable value for the  $R_{zone}$ . Results of the optimization varying the  $R_{zone}$  are shown in

Table 17. These results allow analyzing different scenarios for the construction of the equipment that could affect positively or negatively the purity and efficiency of the process. *Fig. 37* shows graphically a comparison for the best optimization results at each of the evaluated  $R_{zone}$  (1:4, 1:3, 1:2, 1:1, 2:1, 3:1 and 4:1). From

Table 17 and Fig. 37, it is possible to see that the best objective function values reached are for  $R_{zone} = 3/1$  and  $R_{zone} = 4/1$ , where the former is the one with the highest profit fulfilling all the constraints.

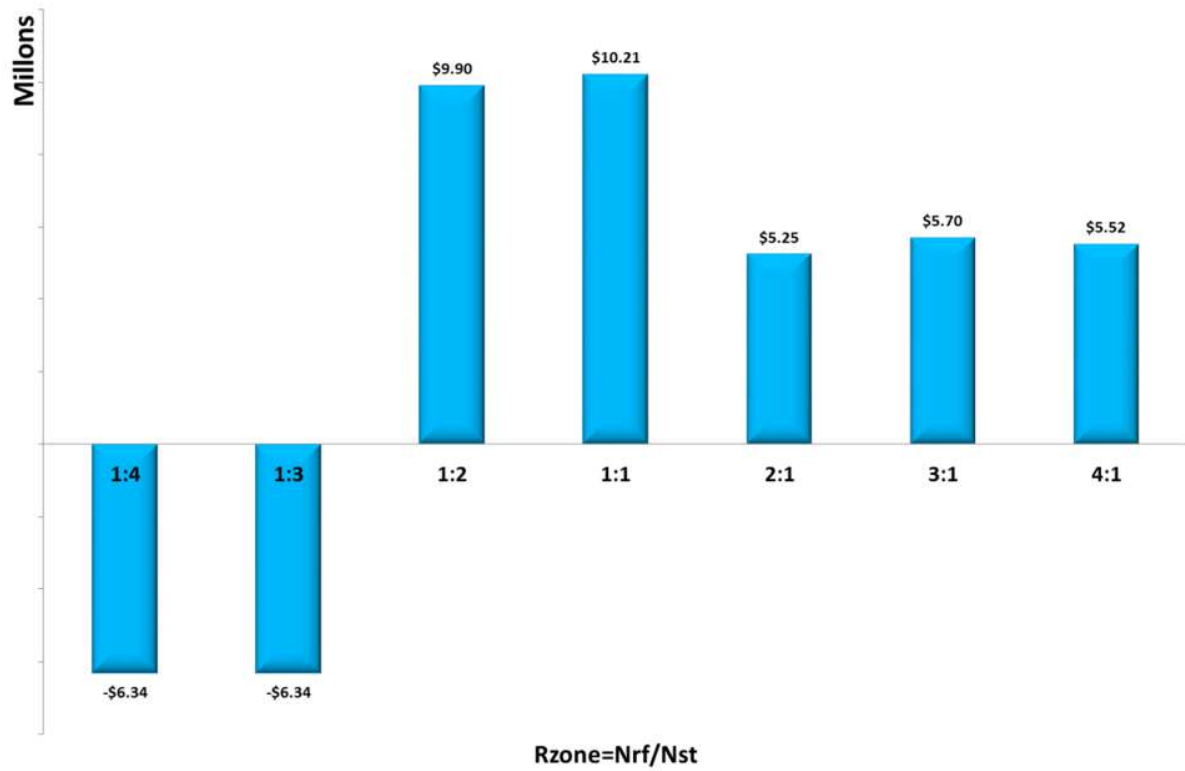


Fig. 37 Optimization results for integrated design in function of  $R_{zone}$  in \$USD



Table 17 Comparison of results for integrated design in function of Rzone

$R_{zone}$	1:4	1:3	1:2	1:1	2:1	3:1	4:1
<b>Decision variables</b>							
$Diam$ [m]	3.35	3.35	1.30	1.14	1.23	0.97	0.97
$reb$	1.02	1.02	1.08	2.37	2.33	2.39	2.39
$Rat$	1.00	1.00	1.00	1.44	1.40	1.27	1.27
$ref$	2.14	2.14	1.76	2.24	1.83	1.94	1.94
$m_{cat}$ [kg]	434.33	434.33	652.85	635.99	694.63	719.48	719.48
$N$	17	17	39	25	33	29	29
<b>Dimensional results</b>							
$N_{rf}$	4	4	10	7	15	6	7
$N_{rxn}$	1	1	9	11	11	21	21
$N_{st}$	12	12	20	7	7	2	1
$H_{bt}$ [m]	0.75	0.75	0.60	0.60	0.60	0.50	0.50
$H_T$ [m]	12.75	12.75	23.40	15.00	19.80	14.50	25.80
$\frac{H_T}{Diam}$	4	4	18	13	16	15	15
<b>Operational results</b>							
$x_{EL,N+2}$	0.24	0.24	0.74	0.93	0.96	0.99	0.98
$\frac{B_{EL}}{[year]}$ [ton]	7402.89	7402.89	15862.36	16749.88	14900.64	14774.82	14689.33
<b>Controllability results</b>							
$M2$	5.00	5.00	5.00	5.00	5.00	5.00	5.00
$M3$	0.0000	0.0000	0.0000	0.0041	0.0005	0.0150	0.0090
$M4(u_1)$	0.0164	0.0164	0.0143	0.0077	0.0099	0.0097	0.0097
$M4(u_2)$	0.0029	0.0029	0.0029	0.0029	0.0029	0.0029	0.0029
$M4(u_3)$	49830.46	49830.46	49736.95	49436.71	49541.57	49544.34	49543.74
$M4(u_4)$	0.0054	0.0054	0.0039	0.0016	0.0016	0.0018	0.0018
$M4(u_5)$	0.0135	0.0135	0.0116	0.0113	0.0122	0.0122	0.0122
$M5$	Not Fulfil	Not Fulfil	Not Fulfil	Not Fulfil	Not Fulfil	Fulfil	Fulfil
<b>Economical results</b>							
$Utility$ (MUSD\$)	-\$6336	-\$6336	\$9904	\$10 207	\$5246	\$5696	\$5522
$C_{RDC,Bu}$ (MUSD\$)	\$99.727	\$99.727	\$105.257	\$92.318	\$105.227	\$100.533	\$100.533
$C_{RDC,Op}$ (MUSD\$)	-\$6236	-\$6236	\$10 010	\$10 299	\$5351	\$5797	\$5623

Although the profits reached for  $R_{zone} = 3/1$  and  $R_{zone} = 4/1$  are quite similar, there are some important advantages of the former with respect to the latter, as follows:

- Using the  $R_{zone} = 3/1$ , resulted in a product with a higher purity (0.99). Although it is important to notice that such advantage did not have an impact on the results, because the objective function used considered that the product (ethyl lactate) will have the same selling price independently of its purity.
- Both  $R_{zone}$  reached the same value for decision variables, however the results in purity and utility are better for  $R_{zone} = 3/1$ , this shows that the distribution of the trays in each zone has an influence on the final results of productivity and efficiency.

As mentioned before, the optimization runs that led to the results shown in Table 16, as well as the reported when varying  $R_{zone}$  (

Table 17) did not include a commonly heuristic criteria used traditionally in the design of distillation columns, the ratio  $H_T/Diam$ , which is usually recommended to be fixed in a value of five for vessel (Elizondo, 2007; Turton, Bailie, Whiting, & Shaeiwitz, 2008). However, it is important to mention that during the first optimization runs, such heuristic recommendation was indeed included as a constraint given by  $H_T/Diam = 5$ , and therefore, for that runs, the total numbers of trays were not taken as decision variable.

Table 18 shows the obtained results when the mentioned heuristic was used as constraint. As it can be seen, for most values of  $R_{zone}$ , the optimization was suddenly broken because the quality constraint (Eq. 74) was not fulfilled. An optimal value fulfilling all the constraints was only reached for the case of  $R_{zone} = 4/1$ . Therefore, it is concluded that the traditional heuristic criteria limited (at least in this case) the solution of the optimization problem.

Table 18 Optimization results with heuristic  $H_T/Diam = 5$  for integrated design

$R_{zone}$	$Diam$ [m]	$reb$	$Rat$	$ref$	$m_{cat}$ [kg]	Broken criterion
1:4	1.29	2.18	1.00	2.17	502.88	Desired quality specifications
1:3	1.29	2.18	1.00	2.17	502.88	Desired quality specifications
1:2	2.75	1.93	1.39	1.93	444.85	Desired quality specifications
1:1	2.75	1.93	1.39	1.93	444.85	Desired quality specifications
2:1	2.35	2.00	1.00	2.10	584.67	Desired quality specifications
3:1	2.35	2.00	1.00	2.10	584.67	Desired quality specifications
4:1	2.46	1.33	1.74	1.97	586.90	Neither

For closing this section, it is important to notice that the obtained results show the importance to use a higher number of trays in the rectification zone, in order to assure that the product of interest (in this case the heavy), didn't leave the column at the top, improving its purity at the bottom section.

#### 4.2.2. Results of the Control System Implementation

The control loops shown in *Fig. 36* were implemented for the optimal design selected in  $R_{zone} = 3/1$ . The tuning parameters for each controller were obtained using the Ciancone correlations for disturbance response and are shown in Table 19.

Table 19 Tuning parameters for PI controllers

Control loop	1	2	3	4	5
Controlled Variable	$x_1 (T_{rf})$	$x_2 (T_{rxn})$	$x_3 (T_{st})$	$x_4 (l_C)$	$x_5 (l_B)$
Manipulated variable	$u_1 (L_{Ref})$	$u_2 (F_{LA})$	$u_3 (Q_B)$	$u_4 (D_C)$	$u_5 (B_{EL})$
$K_c$	-0.0020	9.10E-06	412.9724	-0.7285	-0.0405
$T_I$ [sec]	194.40	59948.60	1542.33	68.40	1090.43

The closed-loop behavior is shown in *Fig. 38* to *Fig. 42*, when facing a disturbance in the purity of the Lactic acid feed stream that take place at  $t=10$  hours. As shown in the figures, the control structure proposed in *Fig. 36* is able to keep the process controlled (e.g. the controlled temperatures were kept at the setpoints while the levels are kept inside the desired range).

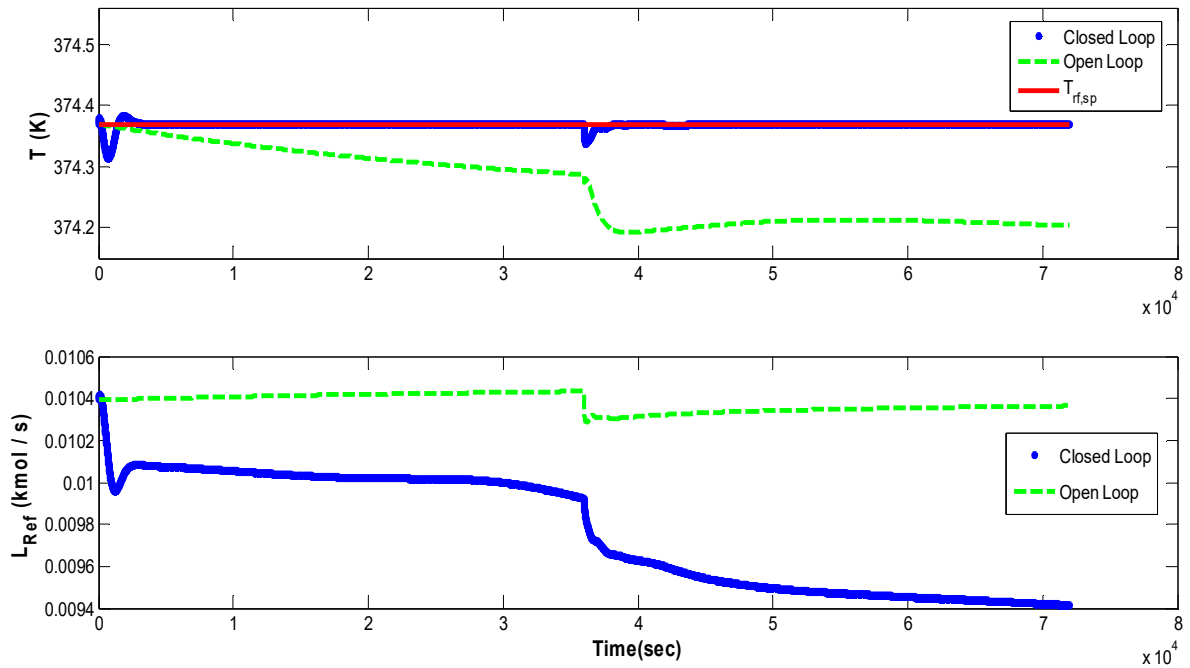


*Fig. 38* Temperature control in Rectifying zone ( $x_1$ ). Temperature in tray 2 (top) and Reflux flow rate (bottom)

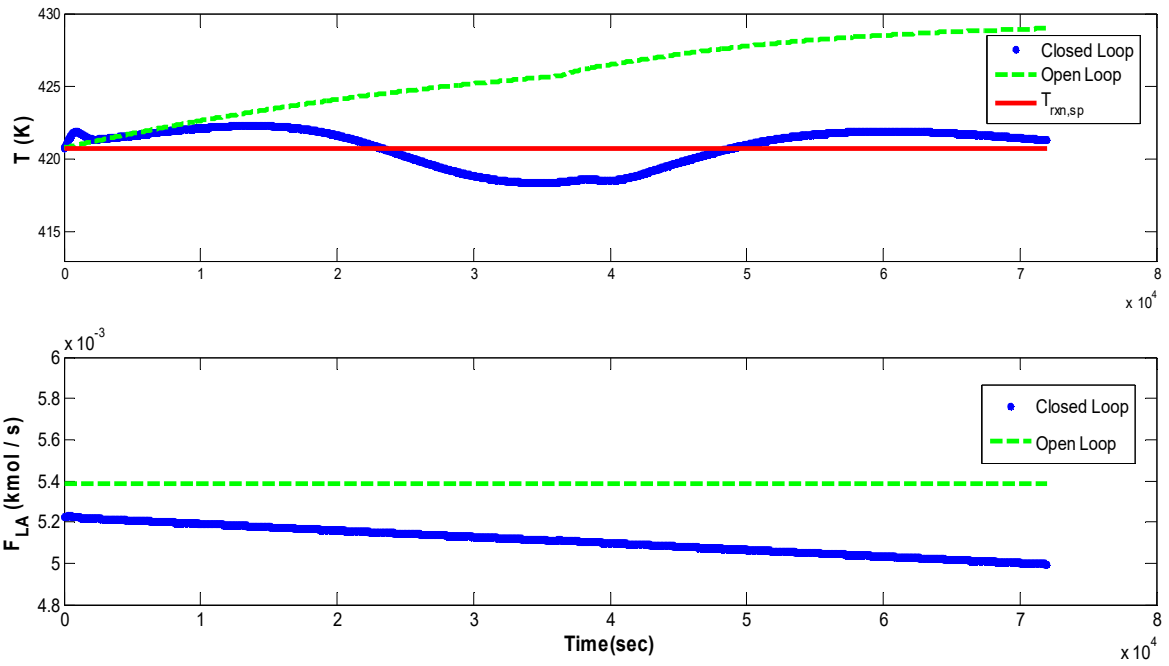


Fig. 39 Temperature control in Reactive zone ( $x_2$ ). Temperature in tray  $N_1 + N_2 - 1$  (top) and Lactic Acid feed stream (bottom)

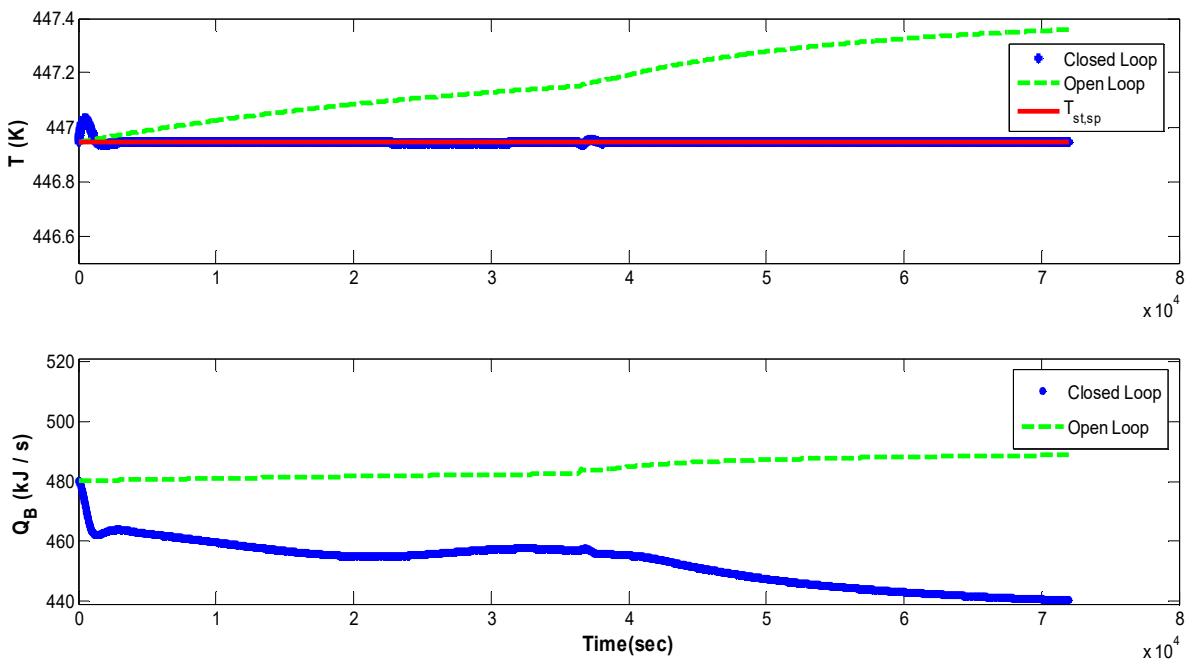
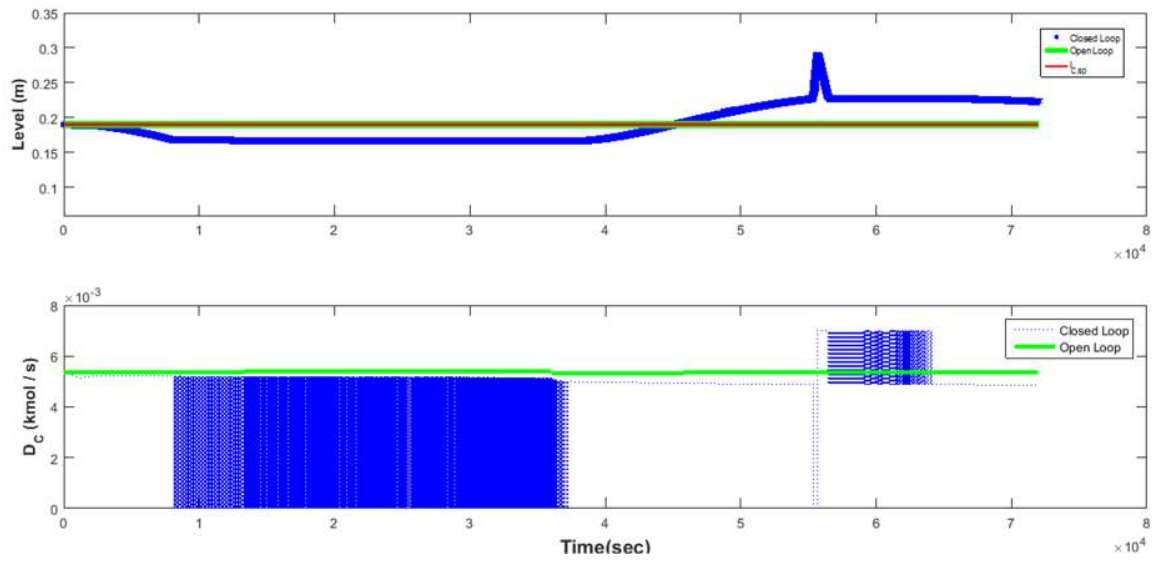
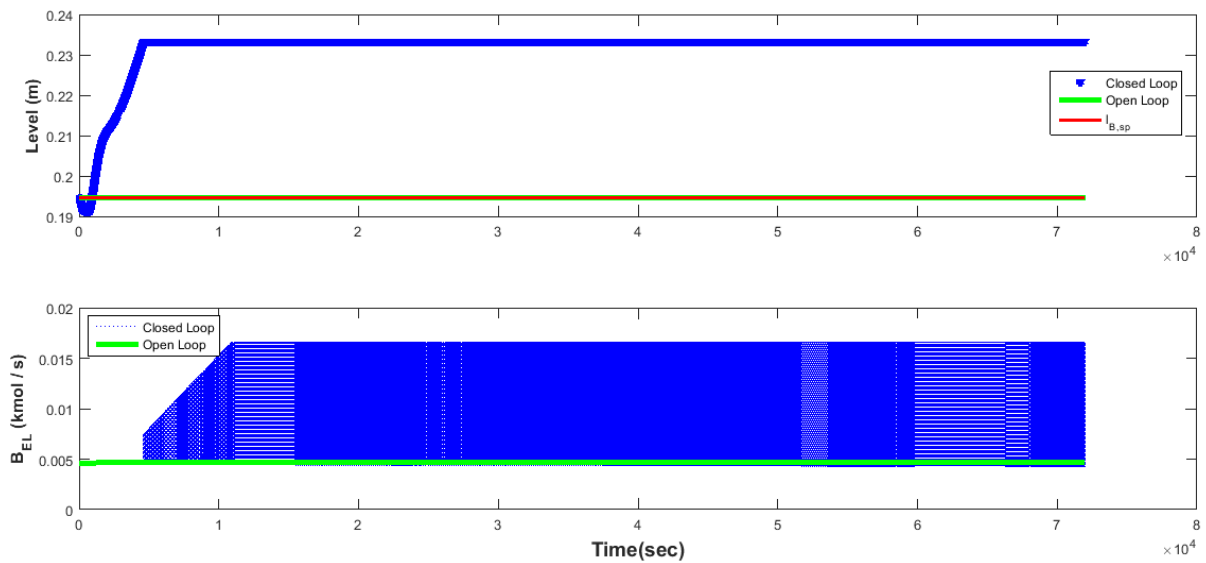


Fig. 40 Temperature control in Stripping zone ( $x_3$ ). Temperature in tray  $N+1$  (top) and Reboiler heat duty (bottom)



**Fig. 41** Level control in the Condenser ( $x_4$ ). Condenser level (top) and Flow of Distillate (bottom)



**Fig. 42** Level control in the Reboiler ( $x_5$ ). Reboiler level (top) and Flow of Bottoms (bottom)

For the case of *Fig. 41* and *Fig. 42* the controllers have behavior like an on-off controller, this is due mainly that the collector and reboiler are modeling as trays, so the dimensions are not the best in this kind of equipment, particularly for the  $H_{weir}$  doing that a small variation in the Distillation and Bottom flows generates a big change in the levels, which requires that the manipulated variable keeps in constant opening and closing of the final control element.



## 5. COMPARISON: INTEGRATED vs. TRADITIONAL SEQUENTIAL DESIGN

In order to compare the design results obtained when the design-control integration methodology is used (applying the practical controllability concept and metrics) against the results when traditional sequential design is applied, optimization was carried out applying traditional design methodology, using the model proposed in chapter 3 and the premises obtained in the same chapter during the validation and sensitivity analysis.

*Fig. 43.* shows the flow diagram that describes the algorithm followed in this work in general for process design (both, traditional and integrated design). As it can be seen, traditional design and integrated design share some algorithm steps. The main difference between both is that the integrated design imposes some additional constraints, which correspond to the controllability metrics mentioned in sub-sections 2.3.6 and 4.1.6. The optimization problem for the traditional design is stated in *Eq. 91 to Eq. 95*, where the objective function is the cost function given in *Fig. 29*; however, as shown in *Fig. 43*, only physical constraints (*Eq. 92*), quality and product specification constraints (*Eq. 94 and Eq. 95*) are used as constraints in this case.

$$\min_{d,v} C_{Total} \quad (Eq. 91)$$

$$s. to \mathbf{d.v}_{lb} < \mathbf{d.v} < \mathbf{d.v}_{ub} \quad (Eq. 92)$$

$$L, V, F > 0 \quad (Eq. 93)$$

$$x_{EL,N+2} \geq 0.85 \quad (Eq. 94)$$

$$B_{EL} \leq 18000 \frac{ton}{year} \quad (Eq. 95)$$

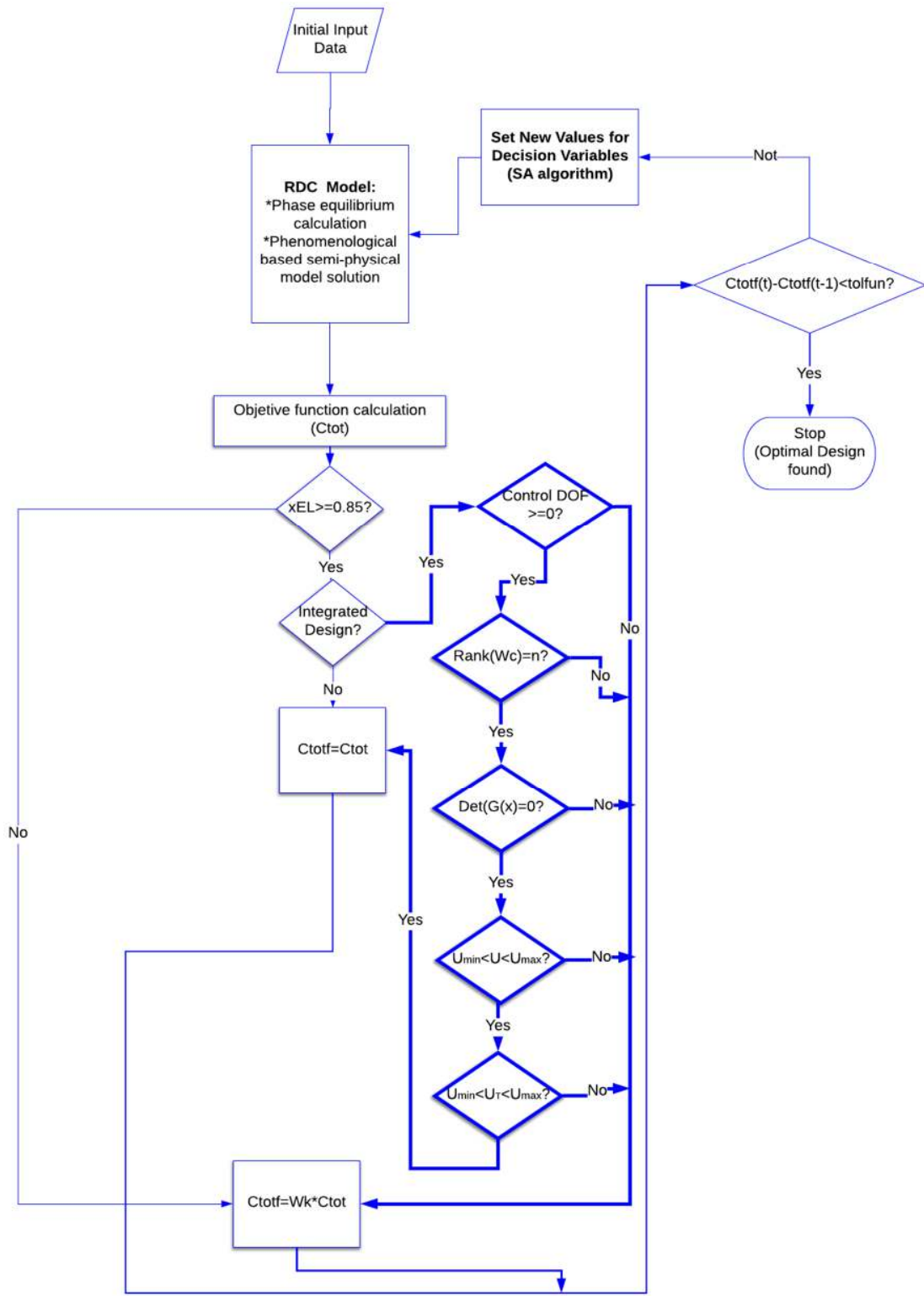


**Fig. 43 General Process Design Algorithm (for Traditional and Integrated Design): Thicker lines indicate steps that are exclusive for Integrated Design Procedure.**

## 5.1. Optimization results for traditional design

For the traditional design, similar runs were performed as in the integrated design case, in order to determine the most suitable  $R_{zone}$ , and also considering and without considering the typical heuristic constraint on the height/ diameter ratio. The best results of the optimization (obtained for a  $R_{zone} = 3/1$ ) were found at a profit too. This set of decision variables is shown in Table 20.

Table 20 Optimal values of decision variables for the traditional design

<i>Diam</i> [m]	<i>reb</i>	<i>Rat</i>	<i>ref</i>	<i>m<sub>cat</sub></i> [kg]	<i>N</i>
1.69	1.85	2.00	1.61	254.14	41

## 5.2. Integrated vs Traditional design

*Fig. 44* shows the results for the profit obtained for the different  $R_{zone}$  tested for both, integrated design and traditional design without heuristic restriction on the length/diameter ratio. Although the traditional design resulted in a higher profit in most compared cases, it will be seen later that the integrated design leads to some advantages/ differences that could be useful for the decision-making during a project evaluation. Furthermore, traditional design failed to obtain a global optimum for the case of  $R_{zone} = 1/2$ . It can also be seen that the fact that the best optimum is located in the  $R_{zone} = 3/1$  for both designs (integrated and traditional), shows that this distribution of the purification stages could be more appropriated for the case studied here.

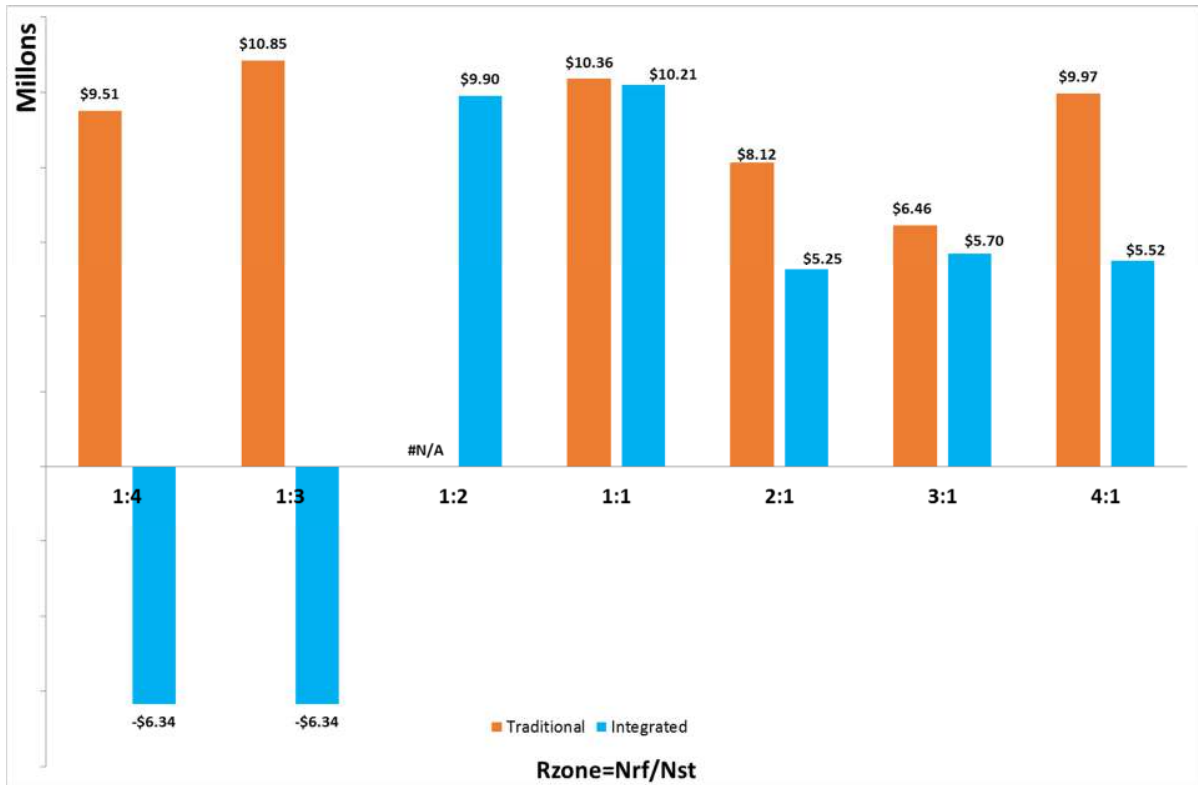


Fig. 44 Profit comparison for integrated and traditional design in \$USD

It must be noticed that the controllability metrics were not used as constraints during the optimization step of the traditional design, but for the sake of comparison, they were evaluated after obtaining the design results. Table 21 presents a comparative summary of the results for the dimensional, operational, controllability and economic parameters, as well as the calculation of a structural stability indicator  $H_T/Diam$ . Besides the economic performance mentioned in the previous paragraph, and taking into account that several of these variables are important during the development of a project, it can be observed from Table 21, that:

- Analyzing the results, it is possible to observe that the traditional design was not able to fulfill all the established requirements (constraints). Including one distribution (1:2) that doesn't reach a global optimum. The

- Table 18 and Table 22 show the broken criterion for each case.
- In four from the seven  $R_{zone}$  values tested; it was not possible to reach the desired purity by the traditional design. For the integrated design this happened for three  $R_{zone}$  values. It can also be seen that the integrated design allows having a good behavior in terms of purity, for each proposed distribution when the number of trays at the rectifying section is higher or equal to the number of trays at the stripping zone. The purity values reached are always higher in the results by the integrated design, so this product could be commercialized to a better price.
- With respect to the first four metrics, it is important to clarify that all the results of the integrated design kept the design between the ranges of operability of the process, in the case of the traditional methodology were did simulations including the calculate of the metrics, however this approach could not assure it for the whole time for all the  $R_{zone}$  values tested.
- In  $R_{zone} = 2/1$  and  $R_{zone} = 3/1$  the results obtained for controllability metric M4 (belonging of forcing control action to the available interval) were lower than zero in some moments of the simulation for the traditional design, particularly in the first hour of operation, and therefore it did not fulfill the fourth practical local controllability metric.
- Most of the  $R_{zone}$  values tested violated the fifth metric (M5, existence of a reachability trajectory), for both, the traditional and the integrated design methodologies (although in more cases for the traditional). For those cases, this means that there is no guarantee of the existence of a linear trajectory for taking back the state variables to the desired set point for the analyzed disturbance scenarios. However, a nonlinear trajectory could exist. Taking this into account, considering hypothetically that there could exist a nonlinear trajectory,  $R_{zone} = 1/1$  for the integrated design shows the best characteristics (fulfillment of the other 4 metrics with higher purity and profit).
- Regarding the ratio of the height and column diameter used as an indicator of structural stability and not as a heuristic constraint, it was found that for the best optimum ( $R_{zone} = 3/1$ ), this ratio is around 14.91 and 14.54 for the integrated design and the traditional design respectively. Therefore, the designs obtained have similar structural behavior.

Table 21 Comparison results for Integrated (Int.) and Traditional (Trad.) design

$R_{zone}$	1:4		1:3		1:2		1:1		2:1		3:1		4:1	
Method.	Int.	Trad.	Int.	Trad.	Int.	Trad.	Int.	Trad.	Int.	Trad.	Int.	Trad.	Int.	Trad.
<b>Decision variables</b>														
$Diam[m]$	3.35	0.85	3.35	1.01	1.30	N.A.	1.14	0.82	1.23	1.63	0.97	1.69	0.97	1.04
$reb$	1.02	1.86	1.02	1.36	1.08	N.A.	2.37	1.76	2.33	1.78	2.39	1.85	2.39	0.91
$Rat$	1.00	1.34	1.00	1.07	1.00	N.A.	1.44	1.36	1.40	1.98	1.27	2.00	1.27	1.30
$ref$	2.14	1.86	2.14	2.06	1.76	N.A.	2.24	2.30	1.83	1.61	1.94	1.61	1.94	1.64
$m_{cat} [kg]$	434.33	450.87	434.33	410.09	652.85	N.A.	635.99	304.81	694.63	281.32	719.48	254.14	719.48	650.42
$N$	17.00	37.00	17.00	27.00	39.00	N.A.	25.00	28.00	33.00	41.00	29.00	41.00	29.00	25.00
<b>Dimensional results</b>														
$N_{rf}$	4.00	4.00	4.00	5.00	10.00	N.A.	7.00	8.00	15.00	26.00	6.00	30.00	7.00	9.00
$N_{rxn}$	1.00	17.00	1.00	9.00	9.00	N.A.	11.00	13.00	11.00	3.00	21.00	2.00	21.00	14.00
$N_{st}$	12.00	16.00	12.00	13.00	20.00	N.A.	7.00	7.00	7.00	12.00	2.00	9.00	1.00	2.00
$H_{bt} [m]$	0.75	0.50	0.75	0.60	0.60	N.A.	0.60	0.50	0.60	0.60	0.50	0.60	0.50	0.60
$H_T [m]$	12.75	18.50	12.75	16.20	23.40	N.A.	15.00	14.00	19.80	24.60	14.50	24.60	25.80	15.00
$\frac{H_T}{Diam}$	3.80	21.81	3.80	16.04	18.06	N.A.	13.13	17.06	16.12	15.10	14.91	14.54	15.00	14.39
<b>Operational results</b>														
$x_{EL,N+2}$	0.24	0.92	0.24	0.76	0.74	N.A.	0.93	0.75	0.96	0.97	0.99	0.93	0.98	0.79
$B_{EL} \left[ \frac{ton}{year} \right]$	7402.89	16836.32	7402.89	16655.68	15862.36	N.A.	16749.88	17326.79	14900.64	17919.73	14774.82	17126.26	14689.33	16714.86
<b>Controllability results</b>														
$M2$	5.0000	5.0000	5.0000	5.0000	5.0000	N.A.	5.0000	5.0000	5.0000	5.0000	5.0000	5.0000	5.0000	5.0000
$M3$	2.00E-09	5.85E-02	2.00E-09	4.05E-03	-1.32E-05	N.A.	4.15E-03	8.81E-02	5.15E-04	1.01E-06	1.50E-02	2.17E-05	9.01E-03	3.05E-04
$M4(u_1)$	0.0164	0.0101	0.0164	0.0123	0.0143	N.A.	0.0077	0.0088	0.0099	0.0091	0.0097	0.0095	0.0097	0.0136
$M4(u_2)$	0.0029	0.0029	0.0029	0.0029	0.0029	N.A.	0.0029	0.0029	0.0029	0.0029	0.0029	0.0029	0.0029	0.0029
$M4(u_3)$	49830.46	49575.93	49830.46	49652.08	49736.95	N.A.	49436.71	49532.03	49541.57	49581.77	49544.34	49573.18	49543.74	49777.02
$M4(u_4)$	0.0054	0.0018	0.0054	0.0034	0.0039	N.A.	0.0016	0.0022	0.0016	0.0004	0.0018	0.0007	0.0018	0.0033
$M4(u_5)$	0.0135	0.0114	0.0135	0.0111	0.0116	N.A.	0.0113	0.0106	0.0122	0.0113	0.0122	0.0115	0.0122	0.0110
$M5$	Not Fulfilled	Not Fulfilled	Not Fulfilled	Not Fulfilled	Not Fulfilled	N.A.	Not Fulfilled	Not Fulfilled	Not Fulfilled	Not Fulfilled	Fulfilled	Fulfilled	Fulfilled	Not Fulfilled
<b>Controllability Metrics Not Fulfilled</b>														
Metrics	M5	M5	M5	M5	M5	N.A.	M5	M5	M5	M4, M5	None	M4	None	M5
<b>Economical results</b>														
Utility (MUSD\$)	-\$6336	\$9506	-\$6336	\$10 852	\$9904	N.A.	\$10 207	\$10 356	\$5246	\$8121	\$5696	\$6460	\$5522	\$9974
$C_{RDC,Bu}$ (MUSD\$)	\$99.727	\$67.986	\$99.727	\$63.349	\$105.258	N.A.	\$92.318	\$46.426	\$105.228	\$69.984	\$100.533	\$68.497	\$100.533	\$93.007
$C_{RDC,op}$ (MUSD\$)	-\$6236	\$9574	-\$6236	\$10 916	\$10 010	N.A.	\$10 299	\$10 403	\$5351	\$8191	\$5797	\$6529	\$5623	\$10 067

Table 22 shows the optimization results for the traditional design when the heuristic height/diameter ratio was included as constraint. It is important to remind that when such constraint is used, the total number of trays is no longer a decision variable. As in the case for the integrated design, when introducing the height/diameter constraint, it was not possible to reach the desired criteria, mainly in terms of the reached product quality.

Table 22 Optimization results with heuristic  $H_T/Diam = 5$  for traditional design

$R_{zone}$	$Diam$ [m]	$reb$	$Rat$	$ref$	$m_{cat}$ [kg]	Broken criterion
1:4	0.87	2.87	1.09	2.03	209.64	Desired quality specifications
1:3	2.40	2.30	1.49	2.06	547.35	Desired quality specifications
1:2	1.92	1.85	2.10	1.93	600.79	Desired quality specifications
1:1	1.60	2.37	1.79	1.83	482.65	Desired quality specifications
2:1	2.35	2.00	1.00	2.10	584.67	Desired quality specifications
3:1	2.35	2.00	1.00	2.10	584.67	Desired quality specifications
4:1	2.35	2.00	1.00	2.10	584.67	Desired quality specifications

Analyzing the results, it is possible to conclude that applying the integrated design methodology to the case study "Ethyl Lactate production from Lactic Acid and Ethanol in a reactive distillation column", it is possible to obtain a design driven to a higher product quality while ensuring the controllability of the process.

## 6. CONCLUSIONS AND FUTURE RESEARCH

- The developed model for predicting the dynamic behavior of the main state variables in a reactive distillation column for ethyl lactate production is a robust and suitable tool for being used in the process design and control system design of the process. This model included reaction mechanisms that fitted better the reaction kinetics for the case studied. Furthermore, the model can be easily adapted to reactive distillation systems where reactions of the type  $aA + bB \leftrightarrow cC + dD$  take place.
- Although both, the obtained results by a traditional design methodology and by the integrated design resulted in a positive profit, it must be noticed that results indicate that the integrated methodology applied in this case properly addresses the combination of decision variables to reach the global optimum, while, for the former case, it was not always possible to converge to a global optimum; although the traditional design fulfilled the function tolerance established like a stopping criteria, none reached the same optimal point from different initial point proved. In contrast, constraints imposed at the integrated design (controllability metrics) directed the optimization towards different optimization regions, resulting in higher purity and profit for most of the  $R_{zone}$  values tested. This allowed a wider analysis for evaluating the feasibility and selecting a process design, without increasing significantly the computational load.
- A control system was designed for the best optimum obtained when comparing the different  $R_{zone}$ , the decisions taken for such control design and the results allow to conclude that:
  - The control structure proposed is adequate to keep the behavior of the main process variables closed to the optimal point (in terms of profit and purity). The override control strategy allowed to keep the reflux ratio and the boil-up ratio close to their optimal values, while assuring safe values for the level at the condenser and at the bottoms of the column.
  - PI controllers can be used for keeping the controlled variables at their set points, in an easy way, which is due to the fact that the practical controllability was already assured during the process design.



### **6.1. Future Work:**

- To Develop an interface for the proposed phenomenological model and simulation algorithm, as a guide, in order to allow the interaction of any user to optimize his/her own case study, for a reactive distillation system with reactions of the type  $aA + bB \leftrightarrow cC + dD$ , through both methodologies, namely integrated design-control in the state space and the traditional one.
- Expand the optimization of the model to other decision variables, such as the location of the feeding points, the number of trays per zone (not as a relation), among other parameters that could also affect the profit for this type of process.
- To incorporate the evaluation of some nonlinear trajectories in order to complement the fifth controllability metric.

## REFERENCES

- Albright, L. (2008). *Albright's chemical engineering handbook*: CRC Press.
- Alvarado-Morales, M., Hamid, M. K. A., Sin, G., Gernaey, K. V., Woodley, J. M., & Gani, R. (2010). A model-based methodology for simultaneous design and control of a bioethanol production process. *Computers & Chemical Engineering*, 34(12), 2043-2061. doi:10.1016/j.compchemeng.2010.07.003
- ARGENTINA, I. (2014). Tabla de compatibilidad química. Retrieved from <http://www.pfenniger.cl/indesur/Compatibilidad%20qu%C3%ADmica.pdf>
- Arroyave Restrepo, J. M., Correa Moreno, L. F., & Duque Lozano, D. (2015). *Diseño conceptual, simulación y optimización del proceso de producción de Lactato de Etilo*. Universidad EAFIT,
- Asteasuain, M., Bandoni, A., Sarmoria, C., & Brandolin, A. (2006). Simultaneous process and control system design for grade transition in styrene polymerization. *Chemical engineering science*, 61(10), 3362-3378.
- Asthana, N. S., Kolah, A. K., Vu, D. T., Lira, C. T., & Miller, D. J. (2006). A kinetic model for the esterification of lactic acid and its oligomers. *Industrial & engineering chemistry research*, 45(15), 5251-5257.
- Bahakim, S. S., & Ricardez-Sandoval, L. A. (2014). Simultaneous design and MPC-based control for dynamic systems under uncertainty: A stochastic approach. *Computers & Chemical Engineering*, 63, 66-81.
- Beresford, R. (2005). Chemical engineering vol. 6. An introduction to chemical engineering design: By RK Sinnott; edited by Coulson and Richardson; published by Pergamon, Oxford, 2005, xvi+ 838 pp.; In: Elsevier.
- Boodhoo, K., & Harvey, A. (2013). *Process intensification technologies for green chemistry: engineering solutions for sustainable chemical processing*: John Wiley & Sons.
- Bykowski, D., Grala, A., & Sobota, P. (2014). Conversion of lactides into ethyl lactates and value-added products. *Tetrahedron Letters*, 55(38), 5286-5289.
- Chan, L. L. T., & Chen, J. (2017). Probabilistic uncertainty based simultaneous process design and control with iterative expected improvement model. *Computers & Chemical Engineering*, 106, 609-620.
- Company, T. D. C. (2018). AMBERLYST™ 15WET – Product Data Sheet. Retrieved from [http://msdssearch.dow.com/PublishedLiteratureDOWCOM/dh\\_09b7/0901b803809b7b11.pdf?filepath=liquidseps/pdfs/noreg/177-03087.pdf&fromPage=GetDoc](http://msdssearch.dow.com/PublishedLiteratureDOWCOM/dh_09b7/0901b803809b7b11.pdf?filepath=liquidseps/pdfs/noreg/177-03087.pdf&fromPage=GetDoc)
- Daengpradab, B., & Rattanaphanee, P. (2015). Process Intensification for Production of Ethyl Lactate from Fermentation-Derived Magnesium Lactate: A Preliminary Design. *International Journal of Chemical Reactor Engineering*, 13(3), 407-412.
- Delgado, P., Sanz, M. T., & Beltrán, S. (2007a). Isobaric vapor–liquid equilibria for the quaternary reactive system: Ethanol+ water+ ethyl lactate+ lactic acid at 101.33 kPa. *Fluid phase equilibria*, 255(1), 17-23.
- Delgado, P., Sanz, M. T., & Beltrán, S. (2007b). Kinetic study for esterification of lactic acid with ethanol and hydrolysis of ethyl lactate using an ion-exchange resin catalyst. *Chemical Engineering Journal*, 126(2), 111-118.
- Elizondo, J. R. E. (2007). Evaluacion Economica Preliminar de Plantas Quimicas Usando Aspen Icarus Process Evaluator 2004.2.

- Figuroa, J., Jaiver, E., Luisa, F., Martinez, M., Patricia, F., Betania, H., . . . Regina, M. (2015). *Evaluation Of Operational Parameters For Ethyl Lactate Production Using Reactive Distillation Process*. Paper presented at the ICHEAP12: 12TH INTERNATIONAL CONFERENCE ON CHEMICAL & PROCESS ENGINEERING.
- Flores-Tlacuahuac, A., & Biegler, L. T. (2005). A robust and efficient mixed-integer non-linear dynamic optimization approach for simultaneous design and control. *Computer Aided Chemical Engineering*, *20*, 67-72.
- Flores-Tlacuahuac, A., & Biegler, L. T. (2007). Simultaneous mixed-integer dynamic optimization for integrated design and control. *Computers & Chemical Engineering*, *31*(5), 588-600.
- Francisco Sutil, M. (2011). Diseño simultáneo de procesos y sistemas de control predictivo mediante índices de controlabilidad basados en normas.
- Gao, J., Zhao, X., Zhou, L., & Huang, Z. (2007). Investigation of ethyl lactate reactive distillation process. *Chemical Engineering Research and Design*, *85*(4), 525-529.
- Gibelhaus, A., Tangkrachang, T., Bau, U., Seiler, J., & Bardow, A. (2019). Integrated design and control of full sorption chiller systems. *Energy*, *185*, 409-422.
- Gutierrez, G., Ricardez-Sandoval, L. A., Budman, H., & Prada, C. (2014). An MPC-based control structure selection approach for simultaneous process and control design. *Computers & Chemical Engineering*, *70*, 11-21. doi:10.1016/j.compchemeng.2013.08.014
- Henson, M. A., & Seborg, D. E. (1997). *Nonlinear process control*: Prentice Hall PTR Upper Saddle River, New Jersey.
- Isidori, A. (1995). *Nonlinear Control Systems* (3 ed.). London: Springer-Verlag London.
- Kenig, E. Y., & Górak, A. (2007). Modeling of reactive distillation. *Modeling of process intensification*, 323-363.
- Kiss, A. A. (2013). *Advanced distillation technologies: design, control and applications*: John Wiley & Sons.
- Lomba, L., Giner, B., Zuriaga, E., Gascón, I., & Lafuente, C. (2014). Thermophysical properties of lactates. *Thermochimica Acta*, *575*, 305-312.
- Lunelli, B. H., de Moraes, E. R., Maciel, M. R. W., & Maciel Filho, R. (2011). Process Intensification for Ethyl Lactate Production Using Reactive Distillation. *Chemical Engineering Transactions*, *24*, 823-828.
- Luyben, M. L., & Luyben, W. L. (1997). *Essentials of process control*: McGraw-Hill New York.
- Luyben, W. L., & Yu, C.-C. (2009). *Reactive distillation design and control*: John Wiley & Sons.
- Mansouri, S. S., Sales-Cruz, M., Huusom, J. K., Woodley, J. M., & Gani, R. (2015). Integrated process design and control of reactive distillation processes. *IFAC-PapersOnLine*, *48*(8), 1120-1125.
- Marlin, T. (2015). Process Control: Designing Processes and Control Systems for Dynamic Performance Modelling. *Chemical Engineering Series, McGraw-Hill, New York*, 78-79.
- Meidanshahi, V., & Adams II, T. A. (2016). Integrated design and control of semicontinuous distillation systems utilizing mixed integer dynamic optimization. *Computers & Chemical Engineering*, *89*, 172-183.
- Mikleš, J., & Fikar, M. (2007). *Process modelling, identification, and control*: Springer.
- Mo, L., Shao-Tong, J., Li-Jun, P., Zhi, Z., & Shui-Zhong, L. (2011). Design and control of reactive distillation for hydrolysis of methyl lactate. *Chemical Engineering Research and Design*, *89*(11), 2199-2206.

- Montoya Sánchez, N. R. *Síntesis, caracterización y evaluación de una resina de intercambio catiónico con forma de empaque para una columna de destilación reactiva*. Universidad Nacional de Colombia,
- Ochoa, S. (2005). Metodología para la Integración Diseño-Control en el espacio de Estados. *M. Sc. Tesis. Universidad Nacional de Colombia*.
- Organics, A. (2009). Ethyl L-Lactate, 97% (GC) Retrieved from <https://wcam.engr.wisc.edu/Public/Safety/MSDS/Ethyl%20lactate.pdf>
- Peña, V., & Yurani, M. (2012). *Metodología de Diseño Simultáneo de Proceso y Control aplicada a un secado por atomización multiproducto para sustancias químicas naturales*. Universidad Nacional de Colombia, Sede Medellín,
- Pereira, C. S., Pinho, S. P., Silva, V. M., & Rodrigues, A. E. (2008). Thermodynamic equilibrium and reaction kinetics for the esterification of lactic acid with ethanol catalyzed by acid ion-exchange resin. *Industrial & Engineering Chemistry Research*, 47(5), 1453-1463.
- Pereira, C. S., Silva, V. M., & Rodrigues, A. E. (2011). Ethyl lactate as a solvent: Properties, applications and production processes—a review. *Green Chemistry*, 13(10), 2658-2671.
- Pereira, C. S. M. (2009). *Process Intensification for the Green Solvent Ethyl Lactate Production based on Simulated Moving Bed and Pervaporation Membrane Reactors*. Department of Chemical Engineering, Faculty of Engineering, University of Porto,
- Rafiei-Shishavan, M., Mehta, S., & Ricardez-Sandoval, L. A. (2017). Simultaneous design and control under uncertainty: A back-off approach using power series expansions. *Computers & Chemical Engineering*, 99, 66-81.
- República-Colombia, B. d. l. Tasa de cambio del peso colombiano (TRM). Retrieved from <http://www.banrep.gov.co/es/trm>
- Ricardez-Sandoval, L. A. (2012). Optimal design and control of dynamic systems under uncertainty: A probabilistic approach. *Computers & Chemical Engineering*, 43, 91-107. doi:10.1016/j.compchemeng.2012.03.015
- Ricardez-Sandoval, L. A., Budman, H., & Douglas, P. (2009). Integration of design and control for chemical processes: A review of the literature and some recent results. *Annual reviews in Control*, 33(2), 158-171.
- Ricardez-Sandoval, L. A., Douglas, P., & Budman, H. (2011). A methodology for the simultaneous design and control of large-scale systems under process parameter uncertainty. *Computers & Chemical Engineering*, 35(2), 307-318.
- Ricardez Sandoval, L., Budman, H., & Douglas, P. (2008). Simultaneous design and control of processes under uncertainty: A robust modelling approach. *Journal of Process Control*, 18(7), 735-752.
- Sakizlis, V., Perkins, J. D., & Pistikopoulos, E. N. (2003). Parametric controllers in simultaneous process and control design. *Computer Aided Chemical Engineering*, 15, 1020-1025.
- Sakizlis, V., Perkins, J. D., & Pistikopoulos, E. N. (2004). Recent advances in optimization-based simultaneous process and control design. *Computers & Chemical Engineering*, 28(10), 2069-2086.
- Scientific, F. (2018). Ethyl L(-)-lactate, 97%. Retrieved from <https://www.fishersci.com/shop/products/ethyl-l-lactate-97-across-organics-4/p-3736465#>
- Sharifzadeh, M. (2013). Integration of process design and control: A review. *Chemical Engineering Research and Design*, 91(12), 2515-2549.
- Smith, C. A., & Corripio, A. B. (2012). *Principles and practice of automatic process control*: Editorial Félix Varela.

- Subawalla, H., & Fair, J. R. (1999). Design guidelines for solid-catalyzed reactive distillation systems. *Industrial & engineering chemistry research*, 38(10), 3696-3709.
- Sundmacher, K., & Kienle, A. (2006). *Reactive distillation: status and future directions*: John Wiley & Sons.
- Taylor, R., & Krishna, R. (2000). Modelling reactive distillation. *Chemical engineering science*, 55(22), 5183-5229.
- Treybal, R. E., & García Rodríguez, A. (1988). *Operaciones de transferencia de masa*.
- Turton, R., Bailie, R. C., Whiting, W. B., & Shaeiwitz, J. A. (2008). *Analysis, synthesis and design of chemical processes*: Pearson Education.
- Vega, P., De Rocco, R. L., Revollar, S., & Francisco, M. (2014). Integrated design and control of chemical processes—Part I: Revision and classification. *Computers & Chemical Engineering*, 71, 602-617.
- Vega, P., Lamanna, d. R., Revollar, S., & Francisco, M. (2014). Integrated design and control of chemical processes—part i: revision and classification. *Computers & Chemical Engineering*.

## APPENDIX

**Table 23 Initial condition for model simulation**

<i>Tray</i>	$x_W$	$x_{Et}$	$x_{LA}$	$x_{EL}$	<i>Holdup [kmol]</i>	<i>T [K]</i>
1	0.2302	0.7697	0.0001	0.0000	2.1676	352.43
2	0.2808	0.7186	0.0006	0.0000	2.0004	352.57
3	0.3388	0.6547	0.0047	0.0017	2.0255	353.72
4	0.3049	0.3969	0.0167	0.2814	1.9803	378.61
5	0.3505	0.3476	0.0282	0.2737	2.0163	381.68
6	0.3810	0.3139	0.0383	0.2669	2.0380	384.20
7	0.3989	0.2933	0.0473	0.2606	2.0464	386.11
8	0.4066	0.2831	0.0557	0.2546	2.0435	387.40
9	0.4066	0.2808	0.0636	0.2490	2.0314	388.15
10	0.4006	0.2846	0.0713	0.2434	2.0123	388.47
11	0.3898	0.2933	0.0791	0.2379	1.9878	388.47
12	0.3749	0.3059	0.0870	0.2322	1.9587	388.23
13	0.3563	0.3222	0.0954	0.2262	1.9255	387.81
14	0.3338	0.3420	0.1044	0.2198	1.8883	387.25
15	0.3074	0.3655	0.1144	0.2127	1.8469	386.59
16	0.2764	0.3928	0.1260	0.2048	1.8008	385.84
17	0.2404	0.4244	0.1396	0.1956	1.7496	385.02
18	0.1989	0.4610	0.1560	0.1842	1.6935	384.13
19	0.1523	0.5054	0.1735	0.1688	1.6368	382.94
20	0.1024	0.5748	0.1780	0.1448	1.6066	380.40
21	0.0513	0.8102	0.0837	0.0548	2.3367	369.16
22	0.0508	0.8106	0.0839	0.0546	2.3368	369.64
23	0.0504	0.8111	0.0842	0.0544	2.3368	370.10
24	0.0499	0.8116	0.0844	0.0541	2.3367	370.56
25	0.0493	0.8121	0.0847	0.0539	2.3366	371.01
26	0.0488	0.8125	0.0850	0.0537	2.3364	371.46
27	0.0484	0.8126	0.0856	0.0534	2.3353	371.92
28	0.0478	0.8069	0.0913	0.0540	2.3143	372.65
29	0.0446	0.7007	0.1548	0.0999	1.7228	382.42